On the Dynamics

of

Creeping Structures

Martin O'Gorman

School of Mathematical Sciences,

Dublin City University.

Supervisor: Dr. D. W. Reynolds.

M.Sc Thesis by Research.

Submitted in fulfilment of the requirements

for the degree of M.Sc. in Applied Mathematical Sciences

at Dublin City University, February, 1999.

I hereby certify that this material, which I now submit for assessment on the programme of study leading to the award of Master of Science in Applied Mathematical Sciences is entirely my own work and has not been taken from the work of others save and to the extent that such work has been cited and acknowledged within the text of my work.

Signed: ________________ ID No: 93700393

Date: 20 February, 1999.

Acknowledgements

David, for your patience, encouragement and excellent supervision. Without you, this thesis would still be a random collection of ideas!

Mum and Dad, without you I would not have achieved this. You have always encouraged me with your inspiring words.

Thanks to the maths postgrads, there have been many, and to the staff in the Maths department.

Kieran Murphy, our many discussions helped clarify a number of points, thanks.

I would like to thank Prof. G. Hunt and Prof. C. Budd for allowing me the opportunity to study under their supervision at the University of Bath. An excellent year.

Paul and Tom, yea can have the table back! Thanks dudes, couldn't have kept going without you.

Dave, for the hardware. I owe you! Paul, for the *software*!

Over the last five years I have been lucky enough to meet some incredible people with whom I have shared many great times. Friendships that will endure. You kept me going, thanks. Lets all get together in New Zealand!

To Granny, Jack and Granda.

Abstract

This thesis considers the dynamics of a viscoelastic Link model. Though the constitutive equation is linear, the problem has a geometrical nonlinearity and an imperfection. This work extends and formalises that done by Hunt and Thompson, which studies the elastic model, and that of Hayman, which studies the quasi-static approximation to the viscoelastic model. The non-linear, dynamic elastic and viscoelastic Link problems and the quasi-static approximation to the latter are rigorously analysed. The equilibria and their stability and bifurcation properties are determined and compared for the perfect and imperfect models. In particular, it is shown that the quasi-static approximation indicates stability at some equilibrium points, corresponding to large deflection, where the dynamic analysis indicates that the system is unstable. Asymptotic approximations to the solution of the linearised problem, subject to different loading strategies, are calculated using multiple scale methods.

Contents

List of Figures

List of Tables

Chapter 1

Introduction

This thesis looks at the dynamic and quasi-static motion of a viscoelastic Link model. The Link model with a Standard Viscoelastic element is illustrated in Figure 1.1. It is a model problem for a transcritical bifurcation with few degrees of freedom. The non-dimensional load λ is the bifurcation parameter. A transcritical bifurcation occurs at the intersection

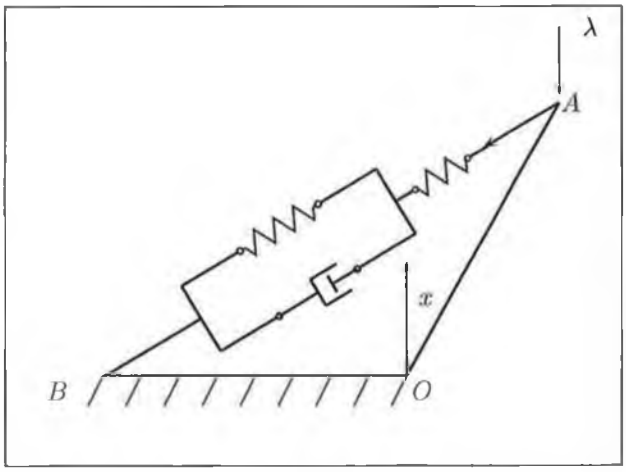

Figure 1.1: The Link Model with Standard Viscoelastic element.

of two branches of equilibria and stability is transferred from one branch to the other, as illustrated in Figure 1.2. We can identify a critical load λ_c at which this change in stability occurs. The non-dimensional model equations are given by

$$\ddot{x} = \lambda(t)\sin x - \cos x\frac{\sqrt{1+\sin x} - \sqrt{1+\sin\nu}}{\sqrt{1+\sin x}} - \frac{\cos x}{\sqrt{1+\sin x}}y, \tag{1.0.1a}$$

$$\dot{y} = -\alpha\{y + \beta(\sqrt{1+\sin x} - \sqrt{1+\sin\nu})\}. \tag{1.0.1b}$$

where $x(t)$ is a measure of displacement, $y(t)$ is the creep stress, $\lambda(t)$ is the load, ν is the initial imperfection, α is related to the relaxation time and $\beta = 1 - G_m$ where G_m is the long-term modulus of elasticity. The elastic buckling behaviour of the Link

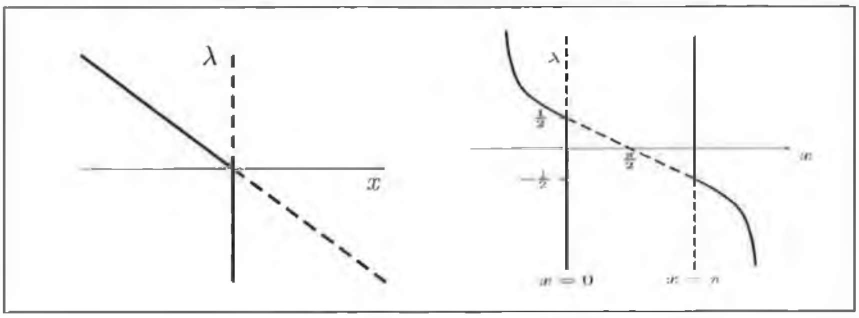

Figure 1.2: (a) A Transcritical Bifurcation. (b) Bifurcation diagram for the elastic system. Solid lines indicate stable equilibrium points and dashed lines indicate unstable equilibrium points. The transcritical bifurcations can be seen at $(x, \lambda) = (0, 1/2)$ and $(x, \lambda) = (\pi, -1/2)$

model has been studied in Hunt and Thompson [18], who looks at the static elastic Link model with imperfection. Equilibrium curves are defined and the stability of the system is investigated. Hayman [14, 15] investigates the Link model with a Maxwell viscoelastic element. He is interested in the creep buckling behaviour of the system. His analysis is restricted to the quasi-static motion of the system. Neither of these sources provide a rigorous mathematical treatment of the model under consideration. Rather, they are interested in the buckling characteristics from a structures viewpoint. This thesis extends the work done in [14, 15, 18]. There is a rigorous treatment of the non-linear, dynamic elastic and viscoelastic Link model and the quasi-static approximation to the nonlinear system.

The dynamic elastic model is a conservative system. The equilibrium curves for the perfect system are reproduced in Figure 1.2. We determine the stability properties of the equilibria and identify two transcritical bifurcation points. The imperfect system is also investigated. We show that the introduction of an imperfection has the effect of reducing the critical load and removing the transcritical bifurcation from the system. In Section 3.3 we investigate the dynamic viscoelastic system. The equilibrium curves can be projected onto the $x\lambda$-plane and compared with those of the elastic system. We show that the effect of the viscoelastic element is to scale the elastic critical load by the factor G_m. This is true in both the perfect case and the imperfect case. The behaviour of the perfect system close to the zero equilibrium branch is analysed in greater detail. We determine conditions on the system parameters λ, α and G_m that allow us to identify the regions in parameter space where the linearised system has one real and two complex eigenvalues. We use these results in Chapter 5 when constructing asymptotic approximations to the solution of the linearised system.

In Chapter 4 we study the quasi-static approximation to the nonlinear system. We extend Hayman's work by assuming that $y(0)$ is non-trivial. Under these conditions there is some residual stress in the spring initially. This is another source of imperfection and this has important consequences for the motion of the system. We show that under this condition, the initial starting position of the system can be on any elastic equilibrium curve. This results in a greater range of possible motions in comparison to those indicated in [14, 15]. We show that the position of equilibrium curves of the quasi-static system is equivalent to those of the dynamic system. However, the results of the quasi-static stability analysis differ from the results predicted by the dynamic analysis. In particular, the quasi-static analysis indicates stability at some equilibrium points, corresponding to large deflections, where the dynamic analysis indicates that the system is unstable. This is true for both the perfect and the imperfect quasi-static systems. We establish a relationship between the dynamic elastic equilibria, the dynamic viscoelastic equilibria and the stability of the quasi-static equilibria. In particular, we show that there are two points at which the stability of the quasi-static equilibrium curve changes from stable to unstable. The first point is equivalent to the critical point on the corresponding dynamic equilibrium curve while the second change occurs at the intersection of the elastic critical point locus with the equilibrium curve.

In Chapter 5 we apply a perturbation technique, the multiple time scale method, to find asymptotic approximations to the solution of the perfect model problem linearised about zero. By imposing the condition that the relaxation time is large, we have $\alpha \ll 1$, giving us a small parameter in the system. The results from Chapter 3 indicate that for $\alpha \ll 1$, the characteristic equation has two complex roots and one real root. This allows us to construct a solution that has both oscillating and exponential components. We analyse the model subject to three loading strategies; the constant load problem, the slowly varying load problem and the parametric loading problem. The results of the constant load problem agree with the analytic results from Chapter 3. In particular, we show that an exponential term decays (grows) for values of load satisfying $\lambda < (>) \lambda_c$, resulting in a stable (unstable) solution. In the slowly varying load problem we write the load as a function of εt, where $\varepsilon \ll 1$. We derive a condition which the time-dependent load must satisfy for the system to remain stable. We show that in certain cases, the system remains stable even if the load occasionally increases above the critical value for the constant load problem. Finally, we look at the parametric load problem where the load is in the form, $\lambda(t) = \lambda_0 + \varepsilon \cos \kappa t$ with λ_0 a constant and $\varepsilon \ll 1$. In the elastic case the problem reduces to the Mathieu equation. The solution to the Mathieu equation can become unstable as a result of a resonance effect due to the interaction of the natural frequency of the system with the frequency of excitation κ. The instabilities are due to oscillations with exponentially increasing amplitude. We investigate the effect that including the viscoelastic element has on these regions of instability. We need to distinguish between instabilities due to oscillations and those due to creep. We show that the viscoelastic element has a stabilising effect on the oscillations and that there is a minimum value of ε below which the system has stable oscillations.

Chapter 2

The Viscoelastic Link Model

2.1 Introduction

The second chapter of this thesis opens with an overview of the theory of viscoelasticity. Desirable properties of viscoelastic materials are detailed and some rheological models are discussed. The viscoelastic element that we use throughout the thesis, the Standard Viscoelastic model, is analysed in detail and its constitutive equation is determined. This equation is required to completely describe the Link model which is introduced later in the chapter. The dynamic equations for the Link model are formulated and supplemented with the constitutive equation for the viscoelastic element, which results in a system comprising of a first order and a second order differential equation. We allow the Link model to have an initial imperfection. Finally, we apply transformations that non-dimensionalise the system. For a more complete introduction to the theory of viscoelasticity and rheological models, the reader is referred to Findley, Lai and Onaran [8], Fabrizio and Morro [7] and Rabotnov [27]. A background to the mechanics of structures is found in Gere and Timoshenko [9].

2.2 Viscoelasticity

The effective modeling of material behaviour requires that we can describe the relationship between stress σ, strain e and time. This relationship is given by the constitutive equation for a given material. The behaviour of some solids can be described simply as elastic and some fluids as viscous. However, for materials that are intermediate between solids and fluids we need to be able to combine the properties of elasticity and viscosity. Such materials are said to be viscoelastic. Viscoelastic materials demonstrate a wide range of behaviour including the following, which are illustrated in Figure 2.1,

a) *Instantaneous elasticity*

This is characterised by an instantaneous strain response to an applied jump in stress.

b) *Creep under constant stress*

Creep is the slow, continuous increase in strain due to a constant stress.

c) *Stress relaxation under constant strain*

Stress relaxation is characterised by a gradual decrease in stress when a material is subjected to a constant strain.

d) *Instantaneous recovery*

This is characterised by an instantaneous decrease in strain following the removal of an applied stress.

e) *Delayed recovery*

Upon removal of an applied stress there may be a slow, continuous recovery of creep strain.

f) *Permanent set*

That part of the strain which is not recovered on removal of an applied stress is referred to as permanent set.

Materials with the properties b), c), e) and f) have memory in the sense that present strain depends on the past history of stress. This is an important concept in the theory

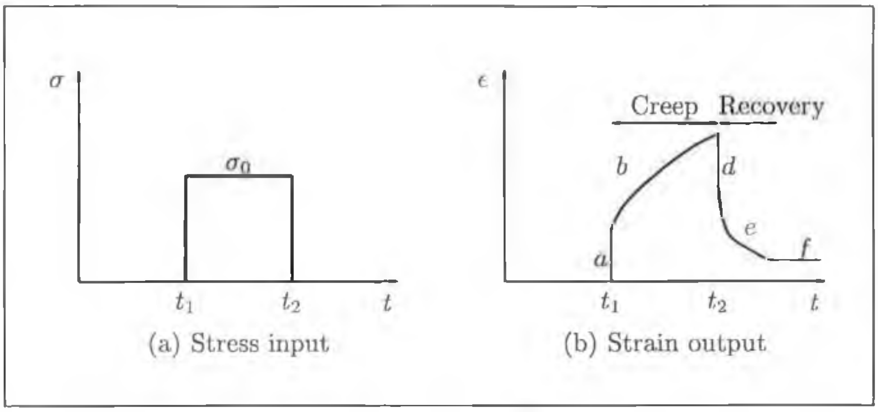

Figure 2.1: The strain response to a piecewise constant stress for a viscoelastic material. A constant stress σ_0 is applied at time t_1 and removed at time t_2. The strain response includes creep and recovery features. Any, or all, of these responses may occur for a typical viscoelastic material.

of viscoelasticity. The total deformation of a material at time t depends not only on the stress at time t but also on all previous stress inputs. Stress history can be written as

$$\sigma^t(s) := \sigma(t-s) \qquad s \geq 0$$

where $\sigma^t(0)$ is the current stress. Thus, if t is the present time, $\sigma^t(s)$ is the stress s time units in the past.

In this work I am concerned with materials that are linearly viscoelastic. A material is said to be linearly viscoelastic if stress is proportional to strain and Boltzmann's superposition principle is satisfied. These conditions can be stated mathematically as

$$e[c_1\sigma_1^t + c_2\sigma_2^t] = c_1e[\sigma_1^t] + c_2e[\sigma_2^t]$$

where e is the strain output, σ_1^t and σ_2^t the stress inputs and c_1, c_2 are stress history constants. The domain of e is the linear space of histories. Boltzmann's superposition principle states that the strain output due to the sum of two different stress histories is equal to the sum of the strain outputs due to the individual stress histories.

2.2.1 Rheological Models

Rheology is the science of deformation and flow. It is the study of those properties of a material which determine its response to applied forces. Rheological models consisting of various combinations of elastic springs and viscous dashpots are used to represent viscoelastic materials. In this section we discuss three common rheological models; the Maxwell model, the Voigt model and the Standard Viscoelastic model. The third model, the Standard Viscoelastic model, is analysed in detail. Both the Maxwell and Voigt models have a number of limitations when used to model solid-like materials. However, the Standard Viscoelastic model retains the desirable features of the Maxwell and Voigt models and overcomes their limitations. This model is used throughout the thesis. Its constitutive equation is derived and its properties are detailed.

The Linear Elastic Spring

Linear elastic springs are used to model elastic behaviour in a material. The linear spring is characterised by a time-independent elastic strain response which is proportional to the stress input. This is illustrated in Figure 2.2[1] The stress-strain relationship is given by Hooke's Law,

$$\sigma = Ee. \tag{2.2.1}$$

The constant E is Young's Modulus and is material dependent. The strain remains constant over time and disappears when the stress is removed. Instantaneous elasticity and recovery are the main characteristics of an elastic material.

[1]Fig 2.2, in common with other diagrams which include a stress input graph, show the constant stress σ_0 beginning at time $t = 0$. This is for illustrative purposes. Both σ and e are defined on $(-\infty, 0)$ and can be non-trivial there.

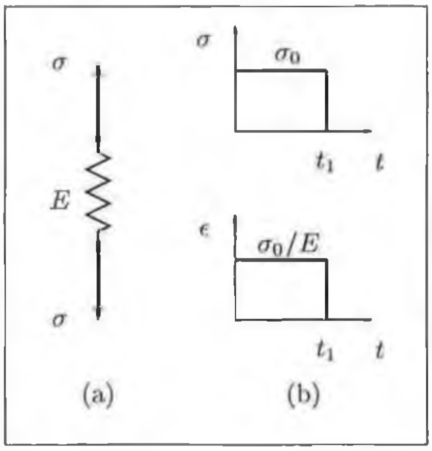

Figure 2.2: (a) The Elastic Spring. (b) Strain response to a piecewise constant stress.

The Linear Viscous Dashpot

The dashpot is used to model viscous behaviour in fluids or fluid-like materials. The stress-strain relationship is characterised by a strain rate response to an applied stress, given by

$$\sigma = \eta \dot{e}, \tag{2.2.2}$$

where η is the constant of viscosity. This is illustrated in Figure 2.3. The dashpot is deformed continuously when a constant stress is applied. Unlike the elastic spring, this deformation is not recoverable and remains as a permanent set.

The Maxwell Model

The Maxwell model consists of a linear spring and linear dashpot in series as shown in Figure 2.4. Using (2.2.1), (2.2.2) and the fact that $e = e_1 + e_2$ we get the following stress-strain relationship for the Maxwell model,

$$\dot{e} = \frac{\dot{\sigma}}{E} + \frac{\sigma}{\eta}.$$

The Maxwell model exhibits instantaneous elasticity (recovery) on loading (unloading).

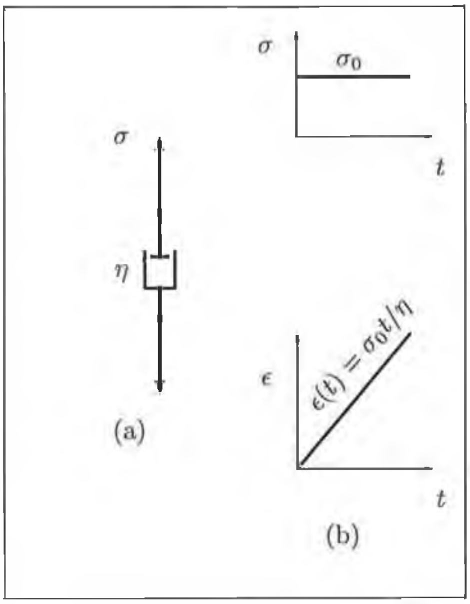

Figure 2.3: (a) The viscous dashpot. (b) The stress-strain relationship.

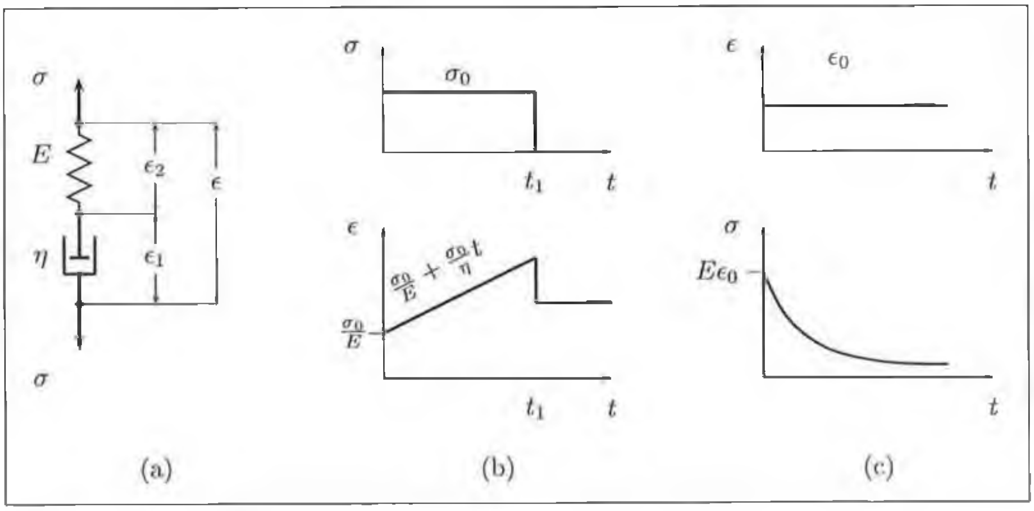

Figure 2.4: (a) The Maxwell Model. (b) Strain response to a constant stress. (c) Stress relaxation due to constant strain.

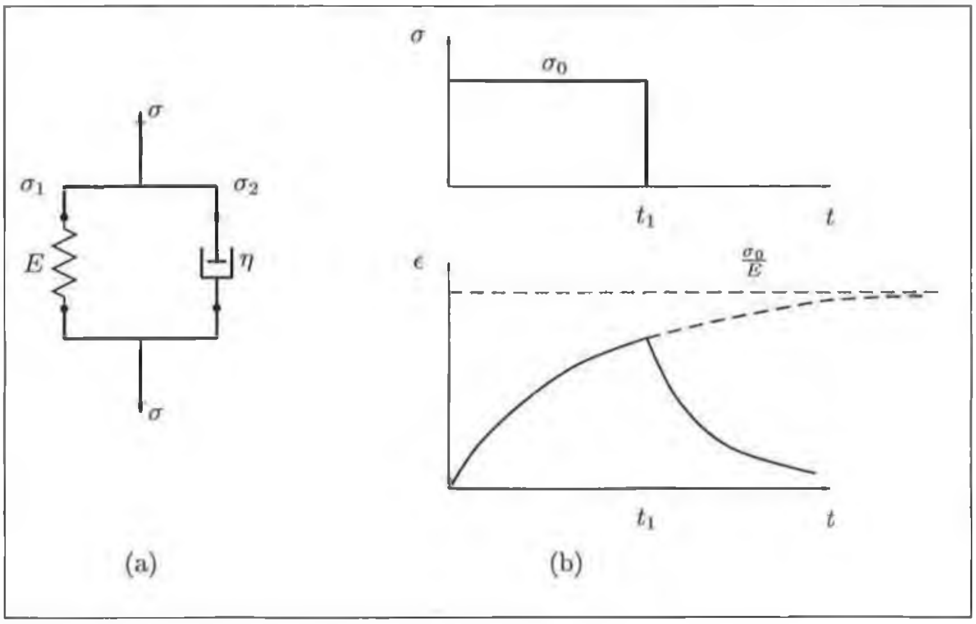

Figure 2.5: (a) The Voigt Model. (b) Strain response to a constant stress.

A creep strain develops under constant stress and a permanent set remains on removal of the stress. If a constant strain is maintained then stress relaxation occurs and stress decays to zero.

The Voigt Model

The Voigt Model consists of a linear spring and linear dashpot in parallel as illustrated in 2.5. Again, using (2.2.1), (2.2.2) and $\sigma = \sigma_1 + \sigma_2$, we get the following stress-strain relationship for the Voigt model,

$$\dot{e} + \frac{E}{\eta}e = \frac{\sigma}{\eta}.$$

The Voigt model has a finite creep limit, σ_0/E, and a decreasing strain rate under constant stress.

While the Maxwell model and the Voigt model have been used to model viscoelastic behaviour in materials, both models are specialised and do not have all the properties a) - f) on page 6. The Maxwell model does not have a finite creep limit and there is no creep

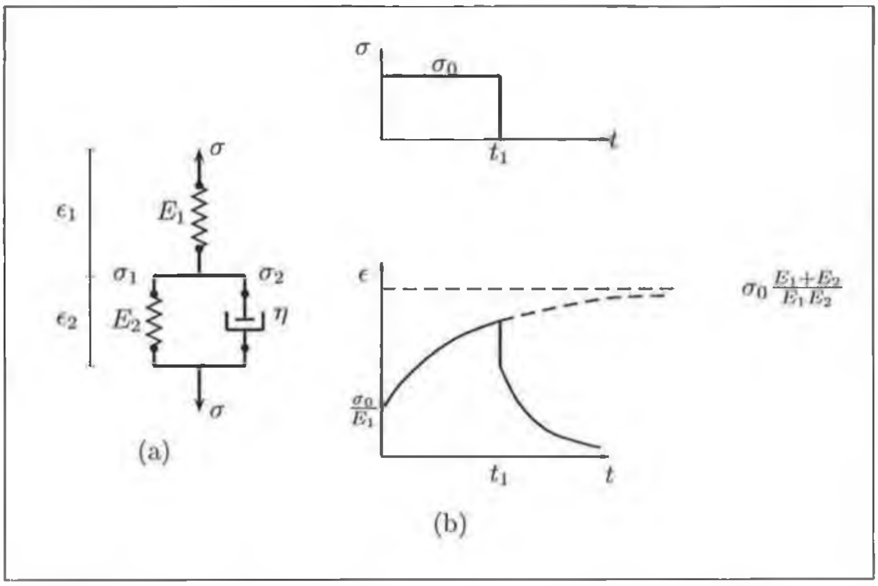

Figure 2.6: (a) The Standard Viscoelastic model. (b) The stress-strain relationship for the standard model.

recovery. The strain due to creep remains as a permanent set once the applied stress is removed. With the Voigt model there is no instantaneous elasticity (recovery) on loading (unloading). Neither does this model exhibit stress relaxation.

2.2.2 The Standard Viscoelastic Model

The Standard Viscoelastic model is a 3-element model that better reproduces the behaviour of real solids under load. This is the model that I will consider throughout this work. The model and its properties are illustrated in Figure 2.6. The model consists of a spring-dashpot pair in parallel combined in series with a spring.

The Constitutive Equation

Let E_1 and E_2 be the spring constants and η the viscous constant. Let σ be the applied stress and e the total deformation. The deformation of the first spring satisfies (2.2.1), or

$$e_1 = \frac{\sigma}{E_1}.$$

The total stress on the spring-dashpot pair is

$$\sigma = \sigma_1 + \sigma_2, \tag{2.2.3}$$

with the spring satisfying

$$\sigma_1 = E_2 e_2,$$

and the dashpot satisfying (2.2.2),

$$\sigma_2 = \eta \dot{e_2}.$$

Thus, for the spring-dashpot pair, (2.2.3) gives

$$\sigma = E_2 e_2 + \eta \dot{e_2}.$$

The total deformation can be written as

$$e = e_1 + e_2. \tag{2.2.4}$$

Differentiating (2.2.4) we get

$$\begin{aligned} \dot{e} &= \dot{e_1} + \dot{e_2}, \\ &= \frac{\dot{\sigma}}{E_1} + \frac{\sigma}{\eta} - \frac{E_2}{\eta} e + \frac{E_2}{E_1 \eta} \sigma. \end{aligned} \tag{2.2.5}$$

Rearranging terms in (2.2.5) and multiplying across by E_1 gives

$$\dot{\sigma} + \frac{E_1 + E_2}{\eta} \sigma = E_1 (\dot{e} + \frac{E_2}{\eta} e). \tag{2.2.6}$$

Now, letting $E = E_1$, $\alpha = (E_1 + E_2)/\eta$ and $\mu = E_2/\eta$ in (2.2.6) we get

$$\dot{\sigma} + \alpha\sigma = E(\dot{e} + \mu e). \tag{2.2.7}$$

This is the differential form of the constitutive equation for the Standard Viscoelastic model.

The differential equation (2.2.7) predicts instantaneous elasticity followed by a time dependent deformation which tends to the limiting value $\sigma_0(E_1+E_2)/(E_1E_2)$, (see Fig.2.6). If the load σ is applied rapidly so that $\dot{\sigma}$ and $\dot{e}$ are large initially then σ and e are negligible and we get $\dot{\sigma} \sim E\dot{e}$. The quantity E is the instantaneous modulus of elasticity. If the stress acts slowly over a long time period the rate of deformation is small and both $\dot{\sigma}$ and $\dot{e}$ become negligible. Then (2.2.7) gives $\sigma \sim (E\mu/\alpha)e$.The quantity $(E\mu)/\alpha = (E_1E_2)/(E_1 + E_2)$ is the long term modulus of elasticity and it relates the stress and deformation in limiting conditions. Solving (2.2.7) for the stress $\sigma(t)$ gives the integral representation of the constitutive equation,

$$\sigma(t) = E\,e(t) - \alpha\,(E - \frac{E\mu}{\alpha})\int_{-\infty}^{t} e(\tau)e^{-\alpha(t-\tau)}\,d\tau. \tag{2.2.8}$$

Letting $G_0 = E$ and $G_\infty = E\mu/\alpha$ we can write (2.2.8) as

$$\sigma(t) = G_0 e(t) + \int_{-\infty}^{t} \dot{G}(t-\tau)e(\tau)\,d\tau, \tag{2.2.9}$$

where $G(t) = G_\infty + (G_0 - G_\infty)e^{-\alpha t}$, $t \geq 0$. We will refer to the long term modulus of elasticity as $G_\infty := \lim_{t\to\infty} G(t)$ and the instantaneous modulus of elasticity as $G_0 := G(0)$. We can rewrite the constitutive equation (2.2.7) in terms of G_0 and G_∞ as

$$\dot{\sigma} + \alpha\sigma = G_0\dot{e} + \alpha G_\infty e. \tag{2.2.10}$$

Solving (2.2.10) for the strain $e(t)$ we get

$$e(t) = J_0\sigma(t) + \int_{-\infty}^{t} \dot{J}(t-\tau)\sigma(\tau)\,d\tau, \tag{2.2.11}$$

where $J(t) = J_0 + (J_0 - J_\infty)e^{-\mu t}$, $J_0 = G_0^{-1}$ and $J_\infty = G_\infty^{-1}$. We can think of $\dot{J}(t)$ as a memory function. The first term in (2.2.11) represents the strain contribution from the current stress. The term inside the integral represents the strain contribution from all the previous stress inputs with $\dot{J}(t)$ determining the current effect of previous stress inputs. In general, $\dot{J}(t)$ is decreasing function, indicating a fading memory property. For the Standard Viscoelastic element we have

$$\dot{J}(t) = \mu(J_\infty - J_0)e^{-\mu t}.$$

Properties of the Standard Viscoelastic Model

The 3-element model exhibits the following characteristics.

1. *Instantaneous Elasticity and Recovery.*

Defining the stress function $\sigma(t)$ by

$$\sigma(t) = \begin{cases} 0, & t < 0, \\ \sigma_0, & t \geq 0, \end{cases} \tag{2.2.12}$$

where σ_0 is constant and using (2.2.11) we can write the strain as

$$\begin{aligned} e(t) &= \sigma_0 \left\{ J_0 - \mu(J_0 - J_\infty) \int_0^t e^{-\mu(t-\tau)} d\tau \right\}, \\ &= \sigma_0 \left\{ J_0 - (J_0 - J_\infty)(1 - e^{-\mu t}) \right\}. \end{aligned} \tag{2.2.13}$$

Setting $t = 0$ in (2.2.13) gives the instantaneous deformation

$$e(0) = \sigma_0 J_0 = \frac{\sigma_0}{G_0}.$$

This instantaneous deformation is recovered on removal of the stress (apply the Boltzmann Superposition Principle).

2. *Finite Creep Limit and Decreasing Strain Rate.*

Under conditions of constant stress σ_0, the strain increases at a decreasing rate until it reaches a finite limit. Taking the limit as $t \to \infty$ in (2.2.13) we get

$$\lim_{t \to \infty} e(t) = \sigma_0 J_\infty = \frac{\sigma_0}{G_\infty},$$

where G_∞ is the long-term modulus of elasticity. Differentiating (2.2.13) we get the (decreasing) strain rate,

$$\dot{e}(t) = -\mu\sigma_0(J_0 - J_\infty)e^{-\mu t} = \mu\frac{G_0 - G_\infty}{G_0 G_\infty}e^{-\mu t}.$$

3. *Stress Relaxation.*

Stress relaxation is a characteristic of certain viscoelastic materials whereby the stress required to maintain a constant strain decreases over time. If a unit strain is imposed at time $t = 0$ and maintained for all time $t \geq 0$, then from (2.2.9) we have

$$\sigma(t) = G_0 + \int_0^t \dot{G}(t-\tau)d\tau = G(t).$$

So, the function

$$G(t) = G_\infty + (G_0 - G_\infty)e^{-\alpha t}, \tag{2.2.14}$$

is the stress relaxation function with $\alpha = 1/t_r$, where t_r is the relaxation time. It demonstrates that the stress required to maintain a constant strain is exponentially decreasing.

2.3 The Link Model

The Link model that is investigated in this thesis has been analysed by various authors in the literature. Hunt and Thompson [18] looks at the static elastic case and derives equilibrium equations. He does not consider the dynamic elastic case or include the viscoelastic element. Hayman [14, 15] considers the quasi-static equations of the Link model with a Maxwell viscoelastic element. He ignores the time dependence due to inertia. In this thesis we are interested in the dynamics of the viscoelastic Link model with a Standard Viscoelastic element. The load is allowed to be time dependent. In the following section the dynamic equations for the Link model with a Standard Viscoelastic element and time-dependent load are formulated.

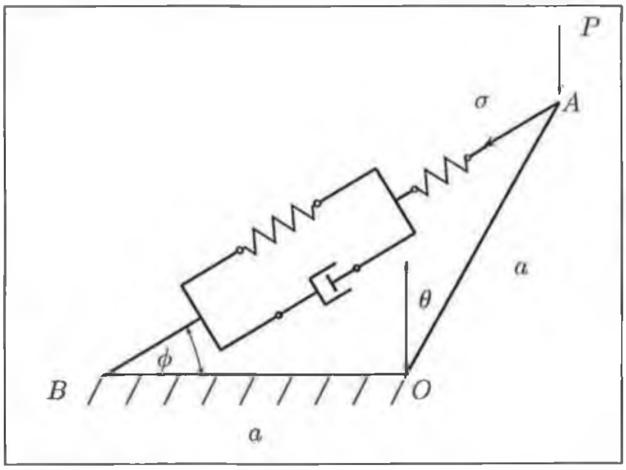

Figure 2.7: The Link Model with Standard Viscoelastic element.

2.3.1 Formulation of the Dynamic Equations

Consider the Link model in Figure 2.7. A light rigid rod of length a is hinged at O. The end A is connected to the point B by a Standard Viscoelastic element. OB is of length a. The viscoelastic element exerts a force $\sigma(t)$ in the direction AB. A time-dependent load $P(t)$ acts vertically downward at A. Conservation of angular momentum about O requires that

$$-ma^2\ddot{\theta}(t) = -aP(t)\sin\theta(t) + a\sigma(t)\sin\phi(t), \tag{2.3.1}$$

where $\phi = \pi/4 - \theta/2$. Now

$$\sin\phi = \sin(\frac{\pi}{4} - \frac{\theta}{2}) = \frac{1}{\sqrt{2}}\frac{\cos\theta}{\sqrt{1+\sin\theta}}.$$

Substituting for ϕ in (2.3.1) and simplifying gives the following dynamic equation,

$$\ddot{\theta} = \frac{P}{ma}\sin\theta - \frac{\sigma}{\sqrt{2}ma}\frac{\cos\theta}{\sqrt{1+\sin\theta}}. \tag{2.3.2}$$

The length of AB is

$$2a\cos\phi = a\sqrt{2(1+\sin\theta)}.$$

As a measure of strain, we choose extension from a natural reference. This natural reference is chosen so that it is stress free. Ideally we want $\theta = 0$ to be the reference state, so that the natural length of AB would be $a\sqrt{2}$. However, later we want to study an imperfection in the Link model and therefore we allow the natural state to be $\theta = \theta_i$, which we consider small. The extension, measured from the reference state, is given by

$$2a\cos\phi - 2a\cos\phi_i = a\sqrt{2}\left\{\sqrt{1+\sin\theta} - \sqrt{1+\sin\theta_i}\right\}, \tag{2.3.3}$$

where $\phi_i = \pi/4 - \theta_i/2$. From (2.3.3), we write the strain as

$$e = \sqrt{1+\sin\theta} - \sqrt{1+\sin\theta_i}. \tag{2.3.4}$$

We assume that the viscoelastic element is composed of a Standard Viscoelastic material. The stress $\sigma(t)$ satisfies (2.2.10) with initial condition

$$\sigma(0) = G_0 e(0) - \alpha(G_0 - G_\infty)\int_{-\infty}^{0} e(\tau)e^{\alpha\tau}\,d\tau,$$

which can be determined from the initial strain history. Define

$$\sigma_c(t) = \sigma(t) - G_0 e(t). \tag{2.3.5}$$

Differentiating (2.3.5) and using (2.2.10) we can write the constitutive equation as

$$\dot{\sigma_c} + \alpha\sigma_c = -\alpha(G_0 - G_\infty)e. \tag{2.3.6}$$

with $\sigma_c(0) = -\alpha(G_0 - G_\infty)\int_{-\infty}^{0} e(\tau)e^{\alpha\tau}d\tau$. Note that $\sigma_c(0) \to 0$ as $\alpha \to 0$. We can think of σ_c as the stress component due to creep. From (2.3.6) and (2.3.2), we see that the equations of motion are

$$\ddot{\theta} = \frac{P}{ma}\sin\theta - \frac{G_0}{\sqrt{2}ma}\frac{\left\{\sqrt{1+\sin\theta} - \sqrt{1+\sin\theta_i}\right\}\cos\theta}{\sqrt{1+\sin\theta}} - \frac{\sigma_c}{\sqrt{2}ma}\frac{\cos\theta}{\sqrt{1+\sin\theta}}. \tag{2.3.7a}$$

$$\dot{\sigma_c} = -\alpha\left(\sigma_c + (G_0 - G_\infty)\left\{\sqrt{1+\sin\theta} - \sqrt{1+\sin\theta_i}\right\}\right). \tag{2.3.7b}$$

We now transform the system into one involving dimensionless variables. Define the following transformations,

$$
\begin{aligned}
x(t) &= \theta\Big(\sqrt{\frac{G_0}{\sqrt{2}ma}}t\Big),\\
y(t) &= \sigma_c\Big(\sqrt{\frac{G_0}{\sqrt{2}ma}}t\Big),\\
\lambda(t) &= P\Big(\sqrt{\frac{G_0}{\sqrt{2}ma}}t\Big)\frac{\sqrt{2}}{G_0}, \hat{\alpha} \qquad\qquad = \alpha\sqrt{\frac{\sqrt{2}ma}{G_0}},\\
\beta &= 1 - \frac{G_\infty}{G_0},\\
\nu &= \theta_i.
\end{aligned}
$$

Applying the above transformations to (2.3.7) gives the non-dimensional system,

$$
\ddot{x} = \lambda(t)\sin x - \cos x\frac{\sqrt{1+\sin x} - \sqrt{1+\sin\nu}}{\sqrt{1+\sin x}} - \frac{\cos x}{\sqrt{1+\sin x}}y, \tag{2.3.8a}
$$

$$
\dot{y} = -\hat{\alpha}\left\{y + \beta\left(\sqrt{1+\sin x} - \sqrt{1+\sin\nu}\right)\right\}. \tag{2.3.8b}
$$

with initial conditions $x(0) = \zeta_1$, $\dot{x}(0) = \zeta_2$, $y(0) = \gamma$ and initial imperfection ν. We call the system with $\nu \neq 0$ the imperfect system. In the limit as $\nu \to 0$ the equations for the imperfect system tend to those of the perfect system. For ease of notation we drop the $\hat{}$ from $\hat{\alpha}$ for the remainder of the thesis. It is useful to note the effect that non-dimensionalising of the variables has on the moduli of elasticity. They have been scaled by the instantaneous modulus G_0 so that the instantaneous modulus is now equal to 1 and the long-term modulus is $G_m = G_\infty/G_0$.

Chapter 3

The Link Model: A Dynamic Analysis

3.1 Introduction

In this chapter we analyse the dynamic system for the Link model. We begin with the elastic system without imperfection. We show that the system is conservative and use this property to calculate the equilibria of the system. The stability properties of the equilibria are also determined. We identify and discuss the bifurcation points of the elastic system. In Section 3.3 we analyse the perfect viscoelastic system. Again, the equilibria and their properties are determined. We discuss the effect that the introduction of the viscoelastic element has on the behaviour of the system. Centre manifold theory is used to identify the type of bifurcation that occurs in the viscoelastic system, with some details of the calculations given in Appendix C. In Section 3.4 we look at the imperfect elastic and viscoelastic models. We compare the equilibria with those found in the perfect case. In appendix A, we give an overview of the theory of ordinary differential equations, and introduce elements of the theory that are used in this chapter. For a fuller account the reader is referred to Guckenheimer and Holmes [11], Hale and Koçak [13] and Glendinning [10]. The stability of the equilibria for the viscoelastic system is determined using the Routh-Hurwitz criterion, which is detailed in Appendix B.

3.2 The Dynamic Elastic System

The dynamic elastic system is obtained by letting $\alpha \to 0$ in (2.3.8). Then $\dot{y}(t) = 0$. Also, since $\sigma_c(0) \to 0$ as $\alpha \to 0$ we have $y(t) = 0$. We consider the constant load model so that the system is autonomous. The model equation is

$$\ddot{x} = \lambda \sin x - \cos x \frac{\sqrt{1+\sin x} - \sqrt{1+\sin \nu}}{\sqrt{1+\sin x}}, \tag{3.2.1}$$

with initial conditions $x(0) = \zeta_1$ and $\dot{x}(0) = \zeta_2$. We first consider the perfect case by setting $\nu = 0$. The imperfect system is discussed in Section 3.4.

3.2.1 Conservation of Energy

If we let

$$v(x,\lambda) = -\left(\lambda \sin x - \cos x \frac{\sqrt{1+\sin x} - \sqrt{1+\sin \nu}}{\sqrt{1+\sin x}}\right)$$

then the perfect elastic system can be written in the form

$$\ddot{x} = -v(x,\lambda), \tag{3.2.2}$$

thus is conservative (see A.6). The energy function is given by

$$E(x,\dot{x},\lambda) = \frac{\dot{x}^2}{2} + V(x,\lambda),$$

where

$$\begin{aligned} V(x,\lambda) &= \int_0^x v(s,\lambda)\,ds \\ &= -\lambda(1-\cos x) + \left(\sqrt{1+\sin x} - 1\right)^2, \end{aligned} \tag{3.2.3}$$

is the potential energy function. The energy function $E(x,\dot{x},\lambda)$ is a constant of the motion of the system.

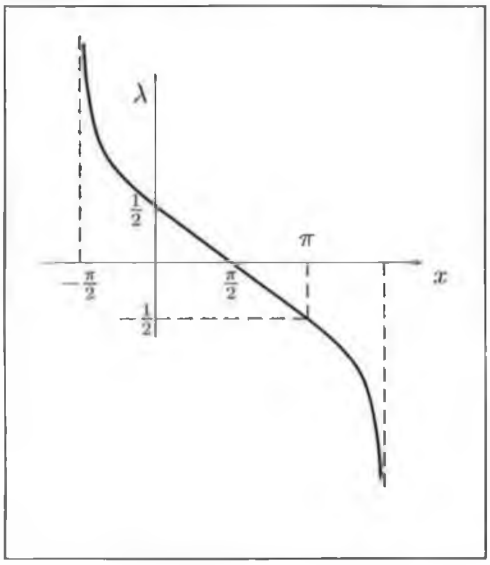

Figure 3.1: The function $\Lambda_E(x)$.

3.2.2 Equilibria

The equilibrium points $\bar{x}$ of the conservative system satisfy $V'(\bar{x}, \lambda) = 0$. The equation

$$0 = V'(x, \lambda) = \lambda \sin x - \frac{\{\sqrt{1 + \sin x} - 1\} \cos x}{\sqrt{1 + \sin x}}, \tag{3.2.4}$$

results in three branches of equilibria for $-\frac{\pi}{2} < x < \frac{3\pi}{2}$,

- the branch $\{(0, \lambda) : \lambda \in \mathbf{R}\}$;
- the branch $\{(\pi, \lambda) : \lambda \in \mathbf{R}\}$;
- the branch $\{(x, \Lambda_E(x)) : \lambda = \Lambda_E(x), -\frac{\pi}{2} < x < \frac{3\pi}{2}\}$;

where

$$\Lambda_E(x) := \frac{\sqrt{1 + \sin x} - 1}{\tan x \sqrt{1 + \sin x}}. \tag{3.2.5}$$

In order to plot the branch $(x, \Lambda_E(x))$ we need to know some properties of Λ_E.

Proposition 1. *The function $\Lambda_E : (-\pi/2, 3\pi/2) \to R$ given by (3.2.5) is a strictly decreasing C^2 invertible function with $\Lambda_E(0) = 1/2, \Lambda_E(\pi/2) = 0, \Lambda_E(\pi) = -1/2$ and $d\Lambda_E/dx(-\pi/2_+) = \infty, d\Lambda_E/dx(3\pi/2_-) = -\infty$.*

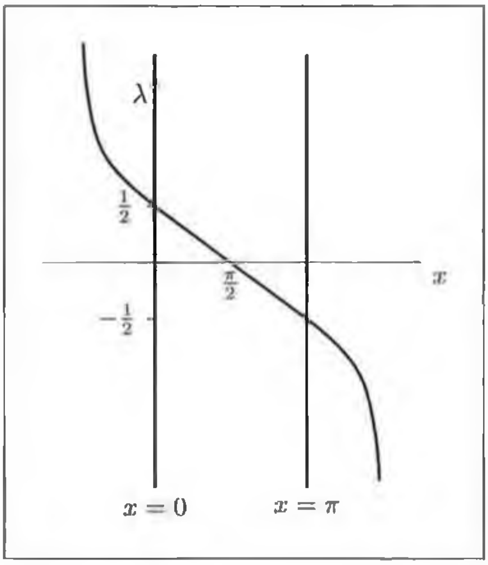

Figure 3.2: The equilibrium curves of the elastic system.

The proof to this proposition is straightforward and the function $\Lambda_E(x)$ is plotted in Figure 3.1. The branches of equilibria are therefore as drawn in Figure 3.2. The $(x, \Lambda_E(x))$ branch intersects the $(0, \lambda)$ branch at $(x, \lambda) = (0, 1/2)$ and intersects the (π, λ) branch at $(x, \lambda) = (\pi, -1/2)$.

3.2.3 Stability Analysis of the Equilibria

We wish to determine the stability of equilibrium points along each of the three branches of equilibria. We are interested in finding the non-hyperbolic equilibrium points and determining if a bifurcation occurs at any of these points.

Proposition 2. *Suppose that $\bar{x}$ is an equilibrium point of the elastic, conservative system* (3.2.2)*, implying that $\bar{x}$ is also a critical point of the potential function $x \to V(\cdot, \lambda)$. Then,*

(i) $\bar{x}$ is an unstable saddle point if $V_{xx}(\bar{x}, \lambda) < 0$.[1]

(ii) $\bar{x}$ is an stable centre point if $V_{xx}(\bar{x}, \lambda) > 0$.

(iii) $\bar{x}$ is an unstable cusp if $V_{xx}(\bar{x}, \lambda) = 0$ and $V_{xxx}(\bar{x}, \lambda) \neq 0$.

[1]The x-subscript denotes partial differentiation with respect to x. Therefore, $V_{xx} = \partial^2 V/\partial x^2$, etc.

Thus, stable centre points correspond to minimum points of the potential function while at maximum points of the potential we have unstable saddle points. The second derivative of the potential function (3.2.3) is

$$V_{xx}(x,\lambda) = -\lambda\cos x - \sin x\frac{\sqrt{1+\sin x}-1}{\sqrt{1+\sin x}} + \frac{1}{2}\frac{\cos^2 x}{(1+\sin x)^{\frac{3}{2}}}. \tag{3.2.6}$$

Proposition 3. *Consider the dynamic autonomous elastic system* (3.2.2)*.*

a. The equilibria $(0,\lambda)$ *are stable for* $\lambda < 1/2$ *and unstable for* $\lambda \geq 1/2$*.*

b. The equilibria (π,λ) *are stable for* $\lambda > -1/2$ *and unstable for* $\lambda \leq -1/2$*.*

c. The equilibria $(\Lambda_E^{-1}(\lambda),\lambda)$ *are stable for* $\lambda > 1/2$ *and* $\lambda < -1/2$*, and unstable for* $-1/2 \leq \lambda \leq 1/2$*.*

The points $(0,1/2)$ *and* $(\pi,-1/2)$ *are unstable cusp points, and non-hyperbolic equilibria.*

Proof. a.) For $(\bar{x},\lambda)$ satisfying $\{(0,\lambda) : \lambda \in \mathbf{R}\}$ we get $V_{xx}(0,\lambda) = -(\lambda - \frac{1}{2})$. Now, from proposition 2, we have

(i) For $\lambda < \frac{1}{2}$, $V_{xx}(0,\lambda) > 0$, implying that $(0,\lambda)$ is a stable centre point.

(ii) For $\lambda > \frac{1}{2}$, $V_{xx}(0,\lambda) < 0$, implying that $(0,\lambda)$ is an unstable saddle point.

(ii) For $\lambda = \frac{1}{2}$, $V_{xx}(0,1/2) = 0$ and $V_{xxx}(0,1/2) \neq 0$, hence $(0,1/2)$ is a non-hyperbolic, unstable cusp point .

b.) For $(\bar{x},\lambda)$ satisfying $\{(\pi,\lambda) : \lambda \in \mathbf{R}\}$ we get $V_{xx}(\pi,\lambda) = \lambda + \frac{1}{2}$. Again, using proposition 2, we have,

(i) For $\lambda > -\frac{1}{2}$, $V_{xx}(\pi,\lambda) > 0$, implying that (π,λ) is a stable centre point.

(ii) For $\lambda < -\frac{1}{2}$, $V_{xx}(\pi,\lambda) < 0$, implying that (π,λ) is an unstable saddle point.

(iii) For $\lambda = -\frac{1}{2}$, $V_{xx}(\pi,\lambda) = 0$ and $V_{xxx}(\pi,\lambda) \neq 0$, hence $(\pi,-1/2)$ is a non-hyperbolic, unstable cusp point.

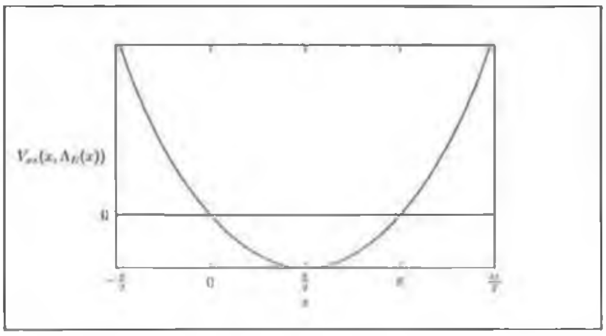

Figure 3.3: The function $V_{xx}(x, \Lambda_E(x))$

c.) The third branch of equilibria has a λ dependency. We need to examine the third derivative of the potential, $V_{xxx}(x, \lambda)$, in order to be able to identify fixed points and regions of increase and decrease of (3.2.6). Differentiating (3.2.6) and substituting (3.2.5) for λ we get

$$V_{xxx}(x, \Lambda_E(x)) = -\frac{3}{4}\frac{\cos x}{(1+\sin x)^{\frac{1}{2}}}, \qquad -\pi/2 < x < 3\pi/2,$$

which has the same sign as $-\cos x$. Thus,

- $V_{xxx}(x, \Lambda_E) < 0$ for $-\frac{\pi}{2} < x < \frac{\pi}{2}$ implying that $V_{xx}(x, \Lambda_E)$ is decreasing;
- $V_{xxx}(x, \Lambda_E) = 0$ for $x = \frac{\pi}{2}$ implying that $V_{xx}(x, \Lambda_E)$ has a critical point;
- $V_{xxx}(x, \Lambda_E) > 0$ for $\frac{\pi}{2} < x < \frac{3\pi}{2}$ implying that $V_{xx}(x, \Lambda_E)$ is increasing;
- $V_{xx}(x, \Lambda_E) = 0$ for $x = 0, x = \pi$.

This information is used to plot $V_{xx}(x, \Lambda_E)$ in Figure 3.3 and we see that

(i) For $x \in (-\frac{\pi}{2}, 0) \cup (\pi, \frac{3\pi}{2})$ we have $V_{xx}(x, \Lambda_E) > 0$ implying that the branch of equilibria over this range of x correspond to stable centre points.

(ii) For $x \in (0, \pi)$ we have $V_{xx}(x, \Lambda_E) < 0$ implying that the branch of equilibria over this range of x correspond to unstable saddle points.

	min.	max.
$\lambda < -1/2$	$0,\ \Lambda_E^{-1}$	π
$-1/2 < \lambda < 1/2$	$0,\ \pi$	Λ_E^{-1}
$\lambda > 1/2$	$\Lambda_E^{-1},\ \pi$	0

Table 3.1: The position of local minimum and maximum points of $V(x, \lambda)$ for different λ values. We can clearly see the interchange between minimum and maximum points, indicating the change in stability of equilibrium points as λ varies.

(iii) For $x = 0, \pi$ we have $V_{xx}(x, \Lambda_E) = 0$ and $V_{xxx}(x, \Lambda_E) \neq 0$, hence these equilibria are unstable cusp points. □

So, we encounter a change in the stability type of equilibria on the $(0, \lambda)$ branch at $\lambda = 1/2$ and on the (π, λ) branch at $\lambda = -1/2$, indicating that the equilibrium points $(\bar{x}, \lambda) = (0, 1/2)$ and $(\bar{x}, \lambda) = (\pi, -1/2)$ are bifurcation points for the system. These equilibria correspond to the intersection points of the $(x, \Lambda_E(x))$ branch with the $(0, \lambda)$ and (π, λ) branches. The change in stability can be clearly seen by examining the critical points of the potential function for various values of λ, as shown in Figure 3.5, Figure 3.6 and Figure 3.4. The local minimum and maximum points are given in Table 3.1. For $-1/2 < \lambda < 1/2$, $V(\cdot, \lambda)$ has local minima at $0, \pi$ and a local maximum at $\Lambda_E^{-1}(\lambda)$. As λ increases through $\lambda = 1/2$, the local minimum at 0 interchanges with the local maximum at $\Lambda_E^{-1}(\lambda)$. The local minimum at π remains unchanged. However, as λ decreases through $\lambda = -1/2$, we encounter an interchange between the the local minima at π and the local maximum at $\Lambda_E^{-1}(\lambda)$. The number of equilibria points changes from two to one and back to two as we pass through the parameter values $\lambda = \pm 1/2$. These bifurcations are discussed in more detail in the next section.

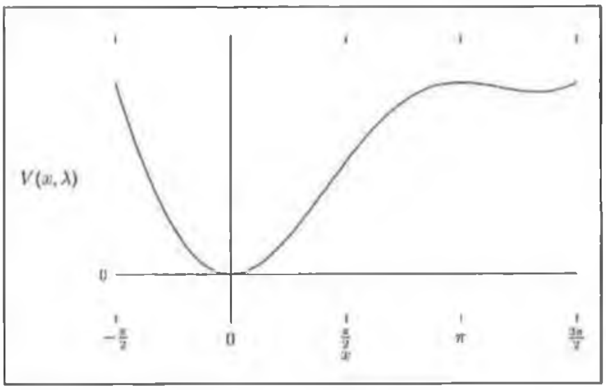

Figure 3.4: Potential function $V(x, \lambda)$ for $\lambda < -1/2$.

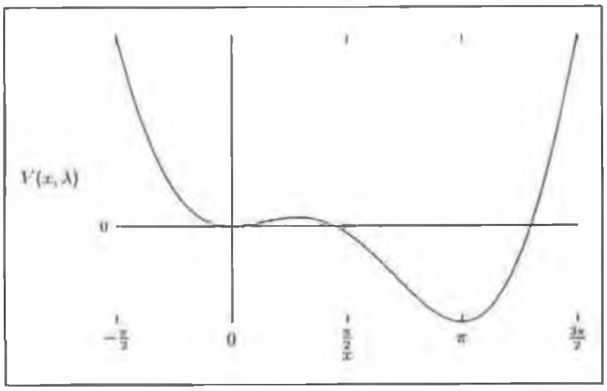

Figure 3.5: Potential function $V(x, \lambda)$ for $-1/2 < \lambda < 1/2$.

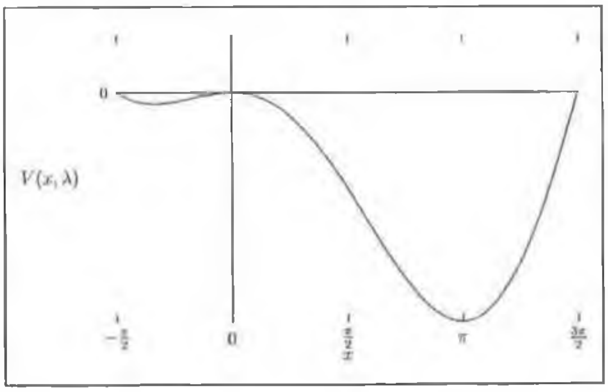

Figure 3.6: Potential function $V(x, \lambda)$ for $\lambda > 1/2$.

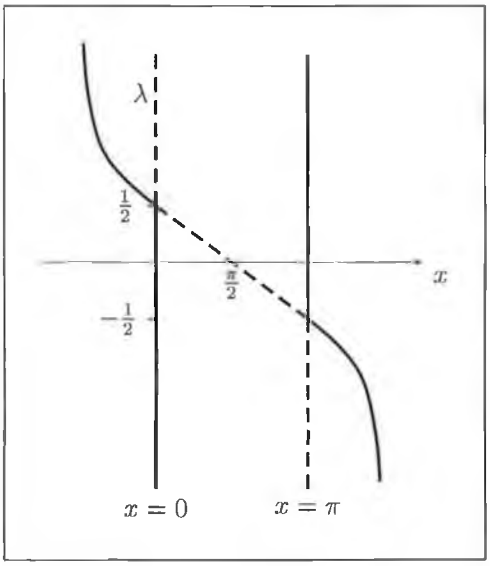

Figure 3.7: Bifurcation diagram for the elastic system. Solid lines indicate stable equilibrium points and dashed lines indicate unstable equilibrium points. The transcritical bifurcations can be seen at $(x, \lambda) = (0, 1/2)$ and $(x, \lambda) = (\pi, -1/2)$

3.2.4 Discussion of Bifurcations

We have identified 3 branches of equilibria for the system, and the stability type of the equilibria on each branch has been determined. The equilibria are plotted in the bifurcation diagram in Figure 3.7

At a bifurcation point there is a qualitative change in the topological features of the flow of the system. In particular we are interested in values of λ at which the number and/or type of equilibrium points changes. We have already seen that the equilibrium point $(x, \lambda) = (0, \frac{1}{2})$ is non-hyperbolic and is a bifurcation point for the system. At this bifurcation point two branches of equilibria coalesce and a change is stability occurs. The origin changes from being stable to unstable and stability is transferred to the branch $(x, \Lambda_E(x))$. This type of bifurcation is called a transcritical bifurcation. There is a reduction in the number of equilibrium points from two to one at the bifurcation point. As λ increases through $\lambda = 1/2$ the number of equilibrium points increases to two again. A similar bifurcation occurs at $(x, \lambda) = (\pi, -1/2)$, where the $(x, \Lambda_E(x))$ branch intersects the (π, λ) branch.

3.3 The Dynamic Viscoelastic System

The dynamic viscoelastic system without imperfection is

$$\ddot{x} = \lambda \sin x - \cos x \frac{\sqrt{1+\sin x} - 1}{\sqrt{1+\sin x}} - \frac{\cos x}{\sqrt{1+\sin x}} y, \tag{3.3.1a}$$

$$\dot{y} = -\alpha \left(y + \beta \left[\sqrt{1+\sin x} - 1 \right] \right). \tag{3.3.1b}$$

$0 < \alpha$ is the normalised relaxation constant and $\beta = 1 - G_m$, where $0 < G_m < 1$ is the normalised long term modulus of elasticity associated with the viscoelastic element.

3.3.1 Equilibria of the Viscoelastic System

Let $\bar{\mathbf{x}} = (\bar{x}, \bar{y}, \lambda)$ be an equilibrium point for the viscoelastic system (3.3.1). From (3.3.1b) we see that equilibrium points satisfy

$$\bar{y} = -\beta \left[\sqrt{1+\sin \bar{x}} - 1 \right]. \tag{3.3.2}$$

For the remainder of this analysis we will refer to the equilibria $(\bar{x}, \bar{y}(\bar{x}), \lambda)$ in terms of $(\bar{x}, \lambda)$. We can view this as a projection of the equilibria onto the $x\lambda$-plane. By substituting (3.3.2) into (3.3.1a) we have that

$$\lambda \sin \bar{x} - G_m \cos \bar{x} \frac{\sqrt{1+\sin \bar{x}} - 1}{\sqrt{1+\sin \bar{x}}} = 0, \tag{3.3.3}$$

giving a relationship between $\bar{x}$ and λ which defines equilibrium curves. We notice immediately that (3.3.3) is equivalent to (3.2.4) with λ replaced by λ / G_m. Hence, it follows that there are 3 branches of equilibrium points for the viscoelastic case,

- the branch $\{(0, \lambda) : \lambda \in \mathbf{R}\}$;

- the branch $\{(\pi, \lambda) : \lambda \in \mathbf{R}\}$;

- the branch $\{(x, \Lambda_V(x)) : \lambda = \Lambda_V(x), -\frac{\pi}{2} < x < \frac{3\pi}{2}\}$;

where

$$\Lambda_V(x) = \frac{G_m\left(\sqrt{1+\sin x} - 1\right)}{\tan x\sqrt{1+\sin x}}. \tag{3.3.4}$$

By proposition 1, $\Lambda_V(x)$ is a strictly decreasing C^2 invertible function with $\Lambda_V(0) = G_m/2$, $\Lambda_V(\pi/2) = 0, \Lambda_V(\pi) = -G_m/2$ and $d\Lambda_V/dx(-\pi/2_+) = \infty, d\Lambda_V/dx(3\pi/2_-) = -\infty$. Thus, the $(x, \Lambda_V(x))$ branch of equilibria intersects the $(0, \lambda)$ branch at $(0, G_m/2)$ and the point of intersection of the $(x, \Lambda_V(x))$ branch with the (π, λ) branch is $(\pi, -G_m/2)$. We can compare the equilibria of the elastic system to those of the viscoelastic system. We see that the $\{(0, \lambda) : \lambda \in \mathbf{R}\}$ and $\{(\pi, \lambda) : \lambda \in \mathbf{R}\}$ branches of equilibria of the elastic system are retained for the viscoelastic system. However, the branch $(x, \Lambda_V(x))$ satisfies $\Lambda_V(x) < \Lambda_E(x)$ for $-\pi/2 < x < \pi/2$ and $\Lambda_V(x) > \Lambda_E(x)$ for $\pi/2 < x < 3\pi/2$. The viscoelastic equilibria are plotted in Fig 3.8. The stability properties are determined in the next section.

3.3.2 Stability Analysis of the Equilibria

The stability type of the equilibrium points of the perfect viscoelastic system can be determined from the linearisation of (3.3.1). In particular, we need to calculate the eigenvalues of the Jacobian matrix. We write the non-linear system in the form

$$\dot{\mathbf{x}} = \mathbf{f}(\mathbf{x}). \tag{3.3.5}$$

Now, let $\mathbf{x} = \bar{\mathbf{x}} + \xi$ where $\bar{\mathbf{x}}$ is an equilibrium point of (3.3.5) and $| \xi | \ll 1$. Then ξ approximately satisfies

$$\dot{\xi} = Df(\bar{\mathbf{x}})\xi,$$

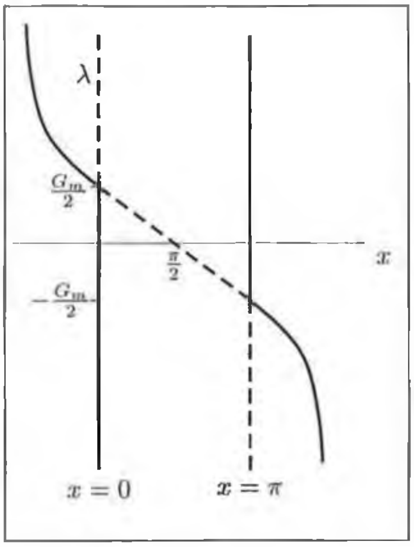

Figure 3.8: The equilibrium branches of the perfect viscoelastic system. Solid lines indicate stable equilibrium points while the dashed lines indicate unstable equilibrium points.

the linearisation about $\bar{\mathbf{x}}$. Here $Df(\bar{\mathbf{x}})$, which is the Jacobian matrix evaluated at $\bar{\mathbf{x}}$, is given by

$$Df(\bar{\mathbf{x}}) = \begin{bmatrix} 0 & 1 & 0 \\ \lambda\cos\bar{x} + \sin\bar{x} + \frac{\sqrt{1+\sin\bar{x}}(\bar{y}(\bar{x})-1)}{2} & 0 & -\frac{\cos\bar{x}}{\sqrt{1+\sin\bar{x}}} \\ -\frac{\alpha\beta}{2}\frac{\cos\bar{x}}{\sqrt{1+\sin\bar{x}}} & 0 & -\alpha \end{bmatrix} \quad (3.3.6)$$

where $\bar{y}(\bar{x})$ is given by (3.3.2). The characteristic equation $\Delta(p)$ of $Df(\bar{\mathbf{x}})$ is

$$\Delta(p) = p^3 + \alpha p^2 + c_1 p + \alpha c_0, \quad (3.3.7)$$

where

$$c_0 = -\left[\lambda\cos\bar{x} + \sin\bar{x} + \frac{\sqrt{1+\sin\bar{x}}(\bar{y}(\bar{x})-1)}{2} + \frac{\beta}{2}\frac{\cos^2\bar{x}}{1+\sin\bar{x}}\right] \quad (3.3.8)$$

and

$$c_1 = -\left[\lambda\cos\bar{x} + \sin\bar{x} + \frac{\sqrt{1+\sin\bar{x}}(\bar{y}(\bar{x})-1)}{2}\right]. \quad (3.3.9)$$

The eigenvalues of (3.3.6) are the roots of the characteristic equation. We want to determine conditions on the model parameters G_m, λ and α given the position of the eigenvalues in the complex plane. In this way we can identify values of the parameters for which stable and unstable solutions exist. We examine each of the three branches of equilibria separately. The eigenvalue analysis indicates the stability of hyperbolic equilibria but for non-hyperbolic equilibrium points we need to use the Centre Manifold theorem to determine the behaviour of the system. Later in chapter 5 we determine solutions to the linearised system $\dot{\xi} = Df(\mathbf{0})\xi$. For this reason we investigate the equilibrium points on the branch $(x, \lambda) = (0, \lambda)$ more closely. In particular, we determine a relationship between G_m, λ and α for which there exists of a pair of complex roots and one other root.

The $\{(0, \lambda) : \lambda \in R\}$ branch of equilibria

By setting $\bar{x} = 0$ in (3.3.8) and (3.3.9), we get the characteristic equation

$$\Delta(p) = p^3 + \alpha p^2 + (\frac{1}{2} - \lambda)p + \alpha(\frac{G_m}{2} - \lambda) \tag{3.3.10}$$

We can determine certain properties of the eigenvalues of (3.3.6) by applying the Routh-Hurwitz criterion to $\Delta(p)$. Also using Rolle's theorem we can determine conditions on λ, G_m and α for which complex eigenvalues will occur. Note that there is always at least one real eigenvalue and that complex eigenvalues will occur as conjugate pairs.

Proposition 4. *The characteristic equation* (3.3.10) *has*

- *Three roots with negative real parts if* $\lambda < \frac{G_m}{2}$.
- *Two roots with negative real parts and a root at the origin if* $\lambda = \frac{G_m}{2}$.
- *Two roots with negative real parts and one positive real root if* $\lambda > \frac{G_m}{2}$.

For $\alpha < \sqrt{3(\frac{1}{2} - \lambda)}$ *there exists a pair of complex conjugate roots to* (3.3.10) *for all* $G_m < 1$. *Otherwise, a complex pair of roots will exist for* $G_m < G_-$ *and* $G_m > G_+$ *where*

$$G_{\pm} = \frac{9\alpha - 4\alpha^3 + 36\alpha\lambda \pm \sqrt{2}(2\alpha^2 + 6\lambda - 3)^{\frac{3}{2}}}{27\alpha}$$

Proof. Applying the Routh-Hurwitz criterion to (3.3.10) we have

$$D_1 = \alpha > 0,$$

$$D_2 = \begin{vmatrix} \alpha & \alpha(\frac{G_m}{2} - \lambda) \\ 1 & \frac{1}{2} - \lambda \end{vmatrix} = \alpha(\frac{1}{2} - \frac{G_m}{2}) > 0,$$

$$D_3 = \begin{vmatrix} \alpha & \alpha(\frac{G_m}{2} - \lambda) & 0 \\ 1 & \frac{1}{2} - \lambda & 0 \\ 0 & \alpha & \alpha(\frac{G_m}{2} - \lambda) \end{vmatrix}$$
$$= \alpha^2(\frac{1}{2} - \frac{G_m}{2})(\frac{G_m}{2} - \lambda)$$

The D_i are strictly positive for $\lambda < G_m/2$. Thus, all roots of the characteristic equation have negative real parts. For $\lambda = \frac{G_m}{2}$ we have $D_3 = 0$. A direct calculation shows us that for this value of λ there is one zero root and 2 roots with negative real parts. Finally, for $\lambda > \frac{G_m}{2}$ the sequence $1, D_1, D_1D_2, \alpha c_0$ has sign sequence $+, +, +, -$ implying 1 root with positive real part for equilibria on the branch $\{(0, \lambda) : \lambda > \frac{G_m}{2}\}$.

We can investigate the roots further using Rolle's Theorem. The first derivative of $\Delta(p)$ is given by

$$\frac{d\Delta}{dp} = 3p^2 + 2\alpha p + (\frac{1}{2} - \lambda),$$

with roots $\alpha_\pm = -\alpha/3 \pm \sqrt{\alpha^2 - 3(\frac{1}{2} - \lambda)}/3$. The roots of $d\Delta(p)/dp$ are complex for $\alpha < \sqrt{3(\frac{1}{2} - \lambda)}$. Rolle's Theorem implies that $\Delta(p)$ has complex roots when this condition is satisfied. Also, $\Delta(p)$ has 2 equal real roots and another real root for $G_m = G_\pm$ where $G_\pm = (9\alpha - 4\alpha^3 + 36\alpha\lambda \pm \sqrt{2}(2\alpha^2 + 6\lambda - 3)^{\frac{3}{2}})/27\alpha$. Thus, a pair of complex roots exists for G_m satisfying $G_m < G_-$, $G_m > G_+$ (see Appendix B). □

Proposition 4 implies that at equilibrium points satisfying $\lambda < G_m/2$ there exists a three-dimensional stable manifold while for $\lambda > G_m/2$ there exists a two-dimensional stable man-

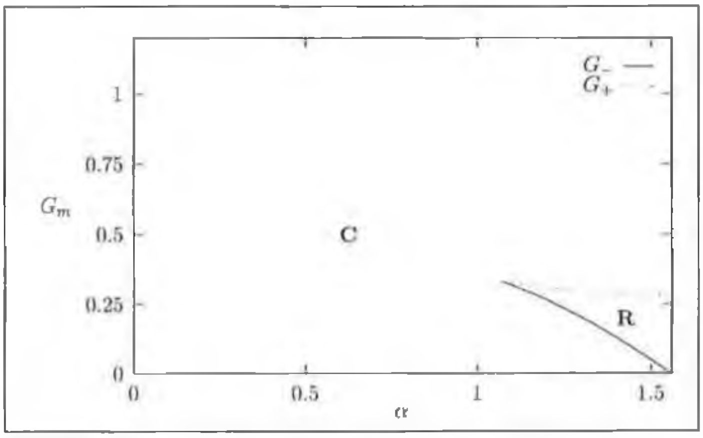

Figure 3.9: Regions in parameter space where real and complex roots exist for $\lambda < 1/2$. The curves G_+ and G_-, which represent the transition between real and complex roots, are shown. In the region marked **C**, the characteristic equation has a pair of complex roots and one real root while in the the region marked **R**, the characteristic equation has 3 real roots.

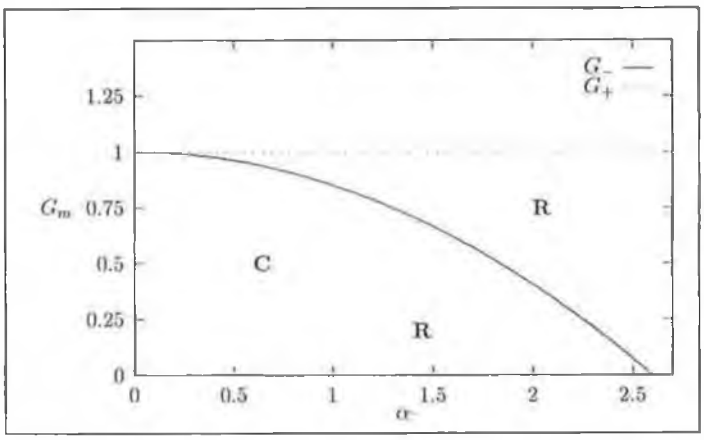

Figure 3.10: Regions in parameter space where real and complex roots exist for the limiting case, $\lambda = 1/2$. Again we show the curves G_+ and G_-. The characteristic equation has a pair of complex roots and one real root in the region marked **C**, while in the the region marked **R**, the characteristic equation has 3 real roots.

ifold and a one-dimensional unstable manifold. The equilibrium point $(\bar{x}, \lambda) = (0, G_m/2)$ has a 2 dimensional stable manifold and a one-dimensional centre manifold. We will investigate the behaviour of the system on the centre manifold later in this chapter. In Figure 3.9 we plot $G_\pm$ vs. α for a typical value of $\lambda \in (0, 1/2)$ and in Figure 3.10 we plot $G_\pm$ vs. α in the limiting case where $\lambda = 1/2$. The curves $G_m = G_\pm$ mark the transition between real and complex roots. At the intersection of the curves we have 3 equal real roots. On the remainder of the curves there are 2 equal real roots and one other root. From these diagrams we can identify the parameter values at which the characteristic equation (3.3.10) has a pair of complex roots. In particular, for $\lambda < 1/2$ we can find some $0 < \alpha \ll 1$ such that a pair of complex roots exists. This fact is used when we construct approximate solutions to the constant load model problem in chapter 5.

The $\{(x, \Lambda_V(x)) : \lambda = \Lambda_V(x), -\frac{\pi}{2} < x < \frac{3\pi}{2}\}$ branch of equilibria

We need to calculate the eigenvalues of the Jacobian matrix (3.3.6) evaluated at the equilibrium point $(\bar{x}, \Lambda_V(\bar{x}))$. Substituting $\Lambda_V(\bar{x})$ for λ and (3.3.2) for $\bar{y}$ in the characteristic equation (3.3.7) and simplifying, we get

$$\Delta(p) = p^3 + \alpha p^2 + c_1 p + \alpha c_0, \tag{3.3.11}$$

where

$$c_0 = -\Bigg[\Lambda_V(\bar{x})\cos\bar{x} + \sin\bar{x} - \frac{\sqrt{1+\sin\bar{x}}}{2}\left(\beta\left(\sqrt{1+\sin\bar{x}} - 1\right) + 1\right) + \frac{\beta}{2}\frac{\cos^2\bar{x}}{1+\sin\bar{x}}\Bigg]$$

and

$$c_1 = -\left[\Lambda_V(\bar{x})\cos\bar{x} + \sin\bar{x} - \frac{\sqrt{1+\sin\bar{x}}}{2}(\beta(\sqrt{1+\sin\bar{x}} - 1) + 1)\right]$$

Proposition 5. *The characteristic equation* (3.3.11) *has*

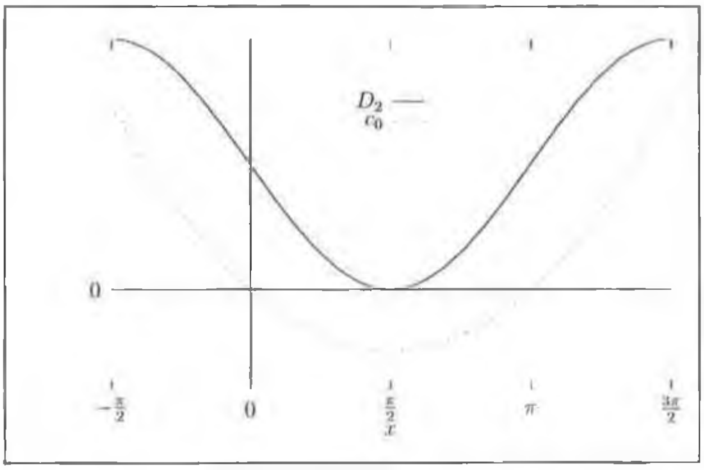

Figure 3.11: Graphs of D_2 and c_0 indicating positive and negative regions.

- *Three roots with negative real parts if* $\bar{x} \in (-\frac{\pi}{2}, 0) \cup (\pi, \frac{3\pi}{2})$;
- *Two roots with negative real parts and a root at the origin if* $\bar{x} = 0$ *or* $\bar{x} = \pi$;
- *Two roots with negative real parts and one positive real root if* $\bar{x} \in (0, \pi)$.

Proof. The Routh-Hurwitz condition is applied to (3.3.11). We need to examine the signs of D_1, D_2 and D_3, where

$$D_1 = \alpha,$$
$$D_2 = \frac{\alpha\beta}{2}\frac{\cos^2\bar{x}}{1+\sin\bar{x}},$$
$$D_3 = \alpha D_2 c_0$$

The plots in Figure 3.11 indicate the sign of D_2 and c_0 where $D_3 = \alpha D_2 c_0$. Clearly, the D_i are strictly positive for $\bar{x} \in (-\frac{\pi}{2}, 0) \cup (\pi, \frac{3\pi}{2})$ implying that all roots of the characteristic equation have negative real parts. For $\bar{x} = 0$ and $\bar{x} = \pi$, D_3 is zero. We calculate the eigenvalues directly to get a root at the origin and two roots with negative real parts. For $\bar{x} \in (0, \pi/2) \cup (\pi/2, \pi)$ the sequence $1, D_1, D_1D_2, \alpha c_0$ has sign sequence $+, +, +, -$, implying that there is one root with positive real part. At $\bar{x} = \pi/2$ we have $D_2 = 0$

and so we need to calculate the root explicitly. We get three real roots, $p_1^* = -\alpha$ and $p_2^* = \pm\sqrt{1 + (\beta(1-\sqrt{2}) - 1)/\sqrt{2}}$. Thus, for $\bar{x} \in (0, \pi/2)$ we have one root with positive real part and two roots with negative real part. $\square$

The $\{(\pi, \lambda) : \lambda \in \mathbf{R}\}$ branch of equilibria

By setting $\bar{x} = \pi$ in (3.3.8) and (3.3.9), the characteristic equation (3.3.7) becomes

$$\Delta(p) = p^3 + \alpha p^2 - (\frac{1}{2} - \lambda)p - \alpha(\frac{G_m}{2} - \lambda) \tag{3.3.12}$$

We state without proof the following proposition. The proof is similar to that of Proposition 4.

Proposition 6. *The characteristic equation* (3.3.12) *will have*

- *Three roots with negative real parts if* $\lambda > -\frac{G_m}{2}$.
- *Two roots with negative real parts and a root at the origin if* $\lambda = -\frac{G_m}{2}$.
- *Two roots with negative real parts and one positive real root if* $\lambda < -\frac{G_m}{2}$.

3.3.3 Stability Analysis of Bifurcation Points

We have determined that the points $(\bar{x}, \lambda) = (0, G_m/2)$ and $(\bar{x}, \lambda) = (\pi, -G_m/2)$ are bifurcation points of the viscoelastic system, occurring at the intersection of 2 branches of equilibria. The stability analysis indicates that at each of these points there is a two-dimensional stable manifold and a one-dimensional centre manifold. We wish to analyse the behaviour of the system at the bifurcation points. The Centre Manifold Theorem (see Appendix A) implies that at a bifurcation point the system can be written locally in co-ordinates on the (stable,unstable and centre) invariant manifolds $W^s \times W^u \times W^c$. The motion on W^s is towards the fixed point and the motion on W^u is away from the fixed point. So the local behaviour can be understood by looking at the motion on the centre manifold. In this section we determine the centre manifold at the equilibrium point $(\bar{x}, \lambda) = (0, G_m/2)$. A similar analysis is used to calculate the centre manifold at second bifurcation point $(\bar{x}, \lambda) = (\pi, -G_m/2)$.

The Centre Manifold at $(\bar{x}, \lambda) = (0, G_m/2)$

The parameter $\mu = \lambda - G_m/2$ is introduced so that the bifurcation point is translated to the origin. The equation

$$\dot{\mu} = 0$$

is added to the system. This will allow us to describe the dynamics close to $\mu = 0$. New co-ordinates (u, v, w) are chosen so that the system is in canonical form. The transformed system is

$$\begin{pmatrix} \dot{u} \\ \dot{v} \\ \dot{w} \\ \dot{\mu} \end{pmatrix} = \begin{pmatrix} -\frac{\alpha}{2} & i\sqrt{\frac{\beta}{2} - (\frac{\alpha}{2})^2} & 0 & 0 \\ -i\sqrt{\frac{\beta}{2} - (\frac{\alpha}{2})^2} & -\frac{\alpha}{2} & 0 & 0 \\ 0 & 0 & 0 & 0 \\ 0 & 0 & 0 & 0 \end{pmatrix} \begin{pmatrix} u \\ v \\ w \\ \mu \end{pmatrix} + \begin{pmatrix} f_1(u, v, w, \mu) \\ f_2(u, v, w, \mu) \\ f_3(u, v, w, \mu) \\ 0 \end{pmatrix} \tag{3.3.13}$$

Details of the canonical transformation and the functions f_1, f_2, f_3 and f_4 are given in the appendix. The center manifold can be represented locally as

$$W_c = \{(u, v, w, \mu) | (u, v) = H(w, \mu), H(0,0) = 0, DH(0,0) = 0\} \tag{3.3.14}$$

where $H(w, \mu) = (h_1(w, \mu), h_2(w, \mu))$ and DH is the Jacobian matrix of $H(w, \mu)$. The conditions on $H(w, \mu)$ given in (3.3.14) imply that h_1 and h_2 can be written as

$$h_1 = h_{11}w^2 + h_{12}w\mu + h_{13}\mu^2 + \ldots \tag{3.3.15}$$

and

$$h_2 = h_{21}w^2 + h_{22}w\mu + h_{23}\mu^2 + \dots \tag{3.3.16}$$

where the h_{ij} are constants to be determined. Thus, on the center manifold the flow is approximated by

$$\begin{pmatrix} \dot{w} \\ \dot{\mu} \end{pmatrix} = \begin{pmatrix} f_3(h_1(w,\mu), h_2(w,\mu), w, \mu) \\ 0 \end{pmatrix} \tag{3.3.17}$$

Following Glendinning [10], we calculate the coefficients h_{ij} to be

$$h_{11} = -\frac{2\beta^2 - 3\beta + \alpha^2(\beta^3 - 3\beta + 6)}{4\beta^2}, \tag{3.3.18a}$$

$$h_{21} = -\alpha\frac{4\beta^2 - 9\beta + \alpha^2(\beta^3 - 3\beta + 6)}{8\sqrt{\frac{\beta}{2} - (\frac{\alpha}{2})^2\beta^2}}, \tag{3.3.18b}$$

$$h_{12} = 2\frac{\beta - 2\alpha^2}{\beta^2}, \tag{3.3.18c}$$

$$h_{22} = \frac{\alpha(3\beta - 2\alpha^2)}{\sqrt{\frac{\beta}{2} - (\frac{\alpha}{2})^2\beta^2}}, \tag{3.3.18d}$$

$$h_{13} = h_{23} = 0. \tag{3.3.18e}$$

Substituting the h_{ij} from (3.3.18) into (3.3.15) and (3.3.16) gives

$$u = h_1(w,\mu) = -\frac{2\beta^2 - 3\beta + \alpha^2(\beta^3 - 3\beta + 6)}{4\beta^2}w^2 + 2\frac{\beta - 2\alpha^2}{\beta^2}w\mu + \dots,$$
$$v = h_2(w,\mu) = \frac{\alpha(3\beta - 2\alpha^2)}{\sqrt{\frac{\beta}{2} - (\frac{\alpha}{2})^2\beta^2}}w^2 - \alpha\frac{4\beta^2 - 9\beta + \alpha^2(\beta^3 - 3\beta + 6)}{8\sqrt{\frac{\beta}{2} - (\frac{\alpha}{2})^2\beta^2}}w\mu + \dots$$

A local approximation to the flow on the centre manifold is found by substituting (3.3.15), (3.3.16) and (3.3.18) into

$$\dot{w} = f_3(h_1(w,\mu), h_2(w,\mu), w, \mu) = C(w,\mu),$$

to get

$$\dot{w} = \frac{\alpha}{4}(1 + \frac{2}{\beta}(\frac{3}{2} - \beta))w^2 + \frac{2\alpha}{\beta}w\mu + \dots \tag{3.3.19}$$

Now, $\alpha > 0$ and $0 < \beta < 1$ so the coefficients of w^2 and $w\mu$ in (3.3.19) are positive. Hence, on the center manifold $\dot{w} = C(w, \mu)$ we have

$$C(0,0) = C_w(0,0) = C_\mu(0,0) = C_{\mu\mu} = 0,$$

$$C_{ww} = \frac{\alpha}{2}(1 + \frac{2}{\beta}(\frac{3}{2} - \beta)) > 0, \; C_{w\mu} = \frac{2\alpha}{\beta} > 0,$$

and thus $C(w, \mu)$ satisfies the conditions for a transcritical bifurcation at $(w, \mu) = (0, 0)$ (see [10]). Setting $\mu = 0$, we get the equation of motion on the centre manifold,

$$\dot{w} = \frac{\alpha}{4}(1 + \frac{2}{\beta}(\frac{3}{2} - \beta))w^2 + \ldots \tag{3.3.20}$$

where $\frac{\alpha}{4}(1 + \frac{2}{\beta}(\frac{3}{2} - \beta)) > 0$. From (3.3.20) we see that the origin is stable if approached from $w < 0$ (i.e. motion is towards the origin), and unstable if approached from $w > 0$. Thus, the bifurcation point at $(\bar{x}, \lambda) = (0, G_m/2)$ is unstable. The calculations for the centre manifold at the bifurcation point $(\bar{x}, \lambda) = (\pi, -G_m/2)$ proceed in the same fashion and we establish that at this point we also have a transcritical bifurcation and that this bifurcation point is unstable.

3.4 The Imperfect Link Model

In this section we discuss the Link model with an initial imperfection. We are interested in the elastic and viscoelastic equilibrium curves and their stability properties. A similar imperfect elastic model is discussed informally in Hunt and Thompson [18]. Hayman [14, 15] discusses the imperfect viscoelastic equilibria in his quasi-static analysis of the model. However, the formal analysis there is incomplete. The results of the equilibrium analysis in this section are used in the quasi-static analysis of the system in Chapter 4.

3.4.1 The Imperfect Elastic System

Recall that the imperfect model equations are formulated on the assumption that the Link model contains an initial imperfection ν, where ν is the angle that the rod OA makes with the vertical while in the unloaded position (see Figure 2.7). The equation for the imperfect elastic system is

$$\ddot{x} = \lambda \sin x - \cos x \frac{\sqrt{1+\sin x} - \sqrt{1+\sin \nu}}{\sqrt{1+\sin x}}. \tag{3.4.1}$$

We assume that the initial imperfection satisfies $\nu > 0$. The perfect system, (3.2.2), is recovered by taking the limit as $\nu \to 0$ in (3.4.1)

Equilibrium Analysis

The equilibrium points $(\bar{x}, \lambda)$ of (3.4.1) satisfy

$$0 = F(\bar{x}, \lambda) := \lambda \sin \bar{x} - \cos \bar{x} \frac{\sqrt{1+\sin \bar{x}} - \sqrt{1+\sin \nu}}{\sqrt{1+\sin \bar{x}}}. \tag{3.4.2}$$

We can solve (3.4.2) to get an expression for λ in terms of $\bar{x}$,

$$\lambda = \Lambda_E^{\nu}(\bar{x}) := \frac{\sqrt{1+\sin \bar{x}} - \sqrt{1+\sin \nu}}{\tan \bar{x}\sqrt{1+\sin \bar{x}}} \tag{3.4.3}$$

The equilibria $(\bar{x}, \Lambda_E^{\nu}(\bar{x}))$ lie on a curve in phase space. Two typical equilibrium curves are shown in Figure 3.12. The equilibrium curve $(\bar{x}, \Lambda_E(\bar{x}))$ for the perfect elastic case is also shown for comparison. For a given imperfection ν, the equilibrium curve intersects the x-axis at ν, increases to a maximum and then decreases, cutting the x-axis at $\pi/2$. We have the following,

Theorem 1. *For $0 < \nu < \pi/2$, the function $\Lambda_E^{\nu} : (0, \pi/2) \to \mathbf{R}$ defined in (3.4.3) satisfies $\Lambda_E^{\nu}(x) > 0$ for $\nu < x < \pi/2$, and has a single maximum point at $x_c \in (\nu, \pi/2)$. The equilibria $(\bar{x}, \Lambda_E^{\nu}(\bar{x}))$ are stable if $0 < \bar{x} < x_c$ and unstable if $x_c < \bar{x} < \pi/2$.*

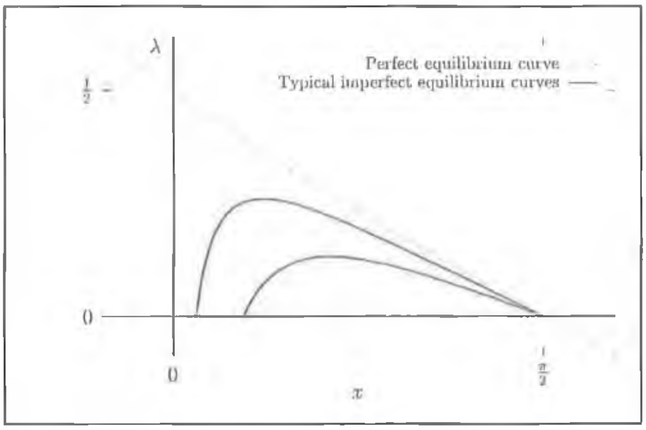

Figure 3.12: Two typical imperfect elastic equilibrium curves are plotted with the perfect elastic equilibrium curve, $(\bar{x}, \Lambda_E(\bar{x}))$, shown for comparison.

Proof. The stability of the equilibrium points is determined by examining the sign of $F_x(\bar{x}, \Lambda_E^{\nu}(\bar{x}))$.[2] The stability changes if $F_x = 0$ and $F_{\lambda x} \neq 0$. We have $F_x(\bar{x}, \Lambda_E^{\nu}(\bar{x})) = -F_\lambda(\bar{x}, \Lambda_E^{\nu}(\bar{x}))\, d\Lambda_E^{\nu}(\bar{x})/dx = \sin x\, d\Lambda_E^{\nu}(\bar{x})/dx$ and $F_{\lambda x} = \cos x \neq 0$ for $\nu < x < \pi/2$. Therefore a change in stability will occur at (x^*, λ^*) satisfying $d\Lambda_E^{\nu}(x^*))/dx = 0$, with $\lambda^* = \Lambda_E^{\nu}(x^*)$. This is the maximum point of the equilibrium curve $\lambda = \Lambda_E^{\nu}(x)$. To determine stability it is sufficient to check the sign of $F_x(\bar{x}, \Lambda_E^{\nu}(\bar{x}))$ at $\bar{x} = \nu$ and $\bar{x} = \pi/2$. We have $F_x(\nu, \Lambda_E^{\nu}(\nu)) < 0$ implying stable centre points for $\nu \leq \bar{x} < x_c$ and $F_x(\pi/2, \Lambda_E^{\nu}(\pi/2)) > 0$ implying unstable saddle points for $x_c \leq \bar{x} < \pi/2$. □

The stability of the imperfect equilibrium curve is shown in Figure 3.13. We define the critical point locus to be the locus of critical points of the equilibrium curves defined for $0 \leq \nu \leq \pi/2$. Rearranging (3.4.3) and differentiating gives us the following implicit equation for the critical point locus,

$$\frac{\partial}{\partial x}\left[(\lambda \tan x - 1)\sqrt{1 + \sin x}\right] = 0. \qquad (3.4.4)$$

Both (3.4.4) and (3.4.2) are referred to in the quasi-static analysis of Chapter 4. In Figure

[2] The subscript denotes partial differentiation with respect to that variable. Thus $F_x = \partial F/\partial x$, etc.

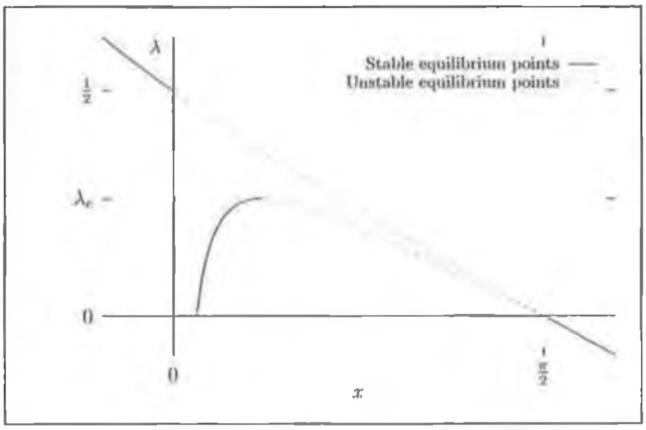

Figure 3.13: Stability of the imperfect equilibrium curve. Stable(unstable) points are indicated by solid(dashed) curves. The imperfect elastic critical load is indicated by λ_c. The perfect case curve is again included for comparison.

3.14 we plot both the equilibrium curves and the critical point locus. The critical point locus (dashed line) and the perfect case equilibrium curve are included. We see that the critical point locus is a decreasing function. This indicates that as the imperfection increases, we have a reduction in the critical load required to cause buckling of the structure.

3.4.2 The Imperfect Viscoelastic System

The equilibrium curves for the imperfect viscoelastic system were studied by Hayman [14, 15] in his quasi-static analysis of the link model. The imperfect elastic equations are supplemented with the creep equation to give

$$\ddot{x} = \lambda(t)\sin x - \cos x\frac{\sqrt{1+\sin x}-\sqrt{1+\sin\nu}}{\sqrt{1+\sin x}} - \frac{\cos x}{\sqrt{1+\sin x}}y, \tag{3.4.5a}$$

$$\dot{y} = -\alpha\{y + \beta(\sqrt{1+\sin x}-\sqrt{1+\sin\nu})\}. \tag{3.4.5b}$$

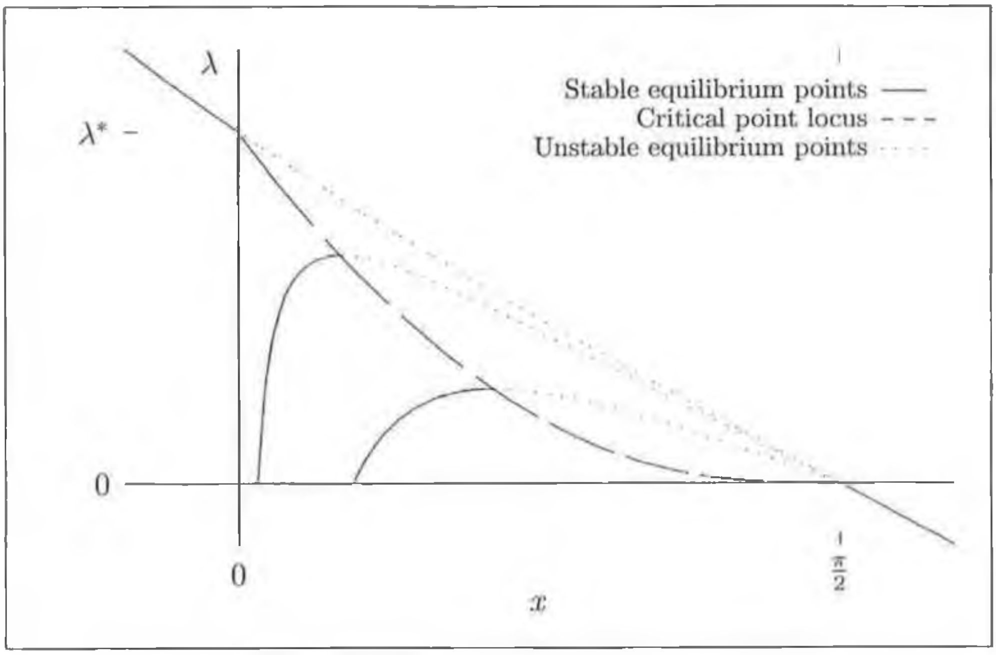

Figure 3.14: The imperfect equilibrium curves and the critical point locus (dashed line) for the elastic and viscoelastic systems. The perfect case equilibrium curve is included for comparison. The perfect critical load is denoted by λ^*. In the elastic case we have $\lambda^* = 1/2$ while in the viscoelastic case we have $\lambda^* = G_m/2$.

The equilibrium points for the imperfect viscoelastic system are in the form $\bar{\mathbf{x}} = (\bar{x}, \bar{y}, \lambda)$. Using (3.4.5b), we can express $\bar{y}$ in terms of $\bar{x}$ to get

$$\bar{y}(\bar{x}) = -\beta\left[\sqrt{1+\sin\bar{x}} - \sqrt{1+\sin\nu}\right]. \tag{3.4.6}$$

As is the case for the perfect system, we can specify an equilibrium point by $(\bar{x}, \lambda)$. Substituting (3.4.6) into (3.4.5) we get the following relationship which must be satisfied by the equilibrium points,

$$\lambda\sin\bar{x} - G_m\cos\bar{x}\frac{\sqrt{1+\sin\bar{x}} - \sqrt{1+\sin\nu}}{\sqrt{1+\sin\bar{x}}} = 0. \tag{3.4.7}$$

Solving for λ we get

$$\Lambda_V^\nu(x) = G_m\frac{\sqrt{1+\sin x} - \sqrt{1+\sin\nu}}{\tan x\sqrt{1+\sin x}}. \tag{3.4.8}$$

These equilibrium curves differ from the imperfect elastic equilibrium curves (3.4.3) by the constant factor G_m. This is similar to the effect that the introduction of the viscoelastic element has on the perfect elastic system. The curves are plotted in Figure 3.14. As in the elastic case, we can define a critical point locus. Rearranging 3.4.8 and imposing the condition that $d\Lambda_V^\nu/dx = 0$, we get the following implicit equation in λ and x,

$$\frac{\partial}{\partial x}\left[(\lambda\tan x - G_m)\sqrt{1+\sin x} + G_m\sqrt{1+\sin\nu}\right] = 0. \tag{3.4.9}$$

Equations (3.4.7) for the equilibrium curve and (3.4.9) for the critical point locus are used in the quasi-static analysis in Chapter 4. Using the Routh-Hurwitz criterion we can determine the stability of the equilibrium points $(\bar{x}, \Lambda_V^\nu(\bar{x}))$. We need to calculate the eigenvalues of the Jacobian matrix evaluated on the imperfect equilibrium curve. The Jacobian differs from (3.3.6) in the term $Df_{21}(\bar{\mathbf{x}})$, which becomes $\lambda\cos\bar{x} + \sin\bar{x} + \sqrt{1+\sin\bar{x}}(\bar{y}(\bar{x}) - \sqrt{1+\sin\nu})/2$, with $\bar{y}(\bar{x})$ given by (3.4.6). Thus, the characteristic equation is

$$\Delta(p) = p^3 + \alpha p^2 + c_1 p + \alpha c_0, \tag{3.4.10}$$

where

$$c_0 = -\left[\Lambda_V^{\nu}(\bar{x})\cos\bar{x} + \sin\bar{x} - \frac{\sqrt{1+\sin\bar{x}}}{2}\left(\beta\left(\sqrt{1+\sin\bar{x}} - \sqrt{1+\sin\nu}\right) + \sqrt{1+\sin\nu}\right)\right.$$
$$\left. + \frac{\beta}{2}\frac{\cos^2\bar{x}}{1+\sin\bar{x}}\right]$$

and

$$c_1 = -\left[\Lambda_V^{\nu}(\bar{x})\cos\bar{x} + \sin\bar{x} - \frac{\sqrt{1+\sin\bar{x}}}{2}\left(\beta\left(\sqrt{1+\sin\bar{x}} - \sqrt{1+\sin\nu}\right) + \sqrt{1+\sin\nu}\right)\right]$$

Note that for $\bar{x} \in (0, \pi/2)$ we have $c_1 > c_0$. The stability properties of the imperfect viscoelastic equilibrium points are given in Theorem 2. In Figure 3.15 we plot c_0 and $d\Lambda_V^{\nu}/dx$ for a typical value of $\nu \in (0, \pi/2)$.

Theorem 2. *Let (x_c, λ_c) be the maximum point on the equilibrium curve $\Lambda_V^{\nu}(x)$. The stability of the equilibrium curve changes at (x_c, λ_c). The equilibrium points $(\bar{x}, \lambda)$ on the curve satisfying $\nu \leq \bar{x} < x_c$ are stable centre points and the equilibrium points $(\bar{x}, \lambda)$ on the curve satisfying $x_c < \bar{x} < \pi/2$ are unstable saddle points. Again, as the imperfection tends to zero we recover the perfect system equilibrium curves.*

Proof. We apply the Routh-Hurwitz criterion to (3.4.10), where D_1, D_2 and D_3 are given by

$$D_1 = \alpha,$$
$$D_2 = \frac{\alpha\beta}{2}\frac{\cos^2\bar{x}}{1+\sin\bar{x}},$$
$$D_3 = \alpha D_2 c_0.$$

From Figure 3.15 we see that both $d\Lambda_V^{\nu}/dx$ and c_0 cross the axis at $\bar{x} = x_c$. For $\nu \leq \bar{x} < x_c$ we have $c_0 > 0$ and for $x_c < \bar{x} < \pi/2$ we have $c_0 < 0$. Also, D_2 has the same value as in the perfect viscoelastic case and is plotted in Fig 3.11. Using this information we can

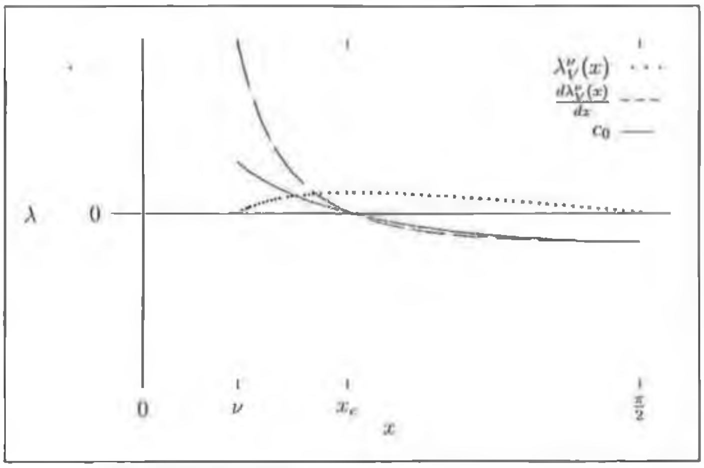

Figure 3.15: Graphs of $d\Lambda_V^\nu/dx$ and c_0 indicating positive and negative regions.

determine the regions in which the D_i are positive, negative or zero. We have $D_i > 0$ for $\bar{x} \in [\nu, x_c)$ implying that all roots of the characteristic equation have negative real parts. For $\bar{x} \in (x_c, \pi/2)$, the sequence $1, D_1, D_1 D_2, \alpha c_0$ has sign sequence $+, +, +, -$, implying that there is one root with positive real part. At $\bar{x} = x_c$ we need to calculate the roots of the characteristic equation exactly. Noting that $c_0 = 0$ and $c_1 > c_0$, we calculate the roots to get a root at the origin and two roots with negative real parts. □

The stability analysis indicates that for equilibrium points satisfying $\bar{x} \in [\nu, x_c)$ there is a three-dimensional stable manifold. At $\bar{x} = x_c$ there is a two-dimensional stable manifold and a one-dimensional centre manifold while for equilibrium points satisfying $\bar{x} \in [x_c, \pi/2)$ there is a two-dimensional stable manifold and a one-dimensional unstable manifold. This is comparable with the perfect case.

Chapter 4

The Link Model:A Quasi-Static Analysis

4.1 Introduction

In this chapter we look at the quasi-static approximation to the non-linear system. We include an imperfection in the system equations. Hayman [14, 15] uses the quasi-static approach in his investigation of the creep buckling behaviour of the Link model. His work is concerned with the phenomenon of creep buckling and he investigates the link between a structures creep buckling behaviour at constant load and its instantaneous buckling and post-buckling behaviour under varying load. Hayman's analysis is limited to Maxwell materials, as well as assuming that the initial creep stress, $y(0)$, is zero. We extend Hayman's work by including a non-trivial initial condition, $y(0) \neq 0$. Under these conditions there is some residual stress in the spring initially. This is another source of imperfection. We discuss the consequences of this. We also investigate the stability of the equilibrium curves in the quasi-static case. The results from this stability analysis differ from the results indicated by the dynamic analysis. In particular, the quasi-static analysis predicts stability at points where the dynamic analysis indicates that the system is unstable. The analysis is valid for both the imperfect system and the perfect system. The results are discussed and illustrated with a series of diagrams in Section 4.4. The quasi-static method is discussed in detail in Hopenstadt [17] while O'Malley [25] provides an excellent introduction to the theory of singular perturbation methods.

4.2 The Quasi-Static Equations

The quasi-static method neglects the dynamic effects due to the structure's inertia but includes the time dependence of displacements due to creep. First we specify circumstances under which this approximation would be valid. The dynamic system of equations (2.3.8) can be written as

$$\ddot{x} = f(x, y, \lambda, \nu), \tag{4.2.1a}$$

$$\dot{y} = -\alpha g(x, y, \nu), \tag{4.2.1b}$$

where

$$f(x, y, \lambda, \nu) = \lambda \sin x - \cos x \frac{\sqrt{1+\sin x} - \sqrt{1+\sin \nu}}{\sqrt{1+\sin x}} - y \frac{\cos x}{\sqrt{1+\sin x}} \tag{4.2.2}$$

and

$$g(x, y, \nu) = y + \beta(\sqrt{1+\sin x} - \sqrt{1+\sin \nu}). \tag{4.2.3}$$

Initial conditions for $x(0)$, $\dot{x}(0)$ and $y(0)$ are given. Now, if we rescale the time t by setting $\tau = \alpha t$, we can rewrite (4.2.1) as

$$\alpha^2 x'' = f(x, y, \lambda, \nu), \tag{4.2.4a}$$

$$y' = g(x, y, \nu), \tag{4.2.4b}$$

where $'$ denotes $d/d\tau$. The transformed system (4.2.4) is a singular perturbation problem. We have a small parameter multiplying the leading order derivative term. We expect a singular solution at $\alpha = 0$ due to the loss of the two initial conditions, $x(0)$ and $\dot{x}(0)$. By letting $\alpha \to 0$ in (4.2.4) we obtain a system of equations which is formally equivalent to the quasi-static problem,

$$0 = f(x, y, \lambda, \nu), \tag{4.2.5a}$$

$$y' = g(x, y, \nu). \tag{4.2.5b}$$

In the context of singularly perturbed systems, (4.2.5) is called the outer problem, and its solution is the outer solution. These equations are supplemented by an initial condition $y(0) = \gamma$, but $x(0), x'(0)$ are not specified. It is possible to derive an initial-value problem for $x(\tau)$ and it is more illustrative to describe the dynamics of the quasi-static problem in terms of the solution to this initial-value problem. We can solve (4.2.5a) for y in terms of x and λ to get

$$y = Y(x, \lambda, \nu), \tag{4.2.6}$$

where

$$Y(x, \lambda, \nu) := (\lambda \tan x - 1)\sqrt{1 + \sin x} + \sqrt{1 + \sin \nu}. \tag{4.2.7}$$

Differentiating (4.2.5a) and substituting for y from (4.2.6) we get an expression for $x'(\tau)$ given by

$$\frac{dx}{d\tau} = Q(x, \lambda, \nu), \tag{4.2.8}$$

where

$$\begin{aligned} Q(x, \lambda, \nu) &= \frac{-f_y\left(x, Y(x, \lambda, \nu), \lambda, \nu\right)\, g\left(x, Y(x, \lambda, \nu), \lambda, \nu\right)}{f_x\left(x, Y(x, \lambda, \nu), \lambda, \nu\right)}, \\ &= \frac{(\lambda \tan x - G_m)\sqrt{1 + \sin x} + G_m\sqrt{1 + \sin \nu}}{\frac{\partial}{\partial x}\left[(\lambda \tan x - 1)\sqrt{1 + \sin x}\right]}. \end{aligned} \tag{4.2.9}$$

This differential equation in $x(\tau)$ is supplemented with an initial condition $x(0) = \zeta$ where ζ satisfies

$$\gamma = Y(\zeta, \lambda, \nu). \tag{4.2.10}$$

Recall from (3.4.3) that the equilibrium curves of the imperfect viscoelastic system satisfy $Y(x, \lambda, \hat{\nu}) = 0$, for some initial imperfection $\nu = \hat{\nu}$. Also, setting the denominator of Q in (4.2.9) to be equal to zero results in the locus of critical points for the elastic system, given by (3.4.4). Knowledge of these curves will be helpful in determining the stability of equilibrium points of the quasi-static system.

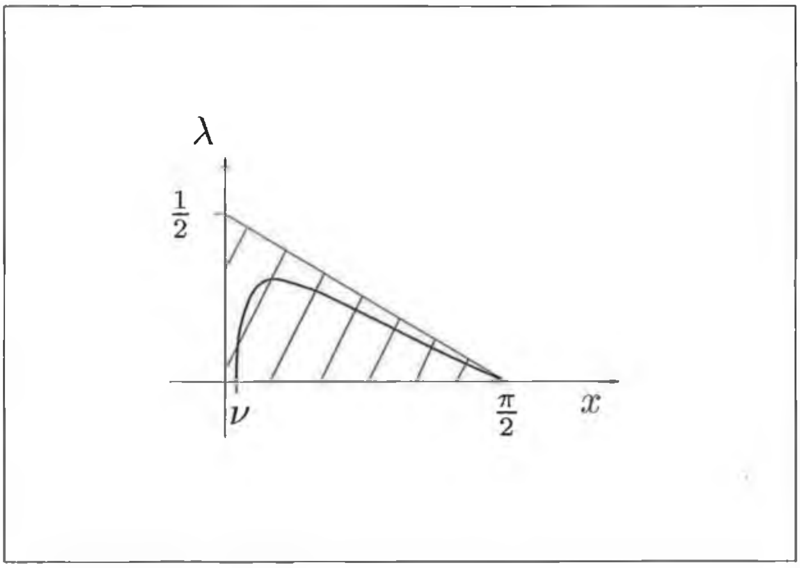

Figure 4.1: Possible initial positions for the quasi-static system. When $y(0) = 0$, the initial position is restricted to the curve beginning at $(\nu, 0)$. Otherwise, the initial position may be anywhere in the shaded region, which is bounded by $x = 0, \lambda = 0$ and $\Lambda_E(x)$.

The Locus of Initial Conditions

The initial condition $x(0) = \zeta$ for the quasi-static system with imperfection ν satisfies

$$\gamma = (\lambda \tan \zeta - 1)\sqrt{1 + \sin \zeta} + \sqrt{1 + \sin \nu}. \tag{4.2.11}$$

This represents a locus of initial conditions in the $x\lambda$-plane. Rearranging (4.2.11) and letting $\sqrt{1 + \sin \hat{\nu}} = \sqrt{1 + \sin \nu} - \gamma$ we get

$$(\lambda \tan \zeta - 1)\sqrt{1 + \sin \zeta} + \sqrt{1 + \sin \hat{\nu}} = 0. \tag{4.2.12}$$

This is equivalent to (3.4.2), the equation for an elastic imperfect equilibrium curve with imperfection $\hat{\nu}$. Thus, for any initial condition $x(0) = \zeta$ of the quasi-static system, the point (ζ, λ), satisfying (4.2.12), lies on an equilibrium curve of the imperfect elastic system. By imposing the restriction that $\gamma = 0$, as in [14, 15], (ζ, λ) is limited to that elastic equilibrium curve with imperfection $\hat{\nu} = \nu$. Non-trivial values of γ allow the initial position (ζ, λ) to lie on any elastic equilibrium curve with imperfection $\hat{\nu}$ satisfying

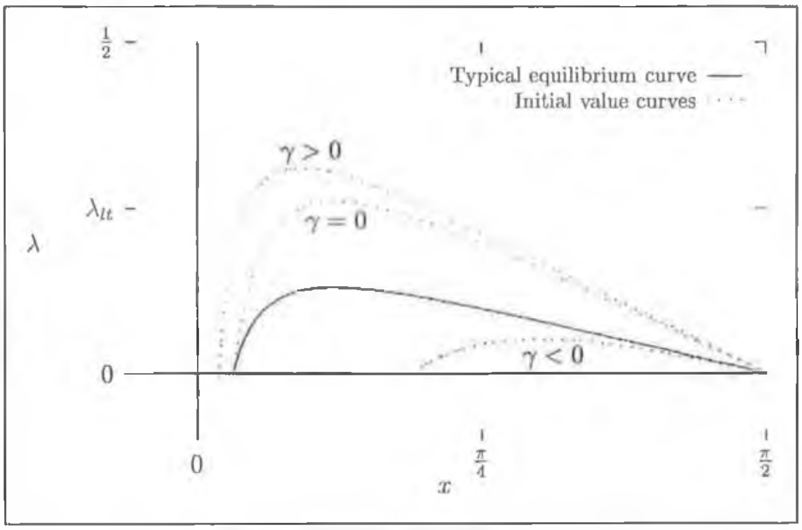

Figure 4.2: Initial value curves for $\gamma < 0, \gamma = 0, \gamma > 0$. Hayman's work is limited to initial conditions on the $\gamma = 0$ curve. The long term critical load $\lambda_{lt} = G_m/2$ is indicated.

$0 < \hat{\nu} < \pi/2$. By allowing non-trivial values for γ, the quasi-static motion can proceed from a variety of initial positions relative to the equilibrium curve. This results in a more complete description of the quasi-static behaviour, and highlights the differences between the quasi-static and the dynamic behaviour of the system. In Figure 4.1 we compare the possible initial positions of the quasi-static system for trivial and non-trivial values of γ. In Fig 4.2 we plot several loci of initial conditions for variable γ with ν fixed. The quasi-static equilibrium curve for fixed ν, which is discussed in the next section, is included for comparison.

4.3 The Quasi-Static Equilibria

The equilibria $(\bar{x}, \lambda)$ for the quasi-static system with imperfection ν satisfy $0 = Q(x, \lambda, \nu)$. From (4.2.8), we have

$$\lambda \tan \bar{x} \sqrt{1 + \sin \bar{x}} - G_m \sqrt{1 + \sin \bar{x}} + G_m \sqrt{1 + \sin \nu} = 0 \tag{4.3.1}$$

Expressing λ in terms of $\bar{x}$ we get

$$\lambda = \Lambda_Q^{\nu}(\bar{x}) := \frac{G_m\sqrt{1+\sin\bar{x}} - G_m\sqrt{1+\sin\nu}}{\tan\bar{x}\sqrt{1+\sin\bar{x}}}. \tag{4.3.2}$$

This is equivalent to (3.4.7), the equation for the long term equilibrium curves of the imperfect viscoelastic system. Again referring to Figure 4.2, we see a typical equilibrium curve for the quasi-static system with associated initial condition curves. We have shown that the equilibrium curves for the quasi-static system are equivalent to those of the dynamic system. We have also established that the initial position of the quasi-static system lies on some curve that is equivalent to an elastic equilibrium curve. We now determine the stability properties of the equilibrium points.

4.3.1 Stability of the Equilibria

The stability of the equilibrium curves can be determined by examining the sign of $Q_x(\bar{x}, \Lambda_Q^{\nu}(\bar{x}), \nu)$. Equilibria satisfying $Q_x(\bar{x}, \Lambda_Q^{\nu}(\bar{x}), \nu) < 0$ are stable while equilibria satisfying $Q_x(\bar{x}, \Lambda_Q^{\nu}(\bar{x}), \nu) > 0$ are unstable. We have the following stability theorem for the quasi-static equilibrium curves.

Theorem 3. *Let (x_c, λ_c) be the maximum point of the equilibrium curve on the $x\lambda$-plane defined by $\lambda = \Lambda_Q^{\nu}(\bar{x})$. Let (x_I, λ_I) be the intersection point of the equilibrium curve $\lambda = \Lambda_Q^{\nu}(\bar{x})$ and the locus of critical points for the imperfect elastic system, defined by*

$$0 = \frac{\partial}{\partial x}\left[(\lambda\tan x - 1)\sqrt{1+\sin x}\right]. \tag{4.3.3}$$

Then, the equilibrium points $(\bar{x}, \Lambda_Q^{\nu}(\bar{x}))$ satisfying $\bar{x} \in [\nu, x_c) \cup (x_I, \pi/2]$ are stable and the equilibrium points satisfying $\bar{x} \in (x_c, x_I)$ are unstable.

Proof. We begin the proof by determining the critical points, if any, of the equilibrium curve. Recall that the equilibrium curve has a critical point (x_c, λ_c) if $Q_x(x_c, \lambda_c, \nu) = 0$ and the stability of the equilibrium curve will change at the critical point if $Q_{\lambda x}(x_c, \lambda_c, \nu) \neq 0$. Differentiating $Q(x, \lambda, \nu)$ w.r.t x, evaluating it on the equilibrium curve and simplifying gives

$$Q_x = \frac{\frac{\partial}{\partial x}\left((\lambda \tan x - G_m)\sqrt{1+\sin x}\right)}{\frac{\partial}{\partial x}\left((\lambda \tan x - 1)\sqrt{1+\sin x}\right)} \tag{4.3.4}$$

Setting the numerator equal to zero gives the critical point locus for the dynamic viscoelastic system. Similarly, setting the denominator equal to zero gives the critical point locus for the dynamic elastic system. As these do not intersect, we cannot have the case $Q_x = 0/0$. Therefore, the critical points satisfy

$$\frac{\partial}{\partial x}((\lambda \tan x - G_m)\sqrt{1+\sin x}) = 0$$

This is simply the maximum point (x_c, λ_c) of the equilibrium curve (4.3.2).

Next, we show that the stability of equilibrium points changes at (x_c, λ_c). Differentiating Q_x with respect to λ gives

$$Q_{\lambda x} = \frac{2 + \sin x\,(2 + \cos^2 x)}{2\lambda(1 + \sin x) + (\lambda \tan x - 1)\cos^3 x}. \tag{4.3.5}$$

Now $0 < \lambda_c < G_m/2$ and $\nu < x_c < \pi/2$ and so, at the maximum point (x_c, λ_c), we have $Q_{x\lambda} \neq 0$. This implies that there is a change in stability at the maximum. By examining the stability at $(\bar{x}, \lambda) = (\nu, 0)$ we can determine the stability for equilibrium points to the left of the critical point. We have $Q_x(\nu, 0) < 0$ implying stability and thus, there is a change in stability from stable to unstable equilibrium points as we cross the maximum point.

Next, we show that there is another change in stability at the point (x_I, λ_I), the intersection point of the elastic critical locus with the quasi-static equilibrium curve. Recall that the denominator in (4.3.4) is zero on the elastic critical locus. If this locus intersects the equilibrium curve then we have $Q_x(x_I, \lambda_I) = \pm\infty$. Also, if an intersection occurs then the intersection point is always to the right of the maximum point of the equilibrium curve. A change in stability may occur as we pass through an intersection point. Indeed, we have $Q_x(\pi/2, 0) < 0$ implying that the equilibrium point $(\bar{x}, \lambda) = (\pi/2, 0)$ is stable. We conclude that the elastic critical locus must have intersected the equilibrium curve, causing a change in stability from unstable equilibrium points to stable equilibrium points. Thus, the equilibrium points (x, λ) satisfying $\bar{x} \in (x_I, \pi/2]$ are stable and the equilibrium points satisfying $\bar{x} \in [x_c, x_I)$ are unstable. □

Equilibrium curves for the quasi-static system in the case $\nu = 0$ and $\nu > 0$ are shown in Figure 4.3. The diagram clearly indicates the stable region that exists for x close to $\pi/2$. This stable region is unique to the quasi-static system.

4.4 Results of the Quasi-Static Analysis

In this section we illustrate the main features of the quasi-static system using a series of diagrams and we discuss the results of the quasi-static analysis. Using Figure 4.2 and Figure 4.3 we can predict the motion of the system for various initial conditions. The motion of $x(\tau)$ for a fixed ν is illustrated in Figure 4.4. We see that the upper right quadrant of the $x\lambda$-plane is divided into four distinct regions. In Figure 4.5, Figure 4.6 and Figure 4.7 we concentrate more closely on the behaviour in each of these regions.

The initial position of the quasi-static system is given in Figure 4.2 for various values of γ. We can compare the initial position with a typical equilibrium curve. We see that it is possible for the initial value to be in any of the regions marked by + or − in Figure 4.4. The critical load λ_c is indicated. It corresponds to the maximum value of *lambda* on the equilibrium curve. For values of load satisfying $\lambda > \lambda_c$, the system is unstable. In the case $\lambda < \lambda_c$, the system may be stable, with motion tending to the stable part of

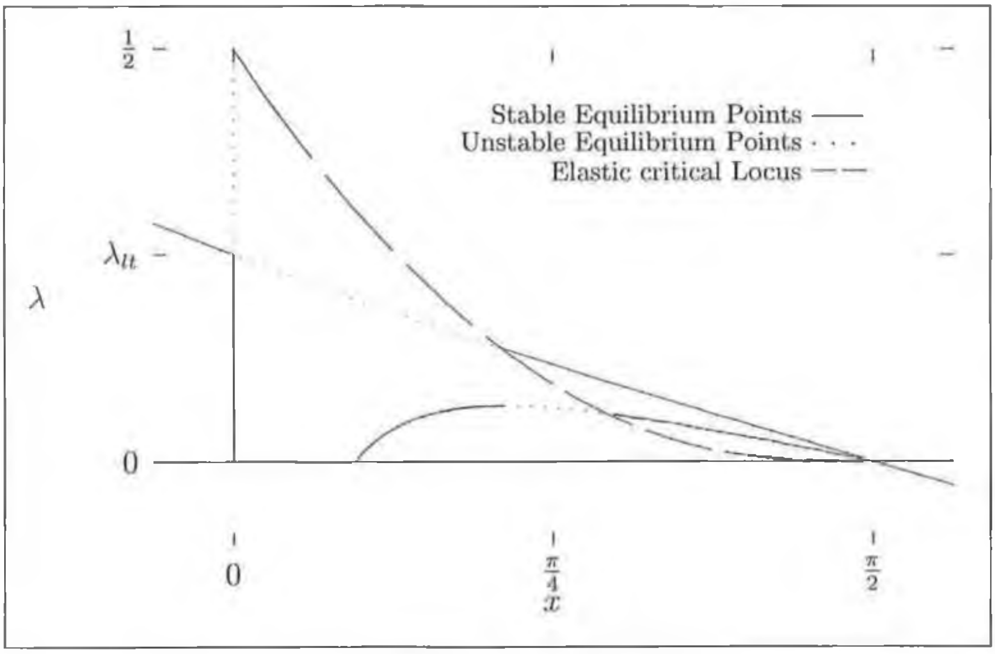

Figure 4.3: Stability of the quasi-static equilibrium curves. The stability of equilibrium points is indicated by solid (stable) and dotted (unstable) lines. Equilibrium curves for the case $\nu = 0$ and $\nu > 0$ are included. The long term critical load is indicated by λ_{lt}. We see a change in the stability at the maximum point of the equilibrium curve representing $\nu > 0$ and also at the intersection of this equilibrium curve with the elastic critical point locus (dashed line). The perfect equilibrium curve changes stability on intersecting the λ-axis and again on intersecting the elastic critical point locus. The stable region close to $x = \pi/2$ is peculiar to the quasi-static analysis.

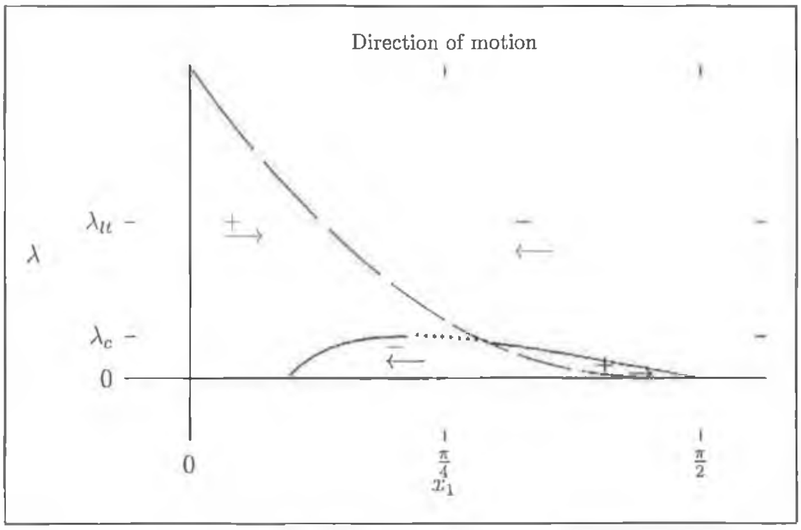

Figure 4.4: Direction of motion of the quasi-static system. The regions marked with + and $\rightarrow$ indicate that x is increasing. Those marked with − and $\leftarrow$ indicate that x is decreasing. A typical equilibrium curve is shown. The elastic critical locus is also included.

the equilibrium curve, or unstable. In Figure 4.5 we illustrate the motion of the system for $\lambda > \lambda_c$. We take two initial values, marked A and A'. Beginning at A, $x(\tau)$ increases until it encounters the elastic locus of critical points. From (4.2.9) we know that at the locus of critical points, $x'(\tau)$ has an infinite displacement rate. Similarly, starting at A', $x(t)$ decreases with the displacement rate tending to minus infinity as $x(\tau)$ tends towards the critical point locus. In Figure 4.6 and Figure 4.7 we demonstrate stable motion of the quasi-static system. In Figure 4.6 the system tends to an equilibrium point $\bar{x}$ satisfying $\nu < \bar{x} < x_c$. This behaviour is also typical of the dynamic viscoelastic system. In Figure 4.7 we see that for certain initial conditions, the system tends towards a stable equilibrium point $\bar{x}$ satisfying $x_I < \bar{x} < \pi/2$. This behaviour is unique to the quasi-static system. From a physical viewpoint, in terms of the Link model in Figure 2.7, this indicates that when the rod is close to a horizontal position, with θ near $\pi/2$, the system can achieve stability in a quasi-static sense. However, the dynamic analysis predicts that the system will tend

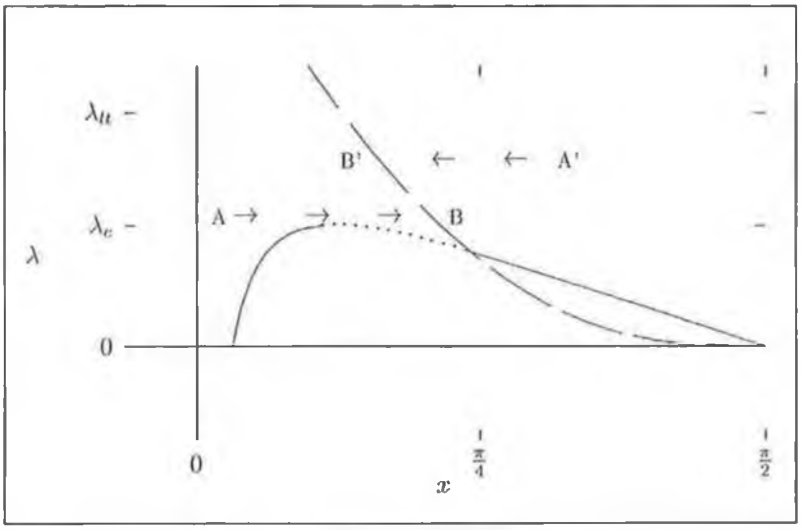

Figure 4.5: Unstable motion for $\lambda > \lambda_c$. As the motion approaches the elastic critical locus (dashed line), an infinite displacement rate is encountered. The long-term critical load, $G/2$, is indicated by λ_{lt}. The equilibrium curve is indicated by the solid (stable) and dotted (unstable) curve with critical load $\lambda = \lambda_c$.

towards the equilibrium at $\bar{x} = \pi$. Finally, is is possible for the system to become unstable for certain initial values (ζ, λ) satisfying $\lambda < \lambda_c$. This occurs when the initial position lies between the unstable part of the equilibrium curve and the elastic locus of critical points. This area is indicated in Figure 4.6 with a single rightarrow. In this case, $x(\tau)$ increases until an infinite displacement rate is encountered at the locus of critical points. Thus, the system is unstable. Again, this motion differs from that indicated by the dynamic analysis, where motion would again tend towards the stable equilibrium point at $\bar{x} = \pi$.

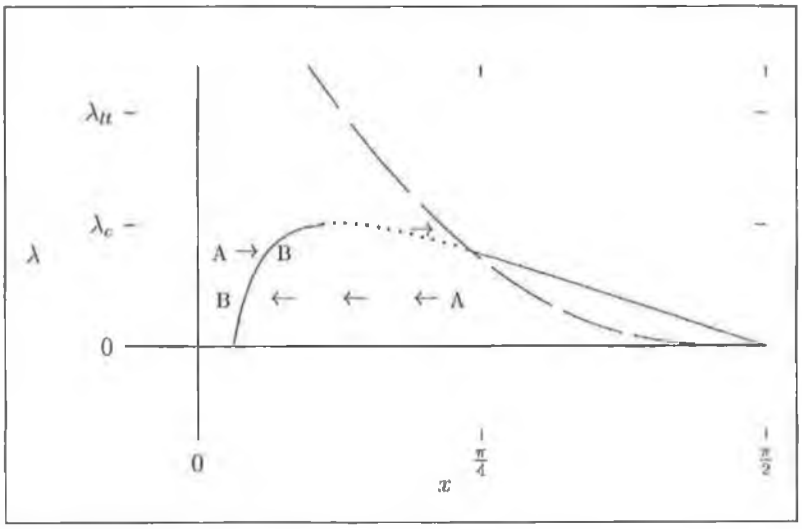

Figure 4.6: Stable and unstable motion for $\lambda < \lambda_c$. The motion may stabilise about the stable part of the equilibrium curve to the left of the elastic critical locus. However, for initial values lying to the right of the unstable part of the equilibrium curve and to the left of the elastic locus, the motion is unstable, encountering an infinite displacement rate.

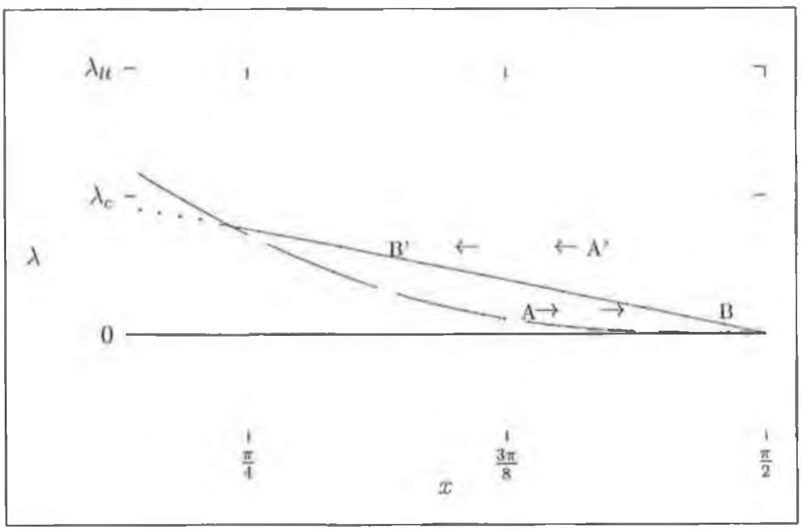

Figure 4.7: Stable motion for values of $\lambda < \lambda_c$ where the initial position is to the right of the elastic critical locus.

Chapter 5

Three Model Problems

5.1 Introduction

In this chapter we apply a perturbation technique, the multiple time scale method, to find asymptotic approximations to the solution of the perfect model problem linearised about zero with large relaxation time. We analyse the model subject to three loading strategies; the constant load problem, the slowly varying load problem and the parametric loading problem. The chapter opens with a general discussion on perturbation techniques, with the main emphasis on the method of multiple scales. The three loading problems are introduced with a brief discussion on each.

We apply the multiple scale method to the constant load viscoelastic model and obtain an asymptotic solution that has an elastic component and a creep component. The solution agrees with the results obtained in the stability analysis of Section 3.3. For unstable solutions we can determine the critical time at which the motion of the system is dominated by the creeping term. The behaviour of the system is demonstrated in a series of graphs. The slowly varying load problem is also analysed using the multiple scale approach. We show that a more complicated time variable is needed to describe motion on a fast time scale. We determine a condition on the loading function to ensure stability in the system. Again we graph the behaviour of the system for various loading functions. Finally we analyse the system subjected to parametric loading. In the elastic case this problem reduces to the Mathieu equation. We are interested in the effect of including a viscoelastic element on the transition curves in parametric space that separate stable and unstable solutions of the Mathieu Equation. The method of strained parameters is used to calculate the new transition curves. The results are discussed and the solution to the problem is presented graphically.

The multiple scale and related techniques are discussed in detail in Cole and Kevorkian [5, 6], Nayfeh and Mook [23] and Holmes [16]. In Murphy [24], the dynamic buckling of linear viscoelastic rods is investigated. Multiple scale solutions are derived for various loading strategies. While there are similarities between the work presented in this chapter and that in [24], the results were derived independently.

5.2 Perturbation Methods

For many problems in applied mathematics it is difficult if not impossible to obtain an exact solution. The problem may be non-linear, have complex boundary conditions, variable coefficients or be multi-dimensional. However, approximate solutions to these problems are often sufficient. There are various methods by which approximate solutions are constructed. Scientific computing can provide highly accurate numerical solutions to otherwise intractable problems. A second option is to use perturbation techniques. Central to this approach is the presence of a small variable ε in the governing equations. Using these techniques we can often determine a reasonably accurate analytic expression for the solution.

5.2.1 The Multiple Time Scale Method

The multiple time scale method is a perturbation technique that can be used to analyse systems which exhibit behaviour on several different time scales. It is a generalisation of the method of strained co-ordinates proposed by the astronomer Lindstedt [21] for the calculation of periodic orbits. The basic idea was first introduced by Stokes [28] in his study of fluid flow. Poincare [26] made extensive use of the ideas underlying multiple time scales in his investigations into the periodic motion of planets. This motion cannot be approximated using a regular asymptotic expansion due to the cumulative effects of small disturbances. These disturbances eventually become non-negligible, resulting in an expansion that is not uniformly valid for times of $O(\varepsilon^{-1})$. The cumulative effects result in, for example, terms proportional to $\varepsilon t \sin kt$. We refer to these terms as mixed secular terms. The word secular, derived from the Latin for century, was used to indicate that the εt term becomes significant when the time t is of the order of a century. Using the Poincare-Lindstedt method a new time $t^{+} = (1 + \varepsilon c_1 + \varepsilon^2 c_2 + \ldots)t$ is defined and the equations are rewritten in terms of this strained time. The constants $c_1, c_2, \ldots$ are chosen to remove secular terms. Multiple time scales is an extension of this idea where multiple independent time variables based on the expansion parameter are used. The use of two independent time scales was proposed explicitly by Kuzmak [20] and independently by Cole and Kevorkian [4]. The latter studied general, weakly nonlinear problems of the form

$$\ddot{y}(t) + y(t) + \varepsilon f(y, \dot{y}, \varepsilon, t) = 0, \qquad y(0) = a, \, \dot{y}(0) = b,$$

using two time-scales, the slow time $\tilde{t} = \varepsilon t$ and the fast time defined by $t^{+} = (1 + \varepsilon^2 c_2 + \varepsilon^3 c_3 + \ldots)t$. They obtain an asymptotic expansion of the solution in the form

$$y(t; \varepsilon) = F(t^{+}, \tilde{t}; \varepsilon) = \sum_{n=0}^{N} F_n(t^{+}, \tilde{t})\varepsilon^n + O(\varepsilon^{N+1})$$

which is uniformly valid (as $\varepsilon \to 0$) on the expanding interval $0 \leq t \leq T$ where $T = O(\varepsilon^{-1})$.

The two-time expansion can be extended further by the introduction of multiple time scales of the form

$$t_k = \epsilon^k t, \; k = 0, 1, 2, \ldots \tag{5.2.1}$$

where each of the time variables t_k is assumed to be independent. An expansion with $N+1$ terms involving $N+1$ time variables is generally uniformly valid on an interval $0 \leq t \leq T$ where $T = O(\varepsilon^{-N})$. The choice of time scales can be more general than (5.2.1). Time variables that are a non-linear function of t and ε may occur. The fundamental assumption of the multiple time scales method with $N+1$ independent time variables t_k, $k = 0, 1, \ldots, N$ is that solutions have a general asymptotic expansion that is uniformly valid (as $\varepsilon \to 0$) in the expanding time interval $0 \leq t \leq T(\varepsilon) = O(\varepsilon^{-N})$ and each term in the general asymptotic expansion can be uniquely expressed as a function of $t_0, t_1, \ldots, t_N$ and a power of ε. This is a powerful assumption and results in the removal of secular terms from the solution. For example, with two independent times defined by $t_0 = t, t_1 = \varepsilon t$, a term of the form $\varepsilon t_0 \sin k t_0$ in the $O(\varepsilon)$ contribution to the expansion violates the uniqueness assumption as it can be included in the $O(1)$ contribution as $t_1 \sin k t_0$. Such a term must be removed by a suitable condition.

5.3 The Model Problems

In this section we introduce the three loading problems that are considered. The first problem we investigate is the viscoelastic model with constant load. The governing equations are

$$\ddot{x} = -\omega x - y,$$
$$\dot{y} = -\alpha\{y + \frac{\beta}{2}x\},$$

where $\omega = (\frac{1}{2} - \lambda)$ and the initial conditions are $x(0) = \zeta_1$, $\dot{x}(0) = \zeta_2$ and $y(0) = \gamma$. As we are interested in the effect of including the viscoelastic element on the elastic system we only consider the case $\omega > 0$. For loads satisfying $\omega \leq 0$ the system is instantaneously unstable. For a large relaxation time we have $\alpha \ll 1$ and so α is a natural small parameter for the system. This is an example of a linear oscillating system with a small viscoelastic effect.

The second problem that we discuss is the viscoelastic model with a slowly varying load $\lambda(t,\varepsilon) = \lambda(\varepsilon t)$ where $\varepsilon \ll 1$. The governing equations are

$$\ddot{x} = -k^2(\varepsilon t)x - y,$$
$$\dot{y} = -\alpha\{y + \frac{\beta}{2}x\},$$

where $k^2(\varepsilon t) = \frac{1}{2} - \lambda(\varepsilon t)$. Again we consider the case $k^2(\varepsilon t) > 0$. For large relaxation times we have $\alpha \ll 1$ and so there are two small parameters in the system. Since we want to investigate both the viscoelastic effect and the effect due to the slowly varying load, we let

$$\alpha = \varepsilon(\alpha_0 + \varepsilon\alpha_1 + \varepsilon^2\alpha_2 + \dots),$$

where the constants $\alpha_0, \alpha_1, \alpha_2 \dots$ are to be determined.

Finally we will analyse the viscoelastic model subject to a load of the form $\lambda(t,\varepsilon) = \lambda_0 + \varepsilon\cos\kappa t$ where again we have $\varepsilon \ll 1$. The load oscillates with small amplitude about the constant value λ_0. This form of loading is known as parametric excitation. It can result in parametric resonance whereby a small excitation can produce a large response when the frequency of the excitation κ is close to an integer multiple of half the natural frequency of the system. The model equations are

$$\ddot{x} = (-\omega + \varepsilon\cos\kappa t)x - y,$$
$$\dot{y} = -\alpha\{y + \frac{\beta}{2}x\},$$

where $\omega = \frac{1}{2} - \lambda_0$. The elastic system obtained by setting $\alpha = 0$ and $y(0) = 0$ is the Mathieu equation, the solutions of which are well known. Of interest are the regions of stability and instability in the ω,ε-plane and the calculation of the transition curves between these regions. We will determine the effect of the viscoelastic element on the transition curves that result from the elastic case. Again we must be careful that we include both the effect due to the viscoelastic element and the effect due to the load. This is achieved by again setting

$$\alpha = \varepsilon(\alpha_0 + \varepsilon\alpha_1 + \varepsilon^2\alpha_2 + \dots).$$

5.4 The Constant Load Problem

In this section we apply the multiple time scale method to the viscoelastic model with constant load and large relaxation time ($\alpha \ll 1$). The governing equations for the model are

$$\ddot{x} = -\omega x - y, \tag{5.4.1a}$$

$$\dot{y} = -\alpha\{y + \frac{\beta}{2}x\}, \tag{5.4.1b}$$

where $\omega = \frac{1}{2} - \lambda > 0$ and the initial conditions are given by $x_1(0) = \zeta_1$, $x_2(0) = \zeta_2$ and $y(0) = \gamma$. We let $\varepsilon = \alpha$. Now, the two-time expansion method with two independent time variables, $\tilde{t} = \varepsilon t$ and $t^+ = (1 + \varepsilon^2 c_2 + \varepsilon^3 c_3 \dots)t$, does not result in a uniformly valid solution on the time interval $0 \leq t \leq T(\varepsilon) = O(\varepsilon^{-2})$ for general initial conditions. To obtain an expansion that is valid on this time interval we require three independent times defined by $t_0 = t, t_1 = \varepsilon t$ and $t_2 = \varepsilon^2 t$. We seek an expansion for $x(t;\varepsilon)$ and $y(t;\varepsilon)$ in the form

$$x(t;\varepsilon) = X(t_0, t_1, t_2; \varepsilon) = X_0(t_0, t_1, t_2) + \varepsilon X_1(t_0, t_1, t_2) + \varepsilon^2 X_2(t_0, t_1, t_2) + \dots \tag{5.4.2}$$

and

$$y(t;\varepsilon) = Y(t_0, t_1, t_2; \varepsilon) = Y_0(t_0, t_1, t_2) + \varepsilon Y_1(t_0, t_1, t_2) + \varepsilon^2 Y_2(t_0, t_1, t_2) + \dots \tag{5.4.3}$$

Derivatives with respect to t are expressed in terms of the new time variables t_0, t_1 and t_2. Let $D_0 = \partial/\partial t_0, D_1 = \partial/\partial t_1$ and $D_2 = \partial/\partial t_2$. Applying the chain rule to d/dt gives

$$\frac{d^k}{dt^k} = \left[(D_0 + \varepsilon D_1 + \varepsilon^2 D_2\right]^k. \tag{5.4.4}$$

Substituting (5.4.2), (5.4.3) and (5.4.4) into (5.4.1) and expanding in powers of ε results in the following sequence of problems:

$O(1)$

$$L(X_0) \equiv D_0^2 X_0 + \omega X_0 = -Y_0, \tag{5.4.5a}$$

$$D_0 Y_0 = 0. \tag{5.4.5b}$$

$O(\varepsilon)$

$$L(X_1) = -2D_0 D_1 X_0 - Y_1, \tag{5.4.6a}$$

$$D_0 Y_1 = -D_1 Y_0 - Y_0 - \frac{\beta}{2} X_0. \tag{5.4.6b}$$

$O(\varepsilon^2)$

$$L(X_2) = -2D_0 D_1 X_1 - -D_1^2 X_0 - 2D_0 D_2 X_0 - Y_2, \tag{5.4.7a}$$

$$D_0 Y_2 = -D_1 Y_1 - Y_1 - \frac{\beta}{2} X_1 - D_2 Y_0 - Y_0 - \frac{\beta}{2} X_0. \tag{5.4.7b}$$

The $O(1)$ problem is solved to give

$$X_0(t_0, t_1, t_2) = A_0^1(t_1, t_2) \cos \sqrt{\omega} t_0 + B_0^1(t_1, t_2) \sin \sqrt{\omega} t_0 - \frac{C_0^1(t_1, t_2)}{\omega}, \tag{5.4.8a}$$

$$Y_0(t_0, t_1, t_2) = C_0^1(t_1, t_2). \tag{5.4.8b}$$

By imposing conditions that remove secular terms in the $O(\varepsilon)$ and $O(\varepsilon^2)$ problems we will be able to determine the dependence of A_0^1, B_0^1 and C_0^1 on the times t_1 and t_2.[1] We

[1]The superscripts $1, \epsilon$ that appear on the functions A_i, B_i, C_i indicate the level at which these functions enter the solution.

substitute for X_0 and Y_0 from (5.4.8) into the right hand side of (5.4.6) to get

$$D_0 Y_1 = -D_1 C_0^1 - \frac{\omega - \beta/2}{\omega} C_0^1 - \frac{\beta}{2}\left[A_0^1 \cos\sqrt{\omega}t + B_0^1 \sin\sqrt{\omega}t\right] \tag{5.4.9}$$

Now, unless we set $-D_1 C_0^1 - \frac{\omega-\beta/2}{\omega} C_0^1 = 0$ in (5.4.9) we will introduce a secular term into the solution. Solving this for C_0^1 gives

$$C_0^1(t_1, t_2) = C_0^\varepsilon(t_2) e^{-\frac{\omega-\beta/2}{\omega} t_1} \tag{5.4.10}$$

and we can now solve (5.4.6) for Y_1 to get

$$Y_1(t_0, t_1, t_2) = \frac{\beta}{2\sqrt{\omega}}\left[A_0^1(t_1, t_2)\sin\sqrt{\omega}t - B_0^1(t_1, t_2)\cos\sqrt{\omega}t\right] + C_1^\varepsilon(t_2). \tag{5.4.11}$$

Substituting X_0 and Y_1 into (5.4.6a) gives us two conditions that must be satisfied if the X_1 solution is not to have secular terms. These are

$$\left[D_1 A_0^1 + \frac{\beta}{4\omega} A_0^1\right] \cos\sqrt{\omega}t_0 = 0,$$
$$\left[D_1 B_0^1 + \frac{\beta}{4\omega} B_0^1\right] \sin\sqrt{\omega}t_0 = 0.$$

Solving for $A_0^1(t_1, t_2)$ and $B_0^1(t_1, t_2)$ gives

$$A_0^1(t_1, t_2) = A_0^\varepsilon(t_2) e^{-\frac{\beta}{4\omega} t_1},$$

$$B_0^1(t_1, t_2) = B_0^\varepsilon(t_2) e^{-\frac{\beta}{4\omega} t_1}.$$

Continuing in this fashion we obtain the following expressions for the $X_i(t_0, t_1, t_2)$ to $O(\varepsilon^2)$,

$$\begin{aligned} X_i(t_0, t_1, t_2) &= A_i e^{-\frac{\beta}{4\omega} t_1} \cos(\sqrt{\omega}t_0 - \frac{\beta(1 + 3G_m - 8\lambda)}{32\omega^{3/2}} t_2) \\ &+ B_i e^{-\frac{\beta}{4\omega} t_1} \sin(\sqrt{\omega}t_0 - \frac{\beta(1 + 3G_m - 8\lambda)}{32\omega^{3/2}} t_2) \\ &+ C_i e^{-(1-\frac{\beta}{2\omega})t_1} \end{aligned} \tag{5.4.12}$$

where the constants $A_i = A_i^\varepsilon(0), B_i = B_i^\varepsilon(0)$ and $C_i = C_i^\varepsilon(0)$ are determined from the initial conditions.

The Initial Conditions

The initial conditions are $x_1(0) = \zeta_1$, $x_2(0) = \zeta_2$ and $y(0) = \gamma$. We use these to solve for the unknown constants that appear in the solution. We have $x(0;\varepsilon) = \zeta_1$, $dx(0;\varepsilon)/dt = \zeta_2$ and $y(0;\varepsilon) = \gamma$. Expanding $x(t;\varepsilon)$, $dx(t;\varepsilon)/dt$ and $y(t;\varepsilon)$ in powers of ε and substituting in the solution (5.4.12) evaluated at $t = 0$ gives

$O(1)$

$$\begin{aligned} A_0 + C_0 &= \zeta_1, \\ \sqrt{\omega}B_0 &= \zeta_2, \\ -\omega A_0 &= -r1 - \omega r3. \end{aligned} \tag{5.4.13}$$

$O(\varepsilon)$

$$\begin{aligned} A_1 + C_1 &= 0, \\ \sqrt{\omega}B_1 &= p_1 A_0 + p_3 C_0, \\ -\omega A_1 &= 2\sqrt{\omega}p_1 B_0. \end{aligned} \tag{5.4.14}$$

$O(\varepsilon^2)$

$$\begin{aligned} A_2 + C_2 &= 0, \\ \sqrt{\omega}B_2 &= p_1 A_1 + p_3 C_1 + p_2 B_0, \\ -\omega A_2 &= 2\sqrt{\omega}p_1 B_1 - 2\sqrt{\omega}p_2 A_0 - p_1^2 A_0 - p_3^2 C_0, \end{aligned} \tag{5.4.15}$$

where $p_1 = \beta/(4\omega), p_2 = \beta(1 + 3G_m - 8\lambda)/(32\omega^{3/2})$ and $p_3 = 1 - \beta/(2\omega)$. Solving (5.4.13), (5.4.14) and (5.4.15) for the constants A_i, B_i and C_i gives

$$A_0 = \zeta_1 + \frac{\gamma}{\omega}, B_0 = \frac{\zeta_2}{\sqrt{\omega}}, C_0 = -\frac{\gamma}{\omega}.$$

$$A_1 = -\frac{2\sqrt{\omega}p_1 B_0}{\omega}, B_1 = \frac{p_1 A_0 + p_3 C_0}{\sqrt{\omega}}, C_1 = -A_1.$$

$$A_2 = -\frac{2\sqrt{\omega}p_1B_1 - 2\sqrt{\omega}p_2A_0 - p_1^2A_0 - p_3^2C_0}{\omega}, B_2 = \frac{p_1A_0 + p_3C_0 + p_2B_0}{\sqrt{\omega}};$$

and

$$C_2 = \frac{2\sqrt{\omega}p_1B_1 - 2\sqrt{\omega}p_2A_0 - p_1^2A_0 - p_3^2C_0}{\omega}.$$

We see that each of the constants in the solution is linearly dependent on either one or two of the initial conditions. We have $A_0 = A_0(\zeta_1, \gamma), B_0 = B_0(\zeta_2), C_0 = C_0(\zeta_1), A_1 = A_1(\zeta_2), B_1 = B_1(\zeta_1, \gamma), C_1 = C_1(\zeta_2), A_2 = A_2(\zeta_1, \gamma)$, $B_2 = B_2(\zeta_2)$ and $C_2 = C_2(\zeta_1, \gamma)$. Using these relationships we can determine the non-zero terms of the expansion for any initial values. The need for three independent times in the multiple time scale expansion can now be justified. If we set $\zeta_1 = \zeta_2 = 0$ then we have $C_0 = C_1 = 0$ and the creep component of the solution first appears in the $O(\varepsilon^2)$ term. An expansion to this order is required to include the creep effect and thus obtain a solution that is uniformly valid on the time interval $0 \le t < T = O(\varepsilon^{-2})$.

Analysis of the Multiple Scale Solution

We now discuss the solution obtained using the multiple time scale method with three independent times. In particular, we are interested in the features that the viscoelastic element introduces to the solution compared to the dynamic elastic solution. The multiple scale solution has elastic and creep components. The elastic component is composed of oscillating terms with an exponential amplitude while the creep component is an exponential term. The amplitude of the oscillation is given by $e^{-\frac{\beta}{4\omega}t_1}$ where $\frac{\beta}{4\omega}t_1 > 0$. Thus, the amplitude is exponentially decreasing for all values of the load λ and varies on the slow time scale t_1. The oscillating terms have frequency $\sqrt{\omega}t_0 - \frac{\beta(1+3G_m-8\lambda)}{32\omega^{3/2}}t_2$. The natural frequency of the elastic problem, $\sqrt{\omega}$, is shifted by the $O(\varepsilon^2)$ term $\varepsilon^2\frac{\beta(1+3G_m-8\lambda)}{32\omega^{3/2}}$. This small term is positive for $0 < \lambda < (1 + 3G_m)/8$ and negative for $(1 + 3G_m)/8 < \lambda < 1/2$. Thus,

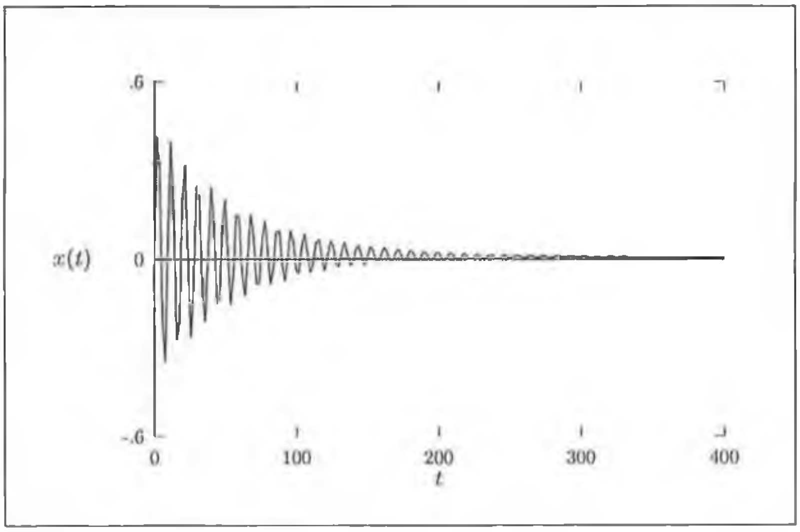

Figure 5.1: A typical multiple scale solution for $\lambda < G_m/2$. The solution is stable and tends to the zero equilibrium position. A numerical solution is also plotted using Mathematica for comparison. However, the solutions are indistinguishable.

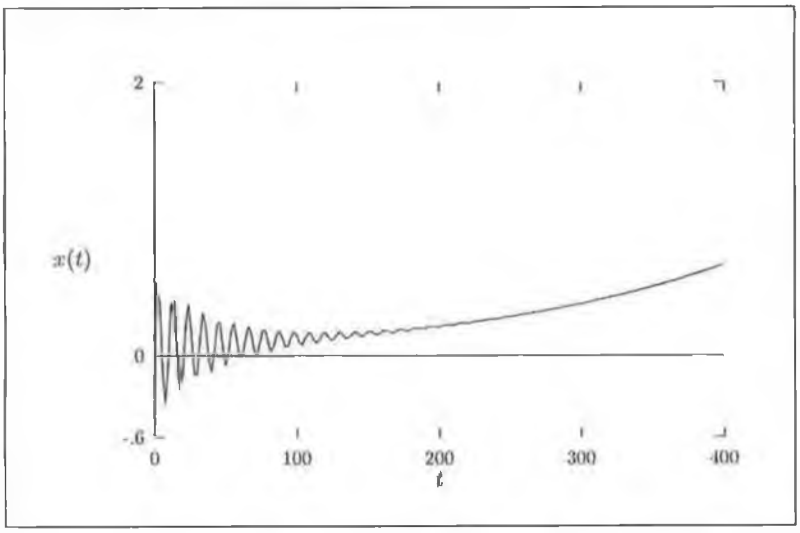

Figure 5.2: A typical multiple scale solution for $G_m/2 < \lambda < 1/2$. Initially, the solution appears to be stable. However, the positive exponential term destabilises the solution. Again we plot a numerical solution for comparison. However, the solutions are indistinguishable over this time interval.

depending on the load value, the frequency of oscillation can be increased or decreased. The slowly modulated oscillations have a stabilising effect on the solution.

The exponential term $e^{-(1-\frac{\beta}{2\omega})t_1}$ results from creep in the system. This creep term varies on the slow time scale t_1. It is exponentially decreasing for $0 \leq \lambda \leq G_m/2$ and this has a stabilising effect on the solution. However, for $G_m/2 < \lambda < 1/2$ the creep term is exponentially increasing on the slow time scale and this will eventually destabilise the solution. Recall that in our stability analysis in Chapter 3 we found that the $(0, \lambda)$ branch of equilibria is stable for $\lambda < 1/2$ in the elastic case while in the viscoelastic case we found that this branch of equilibria was stable for $\lambda < G_m/2$ and unstable in the interval $G_m/2 < \lambda < 1/2$. The multiple scale solution agrees with this.

In Figure 5.1 we plot the multiple scale solution for a typical value of $\lambda < G_m/2$. A numerical solution, generated by the mathematical software package Mathematica, is also plotted. However, the solutions are indistinguishable. The main features of the solution, as discussed above, are apparent. A typical solution for $G_m/2 < \lambda < 1/2$ is plotted in Figure 5.2. We also include a numerical solution. Again, the solutions are indistinguishable. However, if we compare the multiple scale solution with the numerical solution over a much greater time interval, slight differences become apparent.

Critical Times

For values of the parameter λ in the range $G_m/2 < \lambda < 1/2$ we are interested in determining the time at which the exponentially increasing creep term is of the same order of magnitude as the oscillating terms. Physically, this time gives an indication of the useful lifespan of the structure. For general initial conditions we have

$$O(h_{AB}e^{-\frac{\beta}{4\omega}t_1}) = O(h_C e^{(\frac{\beta}{2\omega}-1)t_1}) \tag{5.4.16}$$

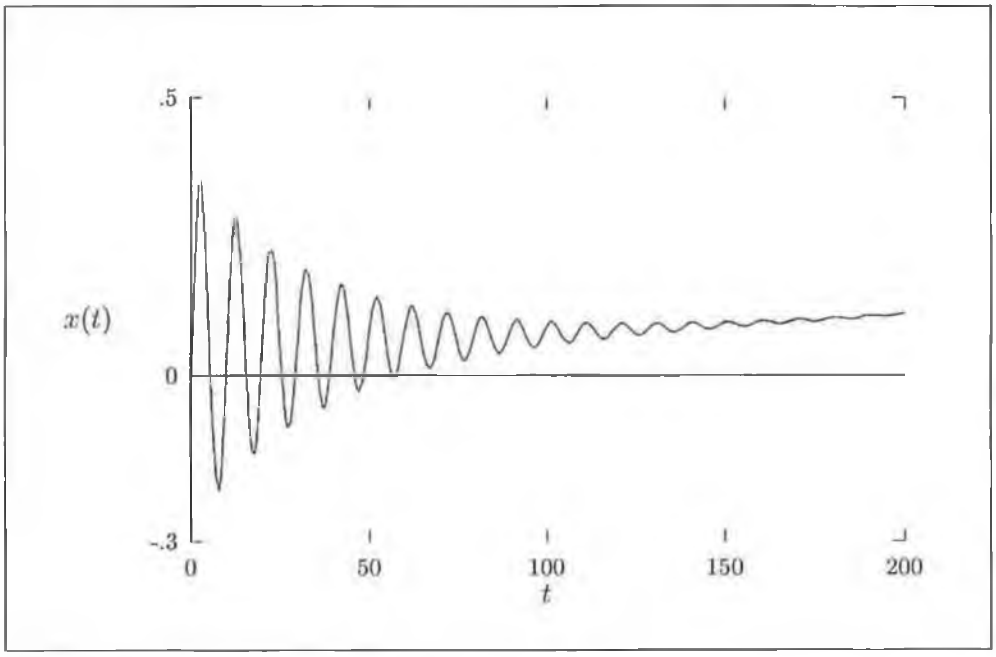

Figure 5.3: A typical unstable multiple scale solution with non-trivial initial conditions and critical time $t_{cr} = 45.717$. Examining the solution we see that the instability does appear in a neighbourhood of this critical time.

where $h_{AB} = A_0 + B_0 + \varepsilon(A_1 + B_1) + \varepsilon^2(A_2 + B_2)$ and $h_C = C_0 + \varepsilon C_1 + \varepsilon^2 C_2$. We solve (5.4.16) for t to get the critical time

$$t_{cr} = \frac{4\omega}{\varepsilon(3\beta - 4\omega)} \ln \left| \frac{h_{AB}(\varepsilon)}{h_C(\varepsilon)} \right|. \tag{5.4.17}$$

For non-trivial initial conditions we have $h_{AB}/h_C = O(1)$ and so $t_{cr} = O(\varepsilon^{-1})$. In Figure 5.3 we plot a typical solution satisfying $G_m/2 < \lambda < 1/2$ with non-trivial initial conditions. We can also calculate the critical time when one or more of the initial conditions are zero. We look at two cases, the first is when we have $\gamma = 0$ and the second is when $\zeta_2 = \gamma = 0$.

Case 1: $\gamma = 0$.

This occurs when the stress due to creep is initially zero, which results in one trivial initial condition, $C_0 = 0$. Therefore the creep component first appears in the solution in the $O(\varepsilon)$ term. We have $h_C = \varepsilon C_1 + \varepsilon^2 C_2$ and so $h_{AB}/h_C = O(\varepsilon)$ giving a critical time that

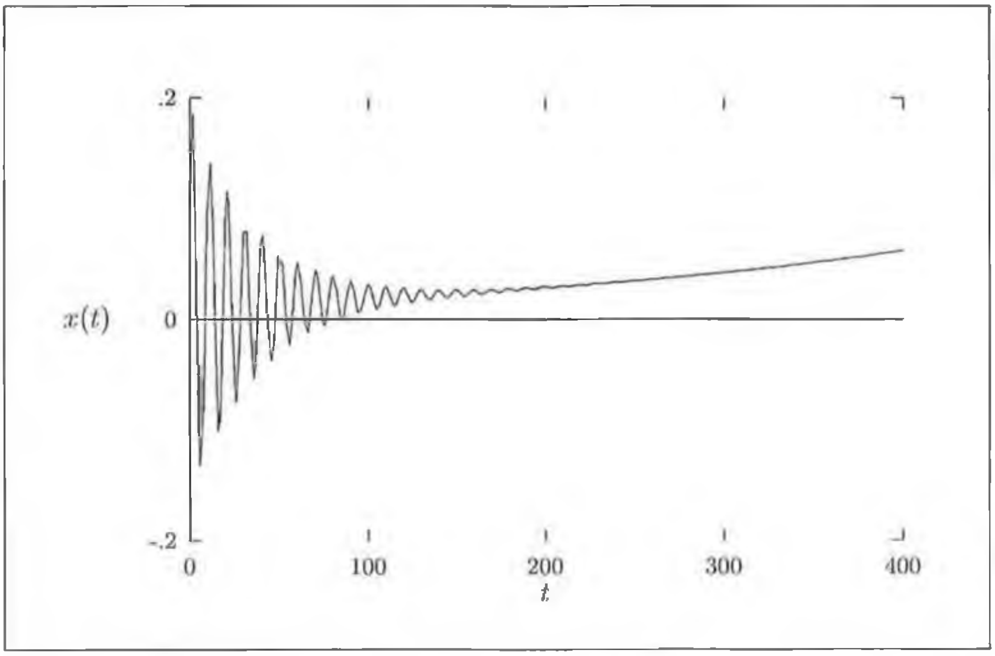

Figure 5.4: A typical unstable multiple scale solution with $\gamma = 0$ and critical time $t_{cr} = 94.773$. Again, we see that the instability becomes apparent in a neighbourhood of this time.

is of order $O(\frac{1}{\varepsilon}\ln|\frac{1}{\varepsilon}|)$. The critical time is increased with this type of initial condition. In Figure 5.4 we plot a typical solution satisfying $\gamma = 0$. The critical time is greater that in the case of non-trivial conditions, as expected.

Case 2: $\zeta_2 = \gamma = 0$

In this case both the initial velocity and the initial creep stress are zero. The creep component of the solution is zero up to $O(\varepsilon)$ as the choice of initial conditions gives $C_0 = 0$ and $C_1 = 0$. We also have $A_0 = B_1 = A_2 = 0$. Substituting these trivial initial values into (5.4.17) gives $h_{AB}/h_C = O(\varepsilon^{-2})$. This results in a critical time that is of order $t = O(\frac{1}{\varepsilon}\ln|\frac{1}{\varepsilon^2}|)$. Again we see an increase in the critical time. This is apparent in Figure 5.5 where we plot a typical solution with $\zeta_2 = \gamma = 0$.

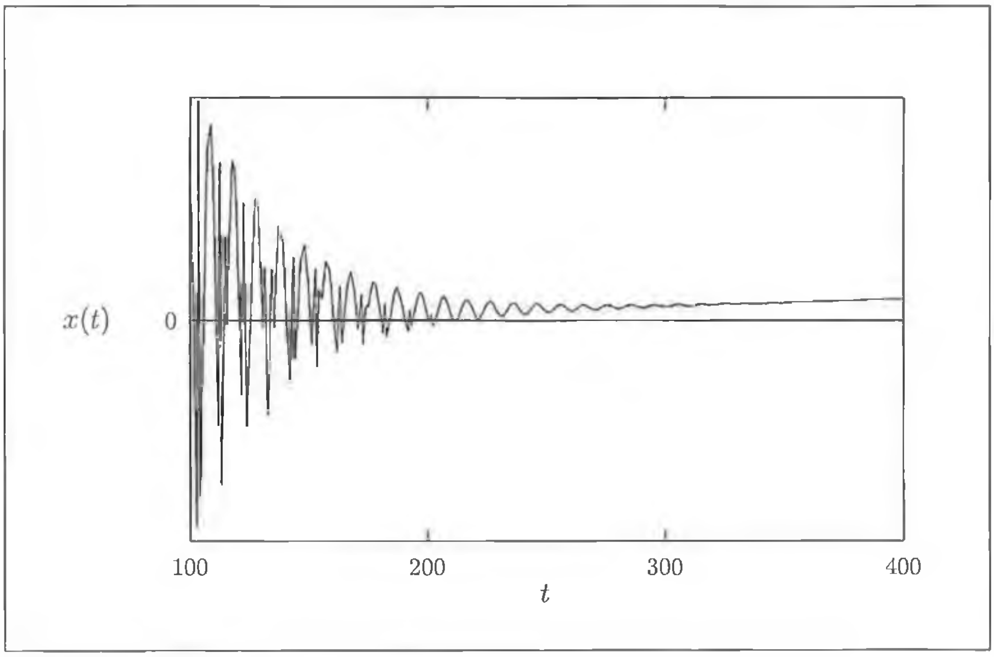

Figure 5.5: A typical unstable multiple scale solution with $\gamma = \zeta_2 = 0$ and critical time $t_{cr} = 218.128$.

5.5 The Slowly Varying Load Model

In this section we consider the effect of a slowly varying load on the Link model. By slowly varying we assume that the load varies on a time-scale that is much longer than the natural time-scale associated with the model. This is a generalisation of the constant load viscoelastic model. Physically we may encounter a slowly varying load in a number of ways. One example may be a slow change in load due to external factors. Also, if the properties of the viscoelastic element change slowly due,for instance, to an aging process, we expect its response to the load to vary. A crude way of modeling this response would be to hold the viscoelastic properties constant and slowly vary the load. The effect of a slowly varying load on an elastic oscillator has been discussed in Cole and Kevorkian [6]. We will extend these ideas to the viscoelastic model. The analysis is not as straightforward as in the constant load problem. The viscoelastic model has a natural small parameter, $\alpha \ll 1$, for large relaxation times. The slowly varying load $\lambda(t;\varepsilon) = \lambda(\varepsilon t)$ introduces another small parameter, $\varepsilon \ll 1$. In order to include both the viscoelastic effect and the slowly varying effect simultaneously we require that $\alpha = O(\varepsilon)$ and so set $\alpha = \varepsilon(\alpha_0 + \alpha_1\varepsilon + \dots)$.

The model equations are

$$\ddot{x} = -k^2(\varepsilon t)x - y, \tag{5.5.1a}$$

$$\dot{y} = -\alpha\{y + \frac{\beta}{2}x\}, \tag{5.5.1b}$$

where $k^2(\varepsilon t) = \frac{1}{2} - \lambda(\varepsilon t)$ and the initial conditions are given by $x_1(0) = \zeta_1$, $x_2(0) = \zeta_2$ and $y(0) = \gamma$. A multiple scale expansion with a fast time $t_0 = t$ fails to provide a uniformly valid approximation for long times as this choice of fast time does not take account of the slow variation in the frequency of the oscillations due to the slowly varying load. Kuzmak [20] recognised that the oscillations in the solution should have a constant frequency with respect to the fast time and so allowed the fast time to have a nonlinear dependence on t. In light of this we choose our fast time to be $t_0 = f(t,\varepsilon)$ where $f(t,\varepsilon)$ is a smooth, non-negative, increasing function of t and satisfies $\varepsilon t \ll f(t,\varepsilon)$ as $\varepsilon \downarrow 0$. We denote the slow time by $t_1 = \varepsilon t$. Substituting $x(t,\varepsilon) = X(t_0,t_1;\varepsilon)$ and $y(t,\varepsilon) = Y(t_0,t_1;\varepsilon)$ into (5.5.1) gives

$$(f_t^2D_0^2 + f_{tt}D_0 + 2\varepsilon f_tD_0D_1 + \varepsilon^2D_1^2)X + k^2X = -Y, \tag{5.5.2a}$$

$$(f_tD_0 + \varepsilon D_1)Y = -\varepsilon(\alpha_0 + a\alpha_1 + \dots)\{Y + \frac{\beta}{2}X\}. \tag{5.5.2b}$$

The terms in (5.5.2a) that result in oscillations on the fast time scale are $f_t^2D_0^2X$ and k^2X. Equating these to zero gives

$$f_t^2D_0^2X + k^2X = 0. \tag{5.5.3}$$

Now, by setting $f_t(t,\varepsilon) = k(\varepsilon t)$ in (5.5.3) the oscillations in the solution will have a constant frequency with respect to the fast time $f(t,\varepsilon)$. Integrating gives the fast time, $f(t,\varepsilon) = \int_0^t k(\varepsilon\tau)d\tau$.

We seek a solution to (5.5.1) in the form

$$x(t;\varepsilon) = X(t_0,t_1;\varepsilon) = X_0(t_0,t_1) + \varepsilon X_1(t_0,t_1) + \ldots \tag{5.5.4a}$$

$$y(t;\varepsilon) = Y(t_0,t_1;\varepsilon) = Y_0(t_0,t_1) + \varepsilon Y_1(t_0,t_1) + \ldots \tag{5.5.4b}$$

Substituting (5.5.4) into (5.5.1) gives the following sequence of problems

$O(1)$

$$k^2D_0^2X_0 + k^2X_0 = -Y_0, \tag{5.5.5a}$$

$$kD_0Y_0 = 0. \tag{5.5.5b}$$

$O(\varepsilon)$

$$k^2D_0^2X_1 + k^2X_1 = -Y_1 - k'D_0X_0 - 2kD_0D_1X_0, \tag{5.5.6a}$$

$$kD_0Y_1 = -D_1Y_0 - \alpha_0(Y_0 + \frac{\beta}{2}X_0). \tag{5.5.6b}$$

$O(\varepsilon^2)$

$$k^2D_0^2X_2 + k^2X_2 = -Y_2 - k'D_0X_1 - 2kD_0D_1X_1 - D_1^2X_0, \tag{5.5.7a}$$

$$kD_0Y_2 = -D_1Y_1 - \alpha_0(Y_1 + \frac{\beta}{2}X_1) - \alpha_1(Y_0 + \frac{\beta}{2}X_0). \tag{5.5.7b}$$

Now, in order to correctly determine a uniformly valid solution to $O(\varepsilon^2)$ it is necessary to include a third time $t_2 = \varepsilon^2 t$. However, the analysis becomes quite complicated. We will calculate the solution to $O(\varepsilon)$. This solution is valid on the time interval $0 < t < O(\varepsilon^{-1})$. The analysis demonstrates the important properties of the solution and solution method.

The slowly varying solution

Solving (5.5.5) for X_0 and Y_0 gives

$$X_0(t_0,t_1) = A_0(t_1)\cos t_0 + B_0(t_1)\sin t_0 - \frac{C_0(t_1)}{k^2(t_1)}, \tag{5.5.8a}$$

$$Y_0(t_0,t_1) = C_0(t_1). \tag{5.5.8b}$$

Substituting (5.5.8) into (5.5.6b) gives

$$kD_0Y_1 = -\alpha_0\frac{\beta}{2}(A_0\cos t_0 + B_0\sin t_0) - C_0' - \alpha C_0(1-\frac{\beta}{2k^2}). \tag{5.5.9}$$

To avoid secular terms in (5.5.9) we impose the condition $-C_0' - \alpha C_0(1-\frac{\beta}{2k^2}) = 0$. Solving for $C_0(t_1)$ gives

$$C_0(t_1) = C_0 e^{-\alpha_0(t_1 - \frac{\beta}{2}K(t_1))}. \tag{5.5.10}$$

where $K(t_1) = \int_0^{t_1}\frac{1}{k^2(\tau)}d\tau$. Now, (5.5.6a) is solved for Y_1 to give

$$Y_1(t_0,t_1) = -\frac{\alpha_0\beta}{2k(t_1)}(A_0(t_1)\sin t_0 - B_0(t_1)\cos t_0) + C_1(t_1). \tag{5.5.11}$$

Substituting (5.5.8a) and (5.5.11) into the (5.5.6a) gives

$$\begin{aligned} k^2D_0^2X_1 + k^2X_1 = &\left(B_0\left[-\frac{\alpha_0\beta}{2k} - k'\right] - 2kB_0'\right)\cos t_0 \\ &+ \left(A_0\left[\frac{\alpha_0\beta}{2k} + k'\right] + 2kA_0'\right)\sin t_0 - C_1 \end{aligned} \tag{5.5.12}$$

We can solve (5.5.12) for X_1. However, we get the two following conditions,

$$\left(B_0\left[-\frac{\alpha_0\beta}{2k} - k'\right] - 2kB_0'\right)\sin t_0 = 0, \tag{5.5.13a}$$

$$\left(A_0\left[\frac{\alpha_0\beta}{2k} + k'\right] + 2kA_0'\right)\cos t_0 = 0, \tag{5.5.13b}$$

that must be satisfied if secular terms are to be avoided. We solve (5.5.13) for $A_0(t_1)$ and $B_0(t_1)$ to get

$$A_0(t_1) = A_0 e^{-\alpha_0\beta/4K(t_1)}\sqrt{k(0)/k(t_1)}, \tag{5.5.14a}$$

$$B_0(t_1) = B_0 e^{-\alpha_0\beta/4K(t_1)}\sqrt{k(0)/k(t_1)}. \tag{5.5.14b}$$

We can now solve (5.5.12) for X_1 to get

$$X_1(t_0, t_1) = A_1(t_1)\cos t_0 + B_1(t_1)\sin t_0 - C_1(t_1)/k^2(t_1). \tag{5.5.15}$$

Substituting for X_1 and Y_1 in the $O(\varepsilon^2)$ problem results in conditions that $A_1(t_1), B_1(t_1)$ and $C_1(t_1)$ must satisfy to prevent the occurrence of secular terms. We get

$$A_1(t_1) = A_1 e^{-\alpha_0\beta/4K(t_1)}\sqrt{k(0)/k(t_1)},$$

$$B_1(t_1) = B_1 e^{-\alpha_0\beta/4K(t_1)}\sqrt{k(0)/k(t_1)},$$

and

$$C_1(t_1) = C_1 e^{-\alpha_0(t_1 - \frac{\beta}{2}K(t_1))}.$$

We see that these terms have the same form as the $O(1)$ terms, as was the case in the constant load problem. We can write the solution as

$$\begin{aligned} x(t;\varepsilon) = {} & (A_0 + \varepsilon A_1)e^{-\alpha_0\beta/4K(t_1)}\sqrt{k(0)/k(t_1)}\cos t_0 \\ & + (B_0 + \varepsilon B_1)e^{-\alpha_0\beta/4K(t_1)}\sqrt{k(0)/k(t_1)} + \varepsilon B_1)\sin t_0 \\ & + (C_0 + \varepsilon C_1)e^{-\alpha_0(t_1 - \frac{\beta}{2}K(t_1))}. \end{aligned} \tag{5.5.16}$$

From the initial conditions we get

$$A_0 = k^2(0)\zeta_1 + \gamma,\ B_0 = \zeta_2,\ C_0 = (1 - k^2(0))\zeta_1 - \gamma,$$

$$A_1 = 2B_0\left[\frac{1}{k^2(0)} - \frac{k'(0)}{2k(0)}\right],\ C_1 = -2B_0\left[\frac{1}{k^2(0)} - \frac{k'(0)}{2k(0)}\right]$$

and

$$B_1 = -A_0\left[\frac{1}{k^2(0)} - \frac{k'(0)}{2k(0)}\right] - \alpha_0 C_0\left[1 - \frac{\beta}{2k^2 0}\right].$$

Analysis of the slowly varying solution

The solution (5.5.16) to the slowly varying load problem has oscillating terms with an exponential amplitude which represent the elastic behaviour of the system and an exponential creep term. This is similar to the constant load problem. In fact, if we set the load $\lambda(\varepsilon t)$ to a constant value, then we recover the solution of the constant load problem, taking into account that the fast times differ by a constant multiple.

The stability of the solution can be determined by looking at the exponential terms in the solution. The oscillating terms are modulated by $e^{-\alpha_0\beta/4K(t_1)}$ where $-\alpha_0\beta/4K(t_1) < 0$ for $\alpha_0 > 0$. Therefore, the amplitude of the oscillations is exponentially decreasing and this has a stabilising effect on the solution. The creep term is of the form $C_0 e^{-\alpha_0(t_1 - \frac{\beta}{2}K(t_1))}$. Again, with $\alpha_0 > 0$ the exponential is decreasing for

$$\frac{\beta K(t_1)}{2t_1} = \frac{\beta}{2t_1}\int_0^{t_1} \frac{1}{\frac{1}{2} - \lambda(\tau)} d\tau < 1. \tag{5.5.17}$$

The solution will be stable if (5.5.17) is satisfied for all values of $t_1 \geq 0$. However, if there exists some time t^* such that $\frac{\beta K(t_1)}{2t_1} > 1$ for all t_1 satisfying $t_1 > t^*$ then the solution becomes unstable. Now, $\beta K(t_1)/(2t_1)$ is bounded below by $\beta < 1$, (let $\lambda = 0$). Also, setting $\lambda(\varepsilon t) = G_m/2$, the critical load for the constant load problem, gives $\beta K(t_1)/(2t_1) = 1$. For constant values of $\lambda > G_m/2$, we have unstable solutions. This agrees with the constant load problem results. If we vary the load periodically about the critical load then we may achieve a stable solution although (5.5.17) is not satisfied over some finite time intervals. This is in contrast to the constant load problem where loads even slightly greater that the critical load cause the system to become unstable. In Figure 5.6 we plot the function $\beta K(t_1)/2t_1$ for a load given by $\lambda(t_1) = 0.25 - 0.2\cos t_1$. The critical load is given by $G_m/2 = 0.35$. The load oscillates about the critical load, reaching a maximum of 0.45 and a minimum of 0.05. We plot the slowly varying solution

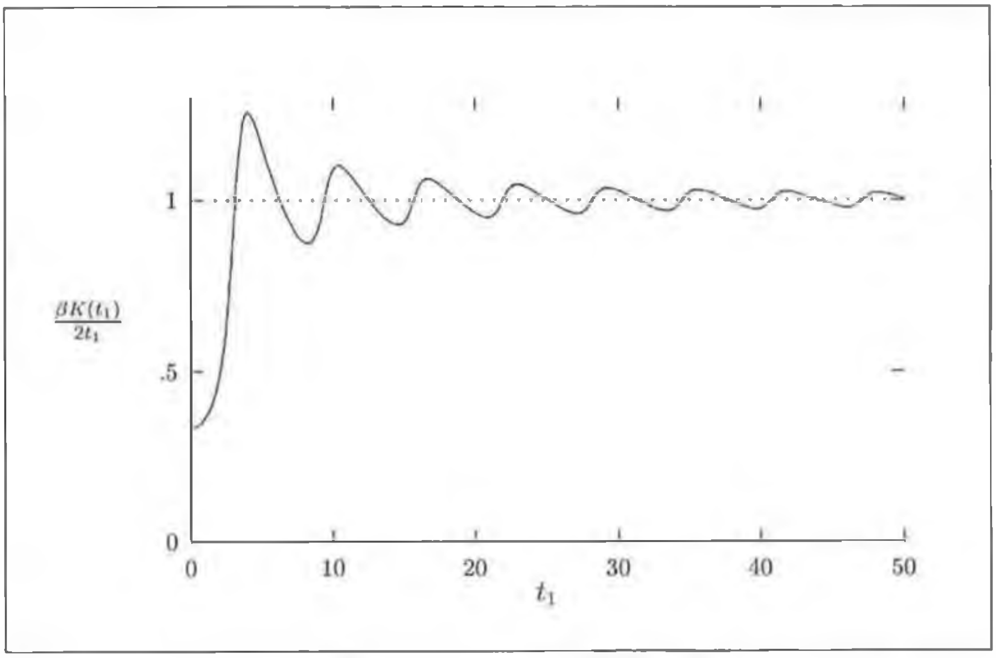

Figure 5.6: The function $\beta K(t_1)/2t_1$, with associated load $\lambda(t_1) = 0.25 - 0.2\cos t_1$, is plotted. The function oscillates about the critical value of 1, decaying with time. The time-scale is given by $t_1 = \varepsilon t$.

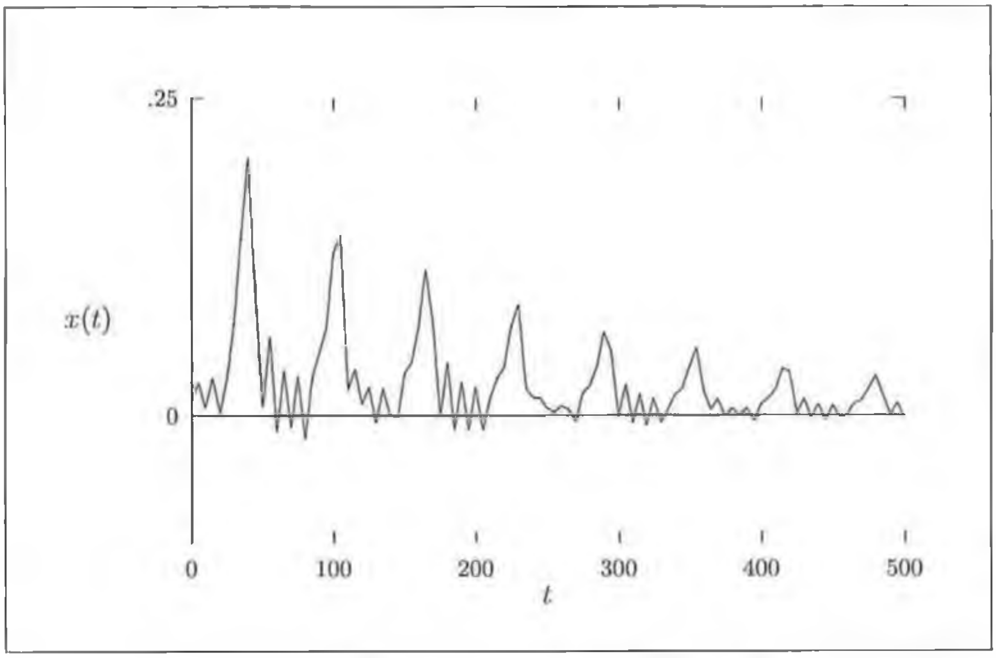

Figure 5.7: The slowly varying solution with load $\lambda(t_1) = 0.25 - 0.2\cos t_1$. The positive peaks in the solution occur at those times when the function $\beta K(t_1)/2t_1$ increases above the critical value of 1. The solution stabilises over time. The time-scale is given by $t_1 = \varepsilon t$.

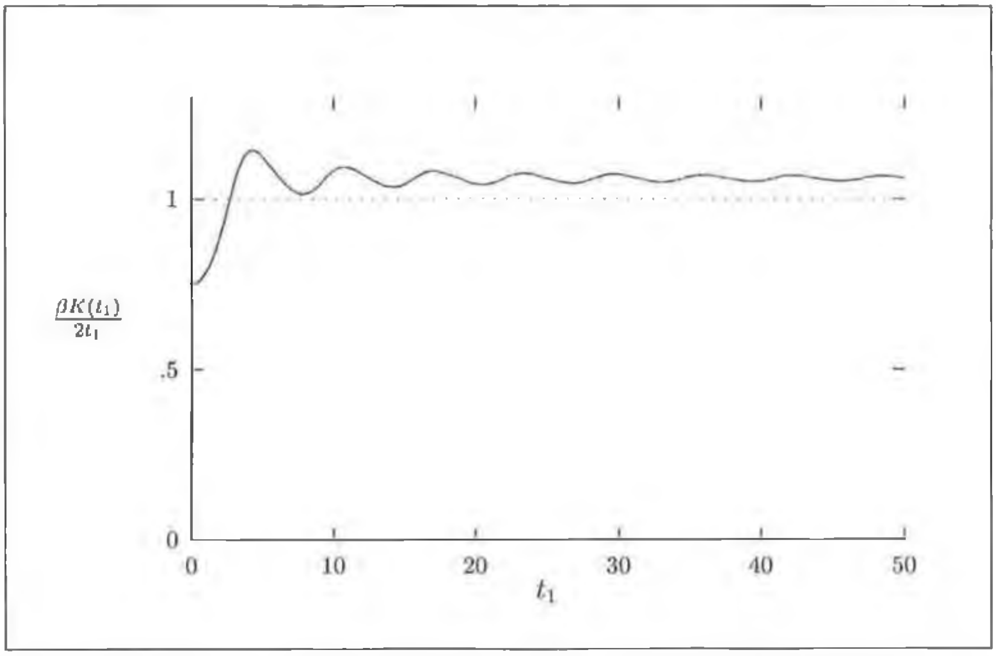

Figure 5.8: The function $\beta K(t_1)/2t_1$ with associated load $\lambda(t_1) = 0.2 - 0.1\cos t_1$, is plotted . The function is oscillating with decaying amplitude, but tends to a value that is greater that the critical value of 1. The time-scale is again given by $t_1 = \varepsilon t$.

in Figure 5.7. Although the load increases periodically above the critical load we see that the solution stabilises as time increases. This is in contrast to the situation shown in Figure 5.9. Here, we plot a solution corresponding to a load $\lambda(t_1) = 0.2 - 0.1\cos t_1$, with critical load given by $G_m/2 = .2$. The solution oscillates evenly about this load. The corresponding function $\beta K(t_1)/2t_1$ is plotted in Figure 5.8.

5.6 The Parametric Load Model

In this section we consider the dynamics of the Link model subjected to a load that oscillates with small amplitude about a constant value. We set $\lambda(t, \varepsilon) = \lambda_0 + \varepsilon \cos \kappa t$

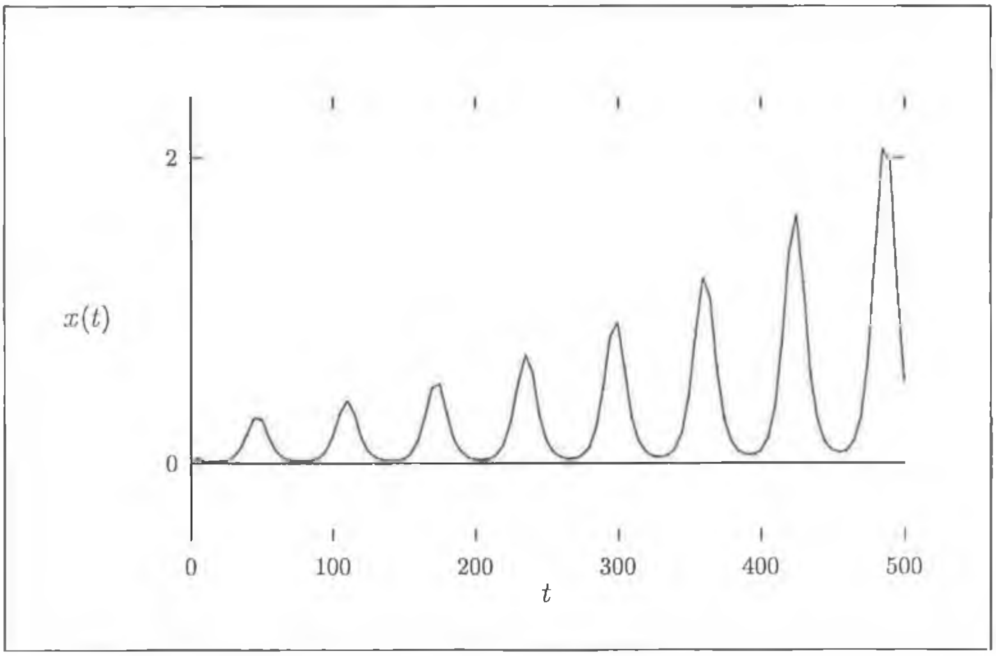

Figure 5.9: The slowly varying solution with load $\lambda(t_1) = 0.2 - 0.1\cos t_1$. The solution becomes unstable, due to the condition $\beta K(t_1)/2t_1 > 1$ being satisfied as $t_1 \to \infty$.

where $\varepsilon \ll 1$. The model equations are

$$\ddot{x} = -(\omega - \varepsilon \cos \kappa t)x - y, \tag{5.6.1a}$$

$$\dot{y} = -\alpha\left\{y + \frac{\beta}{2}x\right\}. \tag{5.6.1b}$$

where $\omega = \frac{1}{2} - \lambda_0$ and $\alpha \ll 1$ and with initial conditions given by $x_1(0) = \zeta_1$, $x_2(0) = \zeta_2$ and $y(0) = \gamma$. The corresponding elastic system, obtained in the limit as $\alpha \to 0$, is the Mathieu equation. We will investigate the effect of the viscoelastic term on the regions of stability and instability of the elastic system, which are well known. In particular we calculate the transition curves between these regions. We begin the analysis with a discussion of the behaviour of solutions to the Mathieu equation, which is based on results in Nayfeh and Mook [23]. We then introduce the viscoelastic element into the model and discuss the effect of its introduction. As the techniques used in calculating the solution are similar to those in Section 5.4 and Section 5.5, some of the details are omitted. Rather, we concentrate on the important points of the analysis.

Analysis of the elastic Mathieu equation

The Mathieu equation is given by

$$\ddot{x} + (\omega - \varepsilon \cos \kappa t)x = 0, \tag{5.6.2}$$

where $\omega = \frac{1}{2} - \lambda_0$ and $\varepsilon \ll 1$. A regular expansion in ε of the solution to (5.6.2) indicates the presence of secular terms and also a breakdown of the solution when $\omega \approx n^2\kappa^2/4$, resulting from the presence of small divisor terms. At these values of ω there is a resonance effect due to the interaction between the natural frequency ω and the frequency of the excitation κ. Using Floquet Theory to analyse the Mathieu equation, we determine that the $\omega\varepsilon$-plane can be separated into regions where the solution is stable (bounded) or unstable (unbounded). The boundaries between these regions are called transition curves and can be represented by $\omega = n^2\kappa^2/4 + \omega_0\varepsilon + \omega_1\varepsilon^2 + \ldots$. To determine the equation of the transition curves and the solution close to these curves, this expansion for ω is substituted into the dynamic equations and the method of multiple scales is applied. The transition curves are seen in Figure 5.10.

The solution to the elastic system without excitation consists of oscillating terms with constant amplitude. The effect of the parametric excitation is to contribute an exponential amplitude to the oscillations. For bounded solutions of the Mathieu equation, the exponential has a complex power, giving a solution that is aperiodic, varying with two frequencies that result from the natural frequency of the elastic system and the parametric excitation frequency. On transition curves the exponential vanishes and the solution is periodic with constant amplitude. For unstable solutions the exponential amplitude has a positive exponent, resulting in an exponentially increasing amplitude and an unbounded

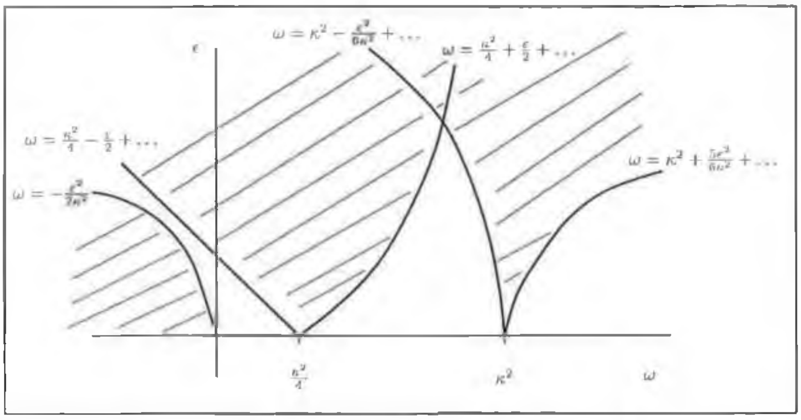

Figure 5.10: The transition curves separating the stable (clear) and unstable (shaded) regions of the $\omega\varepsilon$-plane for the Mathieu equation.

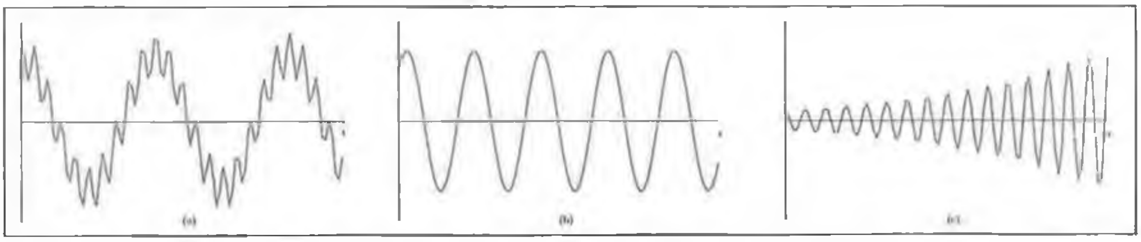

Figure 5.11: Plots of typical solutions to the Mathieu equation. In (a) we have a bounded solution. In (b) we plot the solution on a transition curve while in (c) the solution is unbounded.

solution. In Figure 5.11 we plot typical stable and unstable solution curves to the Mathieu equation.

The viscoelastic Mathieu equation

Now, we wish to investigate the effect of a parametric excitation on the response of the viscoelastic system. We know from Section 5.4 that the viscoelastic system may be unstable due to an exponential creep term. We have seen in the case of the Mathieu equation that the parametric excitation may cause the oscillating terms to become unstable. We concentrate on this latter form of instability in our analysis. Our approach is similar to that described in Nayfeh [23], where the effect that viscous damping has on the regions of stability and instability for the Mathieu equation is investigated. The method of strained parameters is used to determine the equations for the transition curves. We adapt this approach for the viscoelastic model. The method is restrictive in that it only provides solutions to the system on the transition curves. If we required the solution in a neighbourhood of the transition curves we would have to use a more powerful method, such as multiple scales. This is the approach taken by Murphy [24]. The equations of motion are given by (5.6.1). We look for a solution in the form

$$x(t;\varepsilon) = X_0(t) + \varepsilon X_1(t) + \varepsilon^2 X_2(t) + \dots \tag{5.6.3a}$$

$$y(t;\varepsilon) = Y_0(t) + \varepsilon Y_1(t) + \varepsilon^2 Y_2(t) + \dots \tag{5.6.3b}$$

We also expand ω as an asymptotic sequence in ε at the resonance points. We have

$$\omega = \frac{n^2\kappa^2}{4} + \varepsilon\omega_1 + \varepsilon^2\omega_2 + \dots \tag{5.6.4}$$

for $n = 0, 1, \dots$. We determine values for the ω_i by imposing the condition that secular terms be removed from the oscillating component of the solution. The solution obtained in this way is valid on the transition curves and results in an expression for the transition curves.

The creep effect and the parametric effect result in two small parameters, ε and α, for the problem. In order that neither effect dominates, we require that $\alpha = \varepsilon(\alpha_0 + \alpha_1\varepsilon + \dots)$, where $\alpha_0, \alpha_1 \dots$ are constants. We consider two cases, $\omega_0 = \kappa^2/4$ and $\omega_0 = \kappa^2$, (corresponding to $n = 1$ and $n = 2$), and calculate the transition curves at these resonance points. Substituting (5.6.3) and (5.6.4) for $x(t)$, $y(t)$ and ω into (5.6.1) and expanding the system of equations in ε results in the following sequence of problems,

$O(1)$

$$\ddot{X}_0 + \omega_0 X_0 = -Y_0, \tag{5.6.5a}$$

$$\dot{Y}_0 = 0. \tag{5.6.5b}$$

$O(\varepsilon)$

$$\ddot{X}_1 + \omega_0 X_1 = -Y_1 + X_0 \cos \kappa t - \omega_1 X_0, \tag{5.6.6a}$$

$$\dot{Y}_1 = -\alpha_0 (Y_0 + \beta/2\, X_0). \tag{5.6.6b}$$

$O(\varepsilon^2)$

$$\ddot{X}_2 + \omega_0 X_2 = -Y_2 + X_1 \cos \kappa t - \omega_1 X_1 - \omega_2 X_0, \tag{5.6.7a}$$

$$\dot{Y}_2 = -\alpha_0 (Y_1 + \beta/2\, X_1) - \alpha_1 (Y_0 + \beta/2\, X_0). \tag{5.6.7b}$$

Case 1. $\omega_0 = \frac{\kappa^2}{4}$

We solve (5.6.5) to get $Y_0(t) = C_0$ and $X_0(t) = A_0 \cos \omega_0 t + B_0 \sin \omega_0 t - C_0/\omega_0$. These expressions are substituted into (5.6.6b) to give Y_1. Removing secular terms from the oscillating components in (5.6.6a) results in the following conditions which must be satisfied,

$$\sin \frac{\kappa t}{2} \left(\frac{\alpha_0 \beta A_0}{\kappa} - B_0 \left[\omega_1 + \frac{1}{2} \right] \right) = 0, \tag{5.6.8a}$$

$$\cos \frac{\kappa t}{2} \left(\frac{\alpha_0 \beta B_0}{\kappa} + A_0 \left[\omega_1 - \frac{1}{2} \right] \right) = 0, \tag{5.6.8b}$$

where A_0 and B_0 are non-zero constants. Solving (5.6.8) for ω_1 gives

$$\omega_1 = \pm \sqrt{\frac{1}{4} - \left(\frac{\alpha_0 \beta}{\kappa} \right)^2}. \tag{5.6.9}$$

Substituting (5.6.9) into (5.6.4), we write the equation for the transition curves to $O(\varepsilon)$ at $\omega_0 = \kappa^2/4$ as

$$\omega = \frac{\kappa^2}{4} \pm \sqrt{\frac{\varepsilon^2}{4} - \frac{\alpha^2 \beta^2}{\kappa^2}}. \tag{5.6.10}$$

This transition curve is discussed in the next section.

Case 2. $\omega_0 = \kappa^2$

The $O(1)$ equations are solved as in the previous case to give $Y_0(t) = C_0$ and $X_0(t) = A_0 \cos \omega_0 t + B_0 \sin \omega_0 t - C_0/\omega_0$. Using these expressions for X_0 and Y_0 we can solve (5.6.6b) for Y_1. Then, substituting for X_0, Y_0 and Y_1 into (5.6.6a) gives the following conditions for the elimination of secular terms from the oscillating components at the $O(\varepsilon)$ level,

$$\left(\frac{A_0\alpha_0}{\kappa} - \omega_1 B_0\right) \sin \kappa t = 0, \tag{5.6.11a}$$

$$\left(\frac{B_0\alpha_0}{\kappa} + \omega_1 A_0\right) \cos \kappa t = 0, \tag{5.6.11b}$$

where A_0 and B_0 are non-zero. Solving (5.6.11) for α_0 and ω_1 gives $\alpha_0 = \omega_1 = 0$. Thus, we require the $O(\varepsilon^2)$ equations to determine the transition curve at $\omega_0 = \kappa^2$. Using the results from the $O(1)$ and $O(\varepsilon)$ level we can solve (5.6.7b) for Y_2. Finally, substituting the expressions for X_0, X_1 and Y_2 into (5.6.7a) results in the following two conditions which must be satisfied if secular terms are to be removed from the solution at this order,

$$\left(\frac{A_0\alpha_1\beta}{2\kappa} - B_0\left[\frac{1}{12k^2} - \omega_2\right]\right) \sin \kappa t = 0, \tag{5.6.12a}$$

$$\left(\frac{B_0\alpha_1\beta}{2\kappa} - A_0\left[\frac{5}{12k^2} - \omega_2\right]\right) \cos \kappa t = 0. \tag{5.6.12b}$$

We solve (5.6.12) for ω_2 to get

$$\omega_2 = \frac{1}{6\kappa^2} \pm \sqrt{\left(\frac{1}{4\kappa^2}\right)^2 - \frac{\alpha_1^2\beta^2}{4\kappa^2}} \tag{5.6.13}$$

The equation for the transition curve at $\omega_0 = k^2$ is got by substituting (5.6.13) into (5.6.4), giving

$$\omega = \kappa^2 + \frac{\varepsilon^2}{6\kappa^2} \pm \sqrt{\left(\frac{\varepsilon^2}{4\kappa^2}\right)^2 - \frac{\alpha^2\beta^2}{4\kappa^2}}. \tag{5.6.14}$$

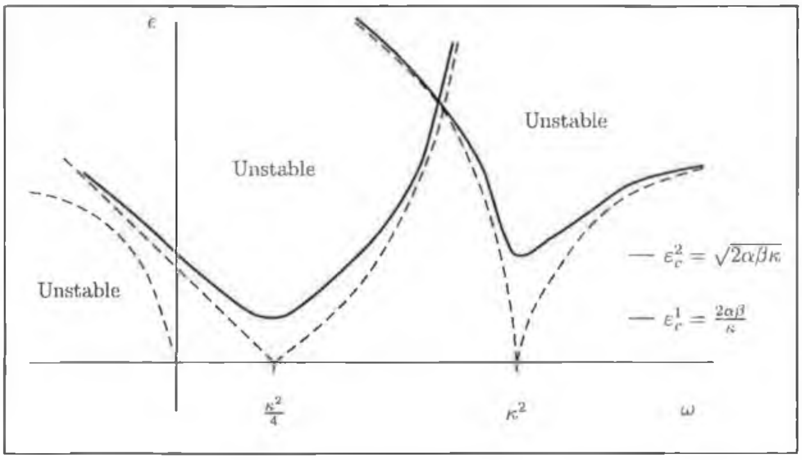

Figure 5.12: Comparison of the viscoelastic transition curves(solid) with those of the Mathieu equation(dashed). The critical values are marked by ε_c^1 for the transition curve at $\omega_0 = \kappa^2/4$ and ε_c^2 for the transition curve at $\omega_0 = \kappa^2$

Analysis of the viscoelastic transition curves

The transition curves for the viscoelastic system are plotted in Figure 5.12. The Mathieu equation curves are included for comparison. Examining the transition curve at $\omega = \kappa^2/4$ we see that it is raised from the ω-axis and is narrow compared to the Mathieu equation curve. There is a critical (minimum) value of the transition curve given by $\varepsilon_c^1 = 2\alpha\beta/\kappa$. For values of ε satisfying $\varepsilon < \varepsilon_c^1$, the system is stable. Thus, the effect of introducing the viscoelastic element is to increase the region of stability and thus it has a stabilising effect on the parametric elastic system. Similarly, we see that the transition curve at $\omega = \kappa^2$ is raised and narrowed compared to the corresponding curve for the elastic case. The critical (minimum) value for ε given by $\varepsilon_c^2 = \sqrt{2\kappa\alpha\beta}$. Thus, the region of stability is again increased.

It is important to distinguish between instabilities due to the parametric excitation and those due to creep. The parametric excitation can destabilise the constant load system by introducing an instability into the oscillating terms while the viscoelastic effect is to introduce an instability by way of an exponentially increasing term. Thus, while we have indicated regions of stability and instability in Figure 5.12, these refer only to instability due to the oscillating terms. There may be an instability due to creep present also and this would eventually destabilise the system.

Chapter 6

Postscript

6.1 Introduction

In this chapter we present a number of issues relating to the dynamics of the Link model. We discuss the system in light of recent work that has been done on nonlinear jump and bifurcation problems with slowly varying parameters. Much of this work is based on the method of multiple time scales and averaging methods, and concerns the calculation of an asymptotic solution to a system of differential equations. We introduce some of the main ideas discussed in Haberman [12] and Marée [22]. Both Haberman and Marée investigate systems with a slowly varying parameter μ. As μ varies through a critical value, corresponding to a bifurcation or jump phenomena, the motion of the system becomes unstable and a new equilibrium position is attained. Although these differential systems differ fundamentally from the the system of equations describing the viscoelastic Link model, the theory offers a new insight into our problem and suggests that further research in this direction may be fruitful. In particular, the use of averaging methods suggests that the application of the theory of near-identity averaging transformations should be investigated. This theory has evolved from the original method of averaging proposed in 1937 by Krylov and Bogoliubov [2] and is presented in detail in Cole and Kevorkian [6]. For a system with a small parameter α, one attempts to find an adiabatic invariant to $O(\alpha^k)$. The procedure involves an averaging transformation of the system. We also discuss the related multiple scale technique due to Kuzmak [20], who investigates strictly nonlinear second-order equation with solutions which are slowly modulated oscillations. We begin the discussion with a background to some of the ideas just mentioned and present some problems that have been examined. An introduction to the theory of adiabatic invariants is presented in Appendix D and a simple example illustrates the idea.

6.2 Recent Developments in Bifurcation Problems with Slowly Varying Parameters

In this section we outline the recent work on bifurcation problems with slowly varying parameters discussed in Haberman [12] and Marée [22]. In Haberman, second order systems of the form

$$\ddot{x} = F(x, \mu) \tag{6.2.1}$$

are considered, where μ is a bifurcation parameter. The nonlinear function $F(x, \mu)$ depends on its arguments in such a way that the system has a either a transcritical bifurcation, pitchfork bifurcation or there is a jump phenomenon. Physically, these systems can be represented by models similar to the Link model. Haberman allows the bifurcation parameter μ to vary slowly by setting $\mu = \mu(\alpha t)$. He then investigates the behaviour of the solution as the bifurcation parameter passes through a critical value. Multiple time scale and matched asymptotic methods are used. The leading order behaviour in the transition layer at the critical point for various phenomena is governed by the first and second Painlevé transcendents (see Ince [19]). Typical behaviour in the case of a transcritical bifurcation is illustrated in Figure 6.1. The solution is initially stable about the zero equilibrium position. As the critical value is passed, the solution may transfer onto the secondary branch of equilibria or it may become unstable and move to some other equilibrium position. In Marée[22], damped second order systems of the form

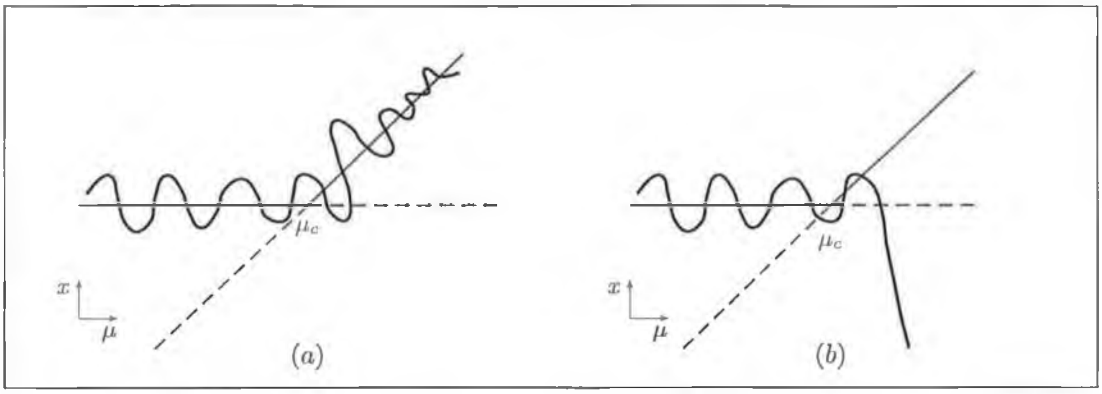

Figure 6.1: The slowly varying solution for a system with a transcritical bifurcation. The solution in (a) remains stable after passing through the bifurcation point $\mu = \mu_c$, moving onto the second equilibrium path. In (b) the solution becomes unstable as the critical point is passed.

$$\ddot{x} = -\alpha k \dot{x} + F(x, \mu(\alpha, t)), \tag{6.2.2a}$$

$$\dot{\mu} = \alpha \tag{6.2.2b}$$

are studied. Thus, the bifurcation parameter $\mu(\alpha, t)$ is slowly varying. This system differs from that discussed in [12] in that there is damping and the rate of change dependence of the bifurcation parameter is specified. Marée determines asymptotic approximations to the solution using the method of averaging and matched asymptotic expansions. Again, the local transition behaviour is described by the first and second Painlevé transcendent. For $\alpha \ll 1$ and $G_m/2 < \lambda < 1/2$, the motion of the system (3.3.1) can be compared to that of (6.2.1) and (6.2.2) in that it appears to stabilise about a zero position but becomes unstable at some critical time. Although the motions are similar, there is a fundamental difference between (6.2.1) and (6.2.2), and the system described by (3.3.1). The former are examples of turning point problems, while the latter has a constant bifurcation parameter and it is the slow onset of creep, with an $O(\alpha)$ rate of change, that destabilises the solution. However, we can view the creep function $y(t)$ as a time-dependent parameter with a rate of change that is of order $O(\alpha)$. In this case, we can make a connection between the creep function $y(t)$ of the system (3.3.1) and the bifurcation parameters of (6.2.1) and (6.2.2). This has been the basis of further work on the Link model.

Averaging Methods

In his 1959 paper, Kuzmak [20] investigates strictly nonlinear second order equations of the form

$$\ddot{x} + g(x, \tau) + \alpha h(x, \dot{x}, \tau) = 0, \tag{6.2.3}$$

where $\tau = \alpha t$. The solutions of (6.2.3) are slowly modulated oscillations. As $\alpha \to 0$, the reduced nonlinear oscillator

$$\ddot{x} + g(x, 0) = 0 \tag{6.2.4}$$

has periodic solutions in some interval $x_0 < x < x_1$. Kuzmak works out the $O(1)$ solution using independent time scales and later work extends these results to higher order. Like (6.2.3), the system (3.3.1) is Hamiltonian when $\alpha \to 0$ and in this case the energy is constant. For $0 < \alpha \ll 1$, the energy varies slowly. While the technique due to Kuzmak cannot be applied directly to (3.3.1), it does suggest that we look at the energy of system and apply some variant of the averaging method.

The method of near-identity averaging transformations would seem to be a possible candidate. This method is applied to systems in the form

$$\frac{dp}{dt} = \alpha F(p, q, t, \alpha), \tag{6.2.5a}$$

$$\frac{dq}{dt} = \omega(p, t, \alpha) + \alpha G(p, q, t, \alpha), \tag{6.2.5b}$$

where $O < \alpha \ll 1$ and the functions F and G are $O(1)$, 2π-periodic functions of q. The basic idea is to transform the dependent variables p and q to new variables P and Q in terms of which the system is as simple as possible to a given order in α. The transformed system is then solved and the solution is used in the transformations relations linking (p, q) to (P, Q) to obtain a solution to the original problem. The variable P will be an adiabatic invariant to $O(\alpha)$ for (6.2.5). One possible advantage of this approach is that an approximate solution to the full nonlinear problem may be possible if suitable transformations are found. However, before the method of near-identity averaging transformations can be applied, we need an initial transformation $(x, \dot{x}) \rightarrow (p, q)$ to express (3.3.1) in the form of (6.2.5). The usual way to achieve this is to let p be a function of the energy E of the reduced system and let q be the phase. Such a transformation is used by Baker, Moore and Spiegel [1] who investigate a system of equations that is similar to (3.3.1). In Appendix D there is a definition of adiabatic invariance and an example that illustrates this type of transformation. While we can define a number of energy functionals for (3.3.1), it remains a goal of further research to successfully obtain a near-identity transformation for the system.

Chapter 7

Conclusions

In this thesis we have considered the dynamic and quasi-static motion of a nonlinear viscoelastic Link model. We have formalised and extended the work done by Hunt and Thompson [18] and Hayman [14, 15]. In Chapter 3 we analysed the dynamic system for the Link model, starting with the elastic system without imperfection. Three equilibrium branches are identified. The stability analysis indicates that the system undergoes a transcritical bifurcation at the intersection points of these equilibria. In the imperfect case, the transcritical bifurcation property is lost and the critical load for the system is reduced in absolute value. The perfect and imperfect viscoelastic system is also studied. By projecting the equilibria of the viscoelastic system onto the $x\lambda$-plane, we are able to compare them with the equilibria of the elastic system. We have shown that the effect of the viscoelastic element is to scale the elastic critical load by the factor G_m. This is true in both the perfect case and the imperfect case. Conditions on the system parameters λ, α and G_m are determined for the perfect system close to the zero equilibrium branch. We find that for $G_m < 1$ and values of λ satisfying $0 \leq \lambda < 1/2$ that there exists some value of $\alpha > 0$ such that the characteristic equation of the linearised system has two complex roots and one real root. These results are used in Chapter 5 when constructing asymptotic approximations to the solution of the linearised system.

In Chapter 4 we study the quasi-static approximation to the nonlinear system. We allow the creep stress to have a non-trivial initial value. This contributes to the imperfection in the model, allowing an increased set of initial positions for the system. This results in a greater range of possible motions in comparison to those indicated in [14, 15]. We have shown that the location of the quasi-static equilibrium curves is equivalent to those of the dynamic system. However, the stability properties differ. There is a change in the stability of the quasi-static equilibrium curve at the point where it intersects the elastic critical locus. To the right of this intersection point the equilibrium curve is stable. This is in contrast to the results indicated by the dynamic analysis. Thus, the quasi-static analysis indicates stability at some equilibrium points, corresponding to large deflections, where the dynamic analysis indicates that the system is unstable. This is one of the main findings of the thesis.

In Chapter 5 we have determined asymptotic approximations to the solution of the perfect model problem linearised about zero. We analyse the model subject to three loading strategies; the constant load problem, the slowly varying load problem and the parametric loading problem. The results of the constant load problem agree with the analytic results from Chapter 3. In particular, we show that an exponential term decays (grows) for values of load satisfying $\lambda < (>) \lambda_c$, resulting in a stable (unstable) solution. For the slowly varying load problem we derive a condition which the time-dependent load must satisfy for the system to remain stable. We show that in certain cases, the system remains stable even if the load occasionally increases above the critical value for the constant load problem. Finally, we look at the parametric load problem. In the elastic case, the problem reduces to the Mathieu equation. We show that the viscoelastic element has a stabilising effect on the oscillations and that there is a minimum value of ε below which the system has stable oscillations.

Appendix A

An Overview of Differential Equation Theory

A.1 Introduction

In this appendix we give a brief overview of the theory of ordinary differential equations. The purpose of the appendix is to provide a background to some of the concepts which are discussed in the thesis. For a more detailed exposition we refer the reader to Guckenheimer and Holmes [11], Hale and Koçak [13] and Glendinning [10]. We begin with definitions of differential equation systems, their solutions and the stability properties of the solutions. We discuss linear and non-linear systems and the relationship between them. There is an introduction to bifurcation theory and the application of the Centre Manifold theorem at bifurcation points. We conclude the overview with a section on conservative systems and their properties.

A.2 Differential equations and stability.

A differential equation of order n is an equation in the form

$$\frac{d^n x}{dt^n} = F\left(x, \frac{dx}{dt}, ..., \frac{d^{n-1}x}{dt^{n-1}}, t\right), \tag{A.2.1}$$

together with a set of initial conditions at $t = t_0$,

$$x(t_0) = a_0, \frac{dx}{dt}(t_0) = a_1, ..., \frac{d^{n-1}x}{dt^{n-1}}(t_0) = a_{n-1}.$$

We can rewrite (A.2.1) as a system of 1^{st} order equations by setting

$$\frac{d^k x}{dt^k} = x_{k+1}$$

for $0 \leq k \leq n-1$. The system of 1^{st}-order equations is

$$\dot{x_k} = x_{k+1}, \qquad 1 \leq k \leq n-1 \tag{A.2.2a}$$

$$\dot{x_n} = F\left(x_1, ..., x_n, t\right). \tag{A.2.2b}$$

We will consider equations of the form

$$\dot{\mathbf{x}} = \mathbf{f}(\mathbf{x}, t) \qquad \mathbf{x} \in \mathbf{R}^n, \tag{A.2.3}$$

where $\mathbf{f} : \mathbf{R}^n \times \mathbf{R}^n \to \mathbf{R}^n$. So, for (A.2.2), we have $\mathbf{f}(\mathbf{x}, t) = (x_2, ...x_n, F(x_1, ..., x_n, t))$ In general the function $\mathbf{f}(\mathbf{x}, t)$ is non-linear. We now give some fundamental results in the theory of ordinary differential equations.

Theorem 4. *(Local Existence and Uniqueness)*

Suppose $\dot{\mathbf{x}} = \mathbf{f}(\mathbf{x}, t)$ and $\mathbf{f} : \mathbf{R}^n \times \mathbf{R} \to \mathbf{R}^n$ is continuously differentiable. Then there exists maximal $t_1 > 0$ and $t_2 > 0$ such that a solution $\mathbf{x}(t)$ with $\mathbf{x}(t_0) = \mathbf{x}_0$ exists and is unique for all $t \in (t_0 - t_1, t_0 + t_2)$.

To emphasize the dependence of the solution $\mathbf{x}(t)$ on the initial condition we write the solution as $\varphi(t, \mathbf{x}_0)$ where $\varphi(t, \mathbf{x}_0) = \mathbf{x}(t)$ and $\varphi(t_0, \mathbf{x}_0) = \mathbf{x}_0$. $\varphi(t_0, \mathbf{x}_0)$ is called the flow through $\mathbf{x}_0$ at time $t = t_0$. Properties of solutions of the system can be defined in terms of the flow. (A.2.3) is said to be autonomous if the time t does not appear explicitly in the right hand side, so that $\mathbf{f} = \mathbf{f}(\mathbf{x})$. There is no loss of generality in taking $t_0 = 0$ if this case. For autonomous systems, the solution can be represented as an integral curve in some phase space.

Definition 1. *The curve $(x_1(t), ..., x_n(t))$ in $\mathbf{R}^n$ is an integral curve of $\dot{\mathbf{x}} = \mathbf{f}(\mathbf{x})$ iff*

$$(\dot{x}_1(t), ..., \dot{x}_n(t)) = f(x_1(t), ..., x_n(t))$$

for all t. Thus, the tangent to the integral curve at $(x_1(t_k), ..., x_n(t_k)$ is $\mathbf{f}(x_1(t_k), ..., x_n(t_k))$.

While it may be difficult to determine an exact solution, information about the behaviour of the system can be deduced from these integral curves.

For many naturally occurring systems there are several associated conserved quantities. These quantities are called first integrals.

Definition 2. *A real-valued, non-constant C^1 function*

$$H : \mathbf{R}^n \to \mathbf{R};\ \mathbf{x} \mapsto H(\mathbf{x})$$

is called a first integral of the differential equation $\dot{\mathbf{x}} = \mathbf{f}(\mathbf{x})$ if H is constant on every integral curve, that is, for any solution $\mathbf{x}(t)$ with initial value $\mathbf{x}(t_0) = \mathbf{x}_0$, the composite function satisfies $H(\mathbf{x}(t)) = H(\mathbf{x}_0)$ for all t for which the solution is defined.

A system containing a conserved quantity is said to be conservative. In certain mechanical systems the total energy of the system is conserved along integral curves. We discuss conserved systems in more detail in Section A.6.

Definition 3. *A point $\bar{\mathbf{x}} \in \mathbf{R}^n \times \mathbf{R}$ is an equilibrium point* (A.2.3) *if*

$$\mathbf{f}(\bar{\mathbf{x}}) = 0.$$

Equilibrium points are fixed points of the flow so we have $\varphi(t, \bar{\mathbf{x}}) = \bar{\mathbf{x}}$. An equilibrium point $\bar{\mathbf{x}}$ is said to be non-degenerate if $\mathbf{f}'(\bar{\mathbf{x}}) \neq 0$. The behaviour of the system close to equilibrium points can be deduced from a stability analysis of these points.

Definition 4. *An equilibrium point $\bar{\mathbf{x}}$ of $\dot{\mathbf{x}} = \mathbf{f}(\mathbf{x})$ is said to stable iff for all $\varepsilon > 0$ there exists a $\delta > 0$ s.t. if $\|\mathbf{x}_0 - \bar{\mathbf{x}}\| < \delta$ then $\|\varphi(t, \mathbf{x}_0) - \bar{\mathbf{x}}\| < \varepsilon$ for all $t \geq 0$. An equilibrium point is said to be unstable if it is not stable.*

Definition 5. *An equilibrium point $\bar{\mathbf{x}}$ of $\dot{\mathbf{x}} = \mathbf{f}(\mathbf{x})$ is asymptotically stable if it is stable and, in addition, there exists a δ s.t. if $\|\mathbf{x}^0 - \bar{\mathbf{x}}\| < \delta$ then $\|\varphi(t, \mathbf{x}^0) - \bar{\mathbf{x}}\| \to 0$ as $t \to \infty$.*

From the definitions we see that a fixed point is stable if solutions which start close to the fixed point remain close to the fixed point for all time. Asymptotic stability implies that a solution that starts close to a fixed point will tend towards the fixed point in the limit as $t \to \infty$.

Suppose that that the nonlinear differential equation (A.2.3) has a fixed point at $\bar{\mathbf{x}}$, then $\mathbf{f}(\mathbf{x})$ can be expanded in a Taylor series about $\bar{\mathbf{x}}$ to give

$$\dot{\mathbf{x}} = Df(\bar{\mathbf{x}})\ \mathbf{x} + h.o.t.$$

where $Df(\bar{\mathbf{x}})$ is the Jacobian matrix of $\mathbf{f}$ evaluated at $\bar{\mathbf{x}}$ defined as

$$Df(\bar{\mathbf{x}}) = \begin{pmatrix} \frac{\partial f_1}{\partial x_1}(\bar{\mathbf{x}}) & \frac{\partial f_1}{\partial x_2}(\bar{\mathbf{x}}) & \dots & \frac{\partial f_1}{\partial x_n}(\bar{\mathbf{x}}) \\ \frac{\partial f_2}{\partial x_1}(\bar{\mathbf{x}}) & \frac{\partial f_2}{\partial x_2}(\bar{\mathbf{x}}) & \dots & \frac{\partial f_2}{\partial x_n}(\bar{\mathbf{x}}) \\ . & . & & . \\ . & . & & . \\ . & . & & . \\ \frac{\partial f_n}{\partial x_1}(\bar{\mathbf{x}}) & \frac{\partial f_n}{\partial x_2}(\bar{\mathbf{x}}) & \dots & \frac{\partial f_n}{\partial x_n}(\bar{\mathbf{x}}) \end{pmatrix} \tag{A.2.4}$$

and $h.o.t$ denotes higher order terms. The equation

$$\dot{\mathbf{x}} = Df(\bar{\mathbf{x}})\ \mathbf{x} \tag{A.2.5}$$

is the linearisation of (A.2.3) at $\bar{\mathbf{x}}$.

Definition 6. *A fixed point is said to be hyperbolic if the eigenvalues of the Jacobian matrix defined at the fixed point have non-zero real parts, otherwise it is non-hyperbolic.*

The stability of hyperbolic fixed points can be determined by calculating the eigenvalues of (A.2.4) evaluated at the fixed point.

Proposition 7. *If the eigenvalues of* (A.2.4), *evaluated at a hyperbolic fixed point* $\bar{\mathbf{x}}$, *have strictly negative real parts then the fixed point* $\bar{\mathbf{x}}$ *is asymptotically stable.*

Proposition 8. *If at least one of the eigenvalues of* (A.2.4), *evaluated at a fixed point* $\bar{x}$, *has a positive real part then the fixed point* $\bar{x}$ *is unstable.*

We can calculate solutions to (A.2.5) system directly. Let

$$\dot{\mathbf{x}} = \mathbf{A}\ \mathbf{x} \tag{A.2.6}$$

be a linear system where $\mathbf{A}$ is a matrix with constant coefficients. Given an initial condition vector $\mathbf{x}_0$ we can write the solution to (A.2.6) as

$$\varphi(t, \mathbf{x}_0) = \mathbf{x}_0 e^{\mathbf{A}t}.$$

So, provided we can calculate this exponential, we can write down solutions to the linear system for any given initial condition.

A.3 Invariant subspaces

While information about the location and stability of fixed points of a system is crucial to understanding the dynamics of the system, we would also like to be able to say something about the long term behaviour of the system. To do this we first need to define invariant subspaces.

Definition 7. *A set M is invariant iff $\forall\ \mathbf{x}_0 \in M$, $\varphi(t, \mathbf{x}_0) \in M$ for all t. A set is forward (resp. backward) invariant if $\forall\ \mathbf{x}_0 \in M, \varphi(t, \mathbf{x}_0) \in M$ for all $t > 0$ (resp. $t < 0$).*

A point in the invariant set will remain in that set during the motion of the system. In the case of (A.2.6) the eigenspaces are invariant subspaces.

Definition 8. *Let $\mathbf{v}_1, ..., \mathbf{v}_{n_s}$ be the n_s eigenvectors of $\mathbf{A}$ whose eigenvalues have strictly negative real parts. Then*

$$E^s(\bar{\mathbf{x}}) = span\{\mathbf{v}_1, ..., \mathbf{v}_{n_s}\}$$

is the stable manifold of $\bar{\mathbf{x}}$.

Definition 9. *Let* $\mathbf{v}_1, ..., \mathbf{v}_{n_u}$ *be the* n_u *eigenvectors of* $\mathbf{A}$ *whose eigenvalues have strictly positive real parts. Then*

$$E^u(\bar{\mathbf{x}}) = span\{\mathbf{v}_1, ..., \mathbf{v}_{n_u}\}$$

is the unstable manifold of $\bar{\mathbf{x}}$.

Definition 10. *Let* $\mathbf{v}_1, ..., \mathbf{v}_{n_c}$ *be the* n_c *eigenvectors of* $\mathbf{A}$ *whose eigenvalues have zero real parts. Then*

$$E^c(\bar{\mathbf{x}}) = span\{\mathbf{v}_1, ..., \mathbf{v}_{n_c}\}$$

is the center manifold of $\bar{\mathbf{x}}$.

Solutions which lie on the stable manifold of $\bar{\mathbf{x}}$ are characterised by exponential decay while those on the unstable manifold are characterised by exponential growth.

A.4 The Nonlinear System $\dot{\mathbf{x}} = \mathbf{f}(\mathbf{x})$

While the linear system, (A.2.6) can be solved explicitly with the solution given by $\varphi(t, \mathbf{x}_0) = \mathbf{x}_0 e^{\mathbf{A}t}$, in general we cannot solve the non-linear system $\dot{\mathbf{x}} = \mathbf{f}(\mathbf{x})$. However, by examining the fixed points of the non-linear system we can determine some facts about its dynamic behaviour. There are two fundamental results of dynamical systems theory which relate the behaviour of the non-linear system to that of the linearised system close to fixed points. Denote the linearisation of $\dot{\mathbf{x}} = \mathbf{f}(\mathbf{x})$ at the fixed point $\bar{\mathbf{x}}$ by

$$\dot{\mathbf{x}} = Df(\bar{\mathbf{x}})\ \mathbf{x}, \quad \mathbf{x} \in \mathbf{R}^n \tag{A.4.1}$$

where $Df(\bar{\mathbf{x}})$ is the Jacobian matrix of $\mathbf{f}$ evaluated at $\bar{\mathbf{x}}$.

Theorem 5. *(Hartman-Grobman)*

If $Df(\bar{\mathbf{x}})$ has no zero or purely imaginary eigenvalues then there is a homeomorphism $\mathbf{h}$ *defined on some neighbourhood U of $\bar{\mathbf{x}}$ which takes orbits of the nonlinear flow to those of the linear flow $e^{Df(\bar{x})t}$. The homeomorphism can be chosen so that parameterisation of orbits by time is preserved.*

Let U be some neighbourhood of $\bar{\mathbf{x}}$, a fixed point of $\dot{\mathbf{x}} = \mathbf{f}(\mathbf{x})$. We define the local stable manifold $W^s_{loc}(\bar{\mathbf{x}})$ by

$$W^s_{loc}(\bar{\mathbf{x}}) = \{\mathbf{x} \in U \mid \varphi(t, \mathbf{x}_0) \to \bar{\mathbf{x}} \text{ as } t \to \infty, \varphi(t, \mathbf{x}_0) \in U \text{ for all } t \geq 0\} \tag{A.4.2}$$

and the local unstable manifold $W^u_{loc}(\bar{\mathbf{x}})$ of $\bar{\mathbf{x}}$ by

$$W^u_{loc}(\bar{\mathbf{x}}) = \{\mathbf{x} \in U \mid \varphi(t, \mathbf{x}_0) \to \bar{\mathbf{x}} \text{ as } t \to -\infty, \varphi(t, \mathbf{x}_0) \in U \text{ for all } t \leq 0\} \tag{A.4.3}$$

Theorem 6. *(Stable Manifold Theorem) Suppose that $\dot{\mathbf{x}} = \mathbf{f}(\mathbf{x})$ has a hyperbolic fixed point $\bar{x}$ and that E^s and E^u are the stable and unstable manifolds of the linearised system $\dot{\mathbf{x}} = \mathbf{Df}(\bar{\mathbf{x}})\ \mathbf{x}$. Then there exists local stable and unstable manifolds $W^s_{loc}(\bar{\mathbf{x}}), W^u_{loc}(\bar{\mathbf{x}})$ to $\dot{\mathbf{x}} = \mathbf{f}(\mathbf{x})$, of the same dimension as E^s and E^u. These manifolds are tangential to E^s and E^u at $\bar{\mathbf{x}}$ and as smooth as the function* $\mathbf{f}$.

The stable manifold theorem shows that the local structure of hyperbolic fixed points of the non-linear flow is the same as for the linearised flow. We can also say something about perturbations of the non-linear system.

Proposition 9. *Let $\bar{\mathbf{x}}$ be a hyperbolic fixed point of $\dot{\mathbf{x}} = \mathbf{f}(\mathbf{x})$ and let*

$$\dot{\mathbf{x}} = \mathbf{f}(\mathbf{x}) + \varepsilon\mathbf{v}(\mathbf{x}), \quad \varepsilon \ll 1 \tag{A.4.4}$$

be a small perturbation to the non-linear system. Then (A.4.4) *has a hyperbolic fixed point close to $\bar{\mathbf{x}}$ which is of the same type as $\bar{\mathbf{x}}$.*

Thus the dynamics in a neighbourhood of a hyperbolic fixed point are invariant to small perturbations of the defining differential equation. The proof is a consequence of the implicit function theorem.

A.5 Bifurcation Theory

In applications, the governing differential equation can depend on a number of parameters. These parameters will typically have some physical representation. For example, the equation for a structure that is subject to loading over time will have a parameter that measures the load at a given time. Bifurcation theory is concerned with the qualitative changes to the topological features of flow as one or more parameters are varied. In particular, we are interested in values of the bifurcation parameters at which these qualitative changes occur. A fundamental observation is that for hyperbolic fixed points the behaviour of the flow is completely determined by the linearised flow and that the topological features at a fixed point persist under small perturbations to the defining equations. Hence, bifurcations of fixed points can only occur at parameter values for which the fixed point is non-hyperbolic. Let

$$\dot{\mathbf{x}} = \mathbf{f}(\mathbf{x}, \mu) \tag{A.5.1}$$

where $\mathbf{f} : \mathbf{R}^n \times \mathbf{R}^k \to \mathbf{R}^n$ be an autonomous system of equations depending on the k-dimensional parameter μ. The equilibrium points of (A.5.1) are given by solutions of the equation $\mathbf{f}(\mathbf{x}, \mu) = 0$. The Implicit Function theorem implies that these equilibria are described by smooth functions of μ away from non-hyperbolic fixed points. These functions describe a branch of equilibria. At a non-hyperbolic equilibrium point $(\bar{\mathbf{x}}, \bar{\mu})$, several branches may come together. In such a case, the point $(\bar{\mathbf{x}}, \bar{\mu})$ is called a bifurcation point. It is useful to plot the branches of equilibria as functions of the parameter. These figures are referred to as bifurcation diagrams. Bifurcations that occur repeatedly are classified according to schemes which are based on concepts of transversality and co-dimension. One of the most important techniques for studying bifurcations is based on the non-hyperbolic equivalent of the Stable Manifold Theorem, called the Centre Manifold Theorem. This generalises the idea of the centre manifold for linear systems to nonlinear systems.

Theorem 7. *(Centre Manifold Theorem.) Let* $\mathbf{f} \in C^r(\mathbf{R}^n)$ *with* $\mathbf{f}(\mathbf{0}) = \mathbf{0}$ *and let* $\mathbf{A} = Df(\mathbf{0})$*. Divide the eigenvalues* λ_i *of* $Df(\mathbf{0})$ *into 3 sets,* σ_s, σ_u *and* σ_c*, with*

$$\mathrm{Re}\ \lambda_i \begin{cases} < 0 & \text{if} \quad \lambda_i \in \sigma_s, \\ = 0 & \text{if} \quad \lambda_i \in \sigma_c, \\ > 0 & \text{if} \quad \lambda_i \in \sigma_u, \end{cases}$$

Let E^s, E^c *and* E^u *be the corresponding generalised eigenspaces. Then there exist* C^r *stable and unstable manifolds* W^s *and* W^u *tangential to* E^s *and* E^u *respectively at* $\bar{\mathbf{x}}$ *and a* C^{r-1} *center manifold,* W^c*, tangential to* E^c *at* $\bar{\mathbf{x}}$*. All these manifolds are invariant, but* W^c *is not necessarily unique.*

The Centre Manifold Theorem implies that at a bifurcation point the system can be written locally in co-ordinates $(\mathbf{x}, \mathbf{y}, \mathbf{z}) \in W^c \times W^s \times W^u$ on the invariant manifolds in the form

$$\dot{\mathbf{x}} = \mathbf{g}(\mathbf{x}) \tag{A.5.2a}$$

$$\dot{\mathbf{y}} = -B\ \mathbf{y} \tag{A.5.2b}$$

$$\dot{\mathbf{z}} = C\ \mathbf{z} \tag{A.5.2c}$$

where B and C are positive definite matrices. The motion on W^s is toward the fixed point and the motion on W^u is away from the fixed point. Therefore, local behaviour can be determined by solving (A.5.2a).

A.6 Conservative Systems

Consider the second order system

$$\dot{x_1} = x_2 \tag{A.6.1a}$$

$$\dot{x_2} = -v(x_1) \tag{A.6.1b}$$

where $v : R \rightarrow R$ is a C^1 function. The motion of (A.6.1) is described by the solution vector $\varphi(t, \mathbf{x}_0)$ which is time dependent. However, there may exist functions of $\varphi(t, \mathbf{x}_0)$ which remain constant during the motion and depend only on the initial conditions. Such functions are called first integrals of the motion. Certain functions play an important role in the physical description of the system, for instance, the energy function. A system is said to be conservative if it has a first integral of the motion. Define the energy function of (A.6.1) by

$$E(x_1, x_2) = \frac{1}{2}x_2^2 + V(x_1), \tag{A.6.2}$$

where

$$V(x_1) = \int_0^{x_1} v(s)ds. \tag{A.6.3}$$

The first term $\frac{1}{2}x_2^2$ in (A.6.2) is called the kinetic energy and (A.6.3) is the potential energy. Differentiating (A.6.2) with respect to time gives

$$\dot{E} = \frac{dE}{dx_1}\dot{x_1} + \frac{dE}{dx_2}\dot{x_2} = v(x_1)x_2 - x_2v(x_1) = 0.$$

Therefore the energy function is an integral of the motion of (A.6.1) and thus the system (A.6.1) is conservative. The potential energy function $V(x_1)$ contains information on the location and stability type of the fixed points of the conservative system. The fixed points are in the form $(\bar{x}_1, 0)$ where $\bar{x}_1$ satisfies $V'(\bar{x}_1) = 0$. Moreover, if we calculate the

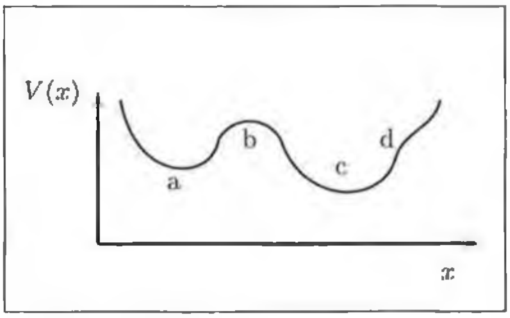

Figure A.1: Potential Function:(a,c) Stable center points (b) Unstable saddle point (d) Unstable cusp point

linearisation of the non-linear system at a fixed point $(\bar{x}_1, 0)$ we get

$$\dot{x} = \begin{pmatrix} 0 & 1 \\ -\ddot{V}(\bar{x}_1) & 0 \end{pmatrix} x.$$

The two eigenvalues of the Jacobian matrix are given by $\pm\sqrt{-V''(\bar{x}_1)}$. We can determine the stability type of non-degenerate equilibrium points by examining these eigenvalues. We see that minimum points of the potential correspond to stable centers while the maximum points of the potential correspond to unstable saddle points. For degenerate fixed points (i.e. $V''(\bar{x}_1) = 0$) we must examine higher order terms of the potential function V. We can rewrite (A.6.1) in terms of the energy function as

$$\dot{x}_1 = \frac{\partial E}{\partial x_2}$$
$$\dot{x}_2 = -\frac{\partial E}{\partial x_1}$$

and therefore the energy function is a Hamiltonian for the system.

The Roots of the Characteristic Polynomial $\Delta(p)$.

In this appendix we present several theorems that are used in the thesis concerning the roots of the characteristic polynomial $\Delta(p)$. The Routh-Hurwitz criterion is used in the stability analysis of equilibrium points. Details of this criterion are found in [3]. The remaining theorems refer to the relationship between the coefficients of $\Delta(p)$ and the existence of complex roots.

Theorem 8. *The Routh-Hurwitz Criterion.*

Let

$$\Delta(p) = p^3 + a_1 p^2 + a_2 p + a_3 \tag{B.0.1}$$

be a cubic polynomial in p. Define the determinants D_1, D_2 and D_3 as

$$D_1 = a_1, D_2 = \det \begin{pmatrix} a_1 & a_3 \\ 1 & a_2 \end{pmatrix}, D_3 = \det \begin{pmatrix} a_1 & a_3 & 0 \\ 1 & a_2 & 0 \\ 0 & a_1 & a_3 \end{pmatrix}$$

The real parts of the roots of (B.0.1) *are strictly negative (nonpositive) if and only if the determinants D_1, D_2 and D_3 are positive (nonnegative). Furthermore, the number of roots with positive real part is equal to the number of sign changes in the sequence* $1, D_1, D_1 D_2, a_3$

Conditions for the existence of a pair of complex roots for (B.0.1) can be determined by applying Rolle's Theorem to $d\Delta/dp = 0$.

Theorem 9. *Existence of complex roots of $\Delta(p)$.*

Let

$$\Delta(p) = p^3 + a_1 p^2 + a_2 p + a_3 \tag{B.0.2}$$

be a cubic polynomial in p. Then, there exists a pair of complex conjugate roots of (B.0.2) *if $a_1 < \sqrt{3a_2}$.*

Proof. From Rolles Theorem we know that $\Delta(p) = 0$ has a pair of complex roots if $d\Delta/dp = 0$ has complex roots. We have

$$\frac{d\Delta}{dp} = 3p^2 + 2a_1 p + a_2$$

with roots α and ϱ given by

$$\alpha = -\frac{a1}{3} \pm \frac{\sqrt{a_1^2 - 3a_2}}{3}$$

Thus, the roots are complex if $a_1 < \sqrt{3a_2}$. □

Proposition 10 below is used in Section 3.3 to determine relationships between the model parameters that ensures the existence of complex roots for the characteristic equation. First we state the following lemma,

Lemma 1. *Let* (B.0.2) *have two equal real roots ρ and one other root ϱ. Let ρ_+ and ρ_- be the roots of $d\Delta/dp$ where $\rho_- < \rho_+$. Then either*

$$\rho = \rho_-,\ \varrho = \frac{3\rho_+ - \rho_-}{2} \text{ and } \rho < \varrho \tag{B.0.3}$$

or

$$\rho = \rho_+\ \varrho = \frac{3\rho_- - \rho_+}{2} \text{ and } \rho > \varrho \tag{B.0.4}$$

Proposition 10. *Let* (B.0.2) *have two equal real roots ρ and one other root ϱ where ρ and ϱ are given by* (B.0.3) *and* (B.0.4)*. We have $a_3 = -\rho^2\varrho$. Let $\Delta^*(p)$ be a perturbation of $\Delta(p)$ where $\Delta^*(p) = p^3 + a_1p^2 + a_2p + a_3^*$. Then, $\Delta^*(p)$ has complex roots for a_3^* satisfying*

$$-\rho_+^2\frac{3\rho_- - \rho_+}{2} < a_3^* < -\rho_-^2\frac{3\rho_+ - \rho_-}{2}$$

Appendix C

Center Manifold Analysis.

In this appendix we include the canonical transformation used in the calculation of the center manifold at the bifurcation point $(\bar{x}_1, \lambda) = (0, G_m/2)$. We also write out the functions f_1, f_2 and f_3. The canonical transformations are

$$\begin{pmatrix} u \\ v \\ w \end{pmatrix} = \begin{pmatrix} 1 & -\frac{2\alpha}{2} & \frac{2}{\beta} \\ \frac{\alpha}{2\sqrt{\frac{\beta}{2}-(\frac{\alpha}{2})^2}} & \frac{\beta-\alpha^2}{\beta\sqrt{\frac{\beta}{2}-(\frac{\alpha}{2})^2}} & \frac{\alpha}{\beta\sqrt{\frac{\beta}{2}-(\frac{\alpha}{2})^2}} \\ 0 & \frac{2\alpha}{2} & -\frac{2}{\beta} \end{pmatrix} \begin{pmatrix} x_1 \\ x_2 \\ y \end{pmatrix}$$

and

$$\begin{pmatrix} x_1 \\ x_2 \\ y \end{pmatrix} = \begin{pmatrix} 1 & 0 & 1 \\ -\frac{\alpha}{2} & \sqrt{\frac{\beta}{2}-(\frac{\alpha}{2})^2} & 0 \\ -\frac{2\alpha^2}{2} & \alpha\sqrt{\frac{\beta}{2}-(\frac{\alpha}{2})^2} & -\frac{\beta}{2} \end{pmatrix} \begin{pmatrix} u \\ v \\ w \end{pmatrix}.$$

The non-linear functions, to quadratic order, are

$$\begin{aligned}
f_1(u,v,w,\mu) =& -\frac{2\alpha}{\beta}\mu(u+w) - \frac{2\alpha}{\beta}\mu((\frac{3}{8}-(\frac{\alpha}{2})^2)u^2 + (\frac{3}{4}-\frac{\beta}{4}-(\frac{\alpha}{2})^2)uw + (\frac{3}{8}-\frac{\beta}{4})w^2 \\
&+ \frac{\alpha\sqrt{\frac{\beta}{2}-(\frac{\alpha}{2})^2}}{2}v(u+w)) - \frac{\alpha}{4}(u+w)^2, \\
f_2(u,v,w,\mu) =& \frac{(1-\frac{\alpha^2}{2})\mu(u+w)}{\sqrt{\frac{\beta}{2}-(\frac{\alpha}{2})^2}} + \frac{\beta-\alpha^2}{\beta\sqrt{\frac{\beta}{2}-(\frac{\alpha}{2})^2}}((\frac{3}{8}-(\frac{\alpha}{2})^2)u^2 + (\frac{3}{4}-\frac{\beta}{4}-(\frac{\alpha}{2})^2)uw \\
&+ (\frac{3}{8}-\frac{\beta}{4})w^2 + \frac{\alpha\sqrt{\frac{\beta}{2}-(\frac{\alpha}{2})^2}}{2}v(u+w)) - \frac{\alpha^2}{8\sqrt{\frac{\beta}{2}-(\frac{\alpha}{2})^2}}(u+v)^2, \\
f_3(u,v,w,\mu) =& \frac{2\alpha}{\beta}\mu(u+w) + \frac{2\alpha}{\beta}\mu((\frac{3}{8}-(\frac{\alpha}{2})^2)u^2 + (\frac{3}{4}-\frac{\beta}{4}-(\frac{\alpha}{2})^2)uw + (\frac{3}{8}-\frac{\beta}{4})w^2 \\
&+ \frac{\alpha\sqrt{\frac{\beta}{2}-(\frac{\alpha}{2})^2}}{2}v(u+w)) + \frac{\alpha}{4}(u+w)^2.
\end{aligned}$$

Adiabatic Invariants

D.1 Introduction

In this appendix we define an adiabatic invariant for the system (D.1.1) and illustrate the concept with a simple example. A fuller account of the theory is given in Cole and Kevorkian [6]. Consider the following system of differential equations in standard form,

$$\frac{dp}{dt} = \alpha F(p, q, t, \alpha), \tag{D.1.1a}$$

$$\frac{dq}{dt} = \omega(p, t, \alpha) + \alpha G(p, q, t, \alpha), \tag{D.1.1b}$$

where $\alpha \ll 1$. We assume that F and G are $O(1)$, 2π periodic functions q.

Definition 11. *A function $\Psi(p, q, t, \alpha)$ with derivative*

$$\frac{d\Psi}{dt} = \psi(p, q, t, \alpha)$$

is an adiabatic invariant to $O(\alpha^k)$ of (D.1.1) *if ψ satisfies the following two conditions,*

(i) $\psi = O(\alpha^{k+1})$,

(ii) ψ has a zero average to $O(\alpha^{k+1})$ over the period of q,

$$\int_0^{2\pi} \psi(p, q, t, \alpha) dq = O(\alpha^{K+2}), \tag{D.1.2}$$

If $\psi \equiv 0$ then Ψ would be an exact invariant. Thus, an adiabatic invariant is constant to a given order in α in an asymptotic sense and the condition on the average of ψ ensures that the error in assuming that Ψ is constant is $O(\alpha^{k+1})$ uniformly in $0 \le t \le T(\alpha) = O(\alpha^{-1})$. Transforming a given system of differential equations to the standard form can often be achieved by looking for a transformation when $\alpha = 0$ and then applying this transformation for $\alpha \neq 0$. This idea is illustrated with a simple example. We consider an oscillator with small damping. The reduced system is Hamiltonian, but this property is lost for $\alpha \neq 0$.

D.2 The Damped Linear Oscillator

The damped linear oscillator is represented by the following second order system,

$$\frac{dx_1}{dt} = x_2, \tag{D.2.1a}$$

$$\frac{dx_2}{dt} = -2\alpha x_2 - x_1, \tag{D.2.1b}$$

where $\alpha \ll 1$. The reduced system is obtained by setting $\alpha = 0$ and results in the linear oscillator. We can express the reduced system in terms of the energy $E(t)$ and phase $q(t)$ using the following transformation,

$$E = \frac{1}{2}(x_2^2 + x_1^2), \tag{D.2.2a}$$

$$q = \tan^{-1}(\frac{x_1}{x_2}). \tag{D.2.2b}$$

Now, allowing α to be non-zero and using (D.2.1) and (D.2.2), we determine $\dot{E}$ and $\dot{q}$ to get

$$\dot{E} = x_2(\dot{x_2} + x_1) = -2\alpha x_2^2 = -2\alpha(2E\cos q^2) = -2\alpha E - 2\alpha E\cos(2q)),$$

$$\dot{q} = 1 + \alpha \sin 2q.$$

This system for E and q is in the standard form (D.1.1). However, E is not an adiabatic invariant to $O(\alpha)$ because $\dot{E}(t)$ does not satisfy (D.1.2) due to the presence of the $-2\alpha E$ term. However, we can define a new variable $J(t)$ in terms of $E(t)$ such that the equation for $\dot{J}(t)$ satisfies (D.1.2), giving us an adiabatic invariant for (D.2.1). Letting $J = \Phi(E, \tau)$, where $\tau = \alpha t$, we get

$$\dot{J} = \Phi_E \dot{E} + \alpha \Phi_\tau = -\alpha(2E\Phi_E - \Phi_\tau) - 2\alpha E \cos(2q)\Phi_E. \tag{D.2.3}$$

Setting $2E\Phi_E - \Phi_\tau = 0$ removes the average term from (D.2.3). We solve this condition to get $\Phi(E, \tau) = 2Ee^{2\tau}$. Substituting for Φ into (D.2.3) gives

$$\dot{J} = 2\alpha J \cos(2q).$$

The equation for $\dot{J}$ contains no average term and satisfies the conditions of an adiabatic invariant to $O(1)$ for the system.

Bibliography

[1] N. H. Baker, D. W. Moore, and E. A. Spiegel. Aperiodic Behaviour of a Non-Linear Oscillator. *Quart. J. Mech. and Appl. Math.*, 24(4):390–420, 1971.

[2] N. N. Bogoliubov and N. M. Krylov. *Introduction to Nonlinear Mechanics.* Princeton University Press, Princeton, 1947.

[3] F. Brauer and J. A. Nohel. *The Qualitative Theory of Ordinary Differential Equations.* Dover Publications, inc. N.Y., 1989.

[4] J. D. Cole and J. Kevorkian. Uniformly Valid Asymptotic approximations for certain differential equations. In *Proc. Internat. Sympos. Nonlinear Differential Equations and Nonlinear Mechanics*, pages 113–120. Academic Press, N.Y., 1963.

[5] J. D. Cole and J. Kevorkian. *Perturbation Methods in Applied Mathematics.* Applied Mathematical Sciences, Springer-Verlag, 1981.

[6] J. D. Cole and J. Kevorkian. *Multiple Scale and Singular Perturbation Methods.* Applied Mathematical Sciences, Springer-Verlag, 1996.

[7] M. Fabrizio and A. Morro. *Mathematical Problems in Linear Viscoelasticity.* SIAM Studies in Applied Mathematics, SIAM, 1992.

[8] W. N. Findley, J. S. Lai, and K. Onaran. *Creep and Relaxation of Nonlinear Viscoelastic Materials with an introduction to Linear Viscoelasticity.* Dover Publications, inc., N.Y., 1989.

[9] J. M. Gere and S. P. Timoshenko. *Mechanics of Materials.* Boston, London, 4th edition, 1997.

[10] P. Glendinning. *Stability, Instability and Chaos: an Introduction to the Theory of Nonlinear Differential Equations.* Cambridge Press, 1994.

[11] J. Guckenheimer and P. Holmes. *Nonlinear Oscillations, Dynamical Systems, and Bifurcations of Vector Fields.* Applied Mathematical Sciences, Springer-Verlag, 1983.

[12] R. Haberman. Slowly varying jump and transition phenomena associated with algebraic bifurcation problems. *SIAM J. Appl. Math.*, 53:69–106, 1979.

[13] J. Hale and H. Koçak. *Dynamics and Bifurcations.* Springer-Verlag, 1991.

[14] B. Hayman. Aspects of Creep Buckling I. The Influence of Post-Buckling Characteristics. *Proc. R. Soc. Lond. A.*, (364):393–414, 1978.

[15] B. Hayman. Aspects of Creep Buckling II. The Effects of Small Deflexion Approximations on Predicted Behaviour. *Proc. R. Soc. Lond. A.*, (364):415–433, 1978.

[16] M. H. Holmes. *Introduction to Perturbation Methods.* Texts in Applied Mathematics, Springer-Verlag, 1995.

[17] F. C. Hoppensteadt. *Analysis and Simulation of Chaotic Systems.* Springer-Verlag, N.Y., 1993.

[18] G. W. Hunt and J. M. T. Thompson. *A General Theory of Elastic Stability.* John Wiley, N.Y., 1973.

[19] E. L. Ince. *Ordinary Differential Equations.* Dover Publications, Dover, N.Y., 1956.

[20] G. N. Kuzmak. Asymptotic Solutions of Nonlinear Second Order Differential Equations with Variable Coefficients. *J. Appl. Math. Mech. (PMM)*, (23):730–744, 1959.

[21] A. Lindstedt. Ueber die integration einer für die störungstheorie wichtigen differentialgleichung. *Astron. Nachr.*, 103:211–220, 1882.

[22] G. J. M. Maré. *Sudden Change in Second Order Nonlinear systems.* PhD thesis, 1995.

[23] D. T. Mook and A. H. Nayfeh. *Nonlinear Oscillations.* Pure and Applied Mathematics, John Wiley and Sons, 1979.

[24] K. Murphy. *Dynamic Buckling of Linear Viscoelastic Rods.* PhD thesis, D.C.U., 1996.

[25] R. E. O'Malley. *Singular Perturbation Methods for Ordinary Differential Equations.* Applied Mathematical Sciences, Springer-Verlag, 1991.

[26] H. Poincaré. *Les Methodes Nouvelles de la Mécanique Celeste*, volume 2. Dover, New York, 1957.

[27] Y. N. Rabotnov. *Creep Problems in Structural Members.* North-Holland, 1969.

[28] G. G. Stokes. On the Theory of Oscillatory Waves. *Cambridge Trans.*, 8:441–473, 1847.